Status of thesis

Title of Thesis: Seismic Attributes of Reservoir E34 at X Field

I SUNDARESAN A/L SATHASIVAM hereby allow my thesis to be placed at the Information Resource Centre (IRC) of Universiti Teknologi PETRONAS (UTP) with the following condition:

1. The thesis becomes the property of UTP
2. The IRC of UTP may make copies of the thesis for academic purpose only.
3. This thesis is classified as
   'CONFIDENTIAL'

The method discussed on this thesis is still not published. The data used are properties of PETRONAS.
The contents of the thesis will remain confidential for Five (5) years.

Remarks on disclosure:
Any modifying of the report or redefine the contents **MUST** get approval from the author and PETRONAS Carigali Sdn. Bhd.

Endorsed by

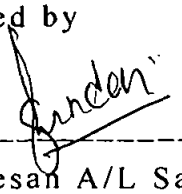

Sundaresan A/L Sathasivam
PETRONAS Carigali Sdn. Bhd.
Exploration Geoscience Group
Date:21 January 2008

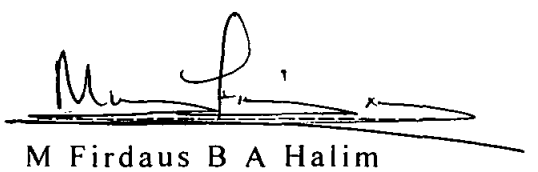

M Firdaus B A Halim
PETRONAS Research Scientific
Sdn.Bhd Geoscience Group
Date:21 January 2008

UNIVERSITI TEKNOLOGI PETRONAS

SEISMIC ATTRIBUTES OF RESERVOIR E34 AT X FIELD

BY

SUNDARESAN A/L SATHASIVAM

A THESIS
SUBMITTED TO THE POSTGRADUATE STUDIES PROGRAMME
AS A REQUIREMENT FOR THE
DEGREE OF MSc in PETROLEUM GEOSCIENCE

JANUARY, 2008

Universiti Teknologi PETRONAS
Bandar Seri Iskandar
31750 Tronoh
Perak Darul Ridzuan

Declaration

I hereby declare that the thesis is based on my original work except for quotations and citations which have been duly acknowledged. I also declare that it has not been previously or concurrently submitted for any other degree at UTP or other institutions.

Signature : 

Name : SUNDARESAN A/L SATHASIVAM

DATE : 21 January 2008

UNIVERSITI TECHNOLOGY PETRONAS

Approval by Supervisor (s)

The undersigned certify that they have read, and recommended to The Postgraduate Studies Programme for acceptance, a thesis entitled **"Seismic Attributes of Reservoir E34 at X Field"** submitted by **Sundaresan A/L Sathasivam** for the fulfillment of the requirements for the Degree of Master of Science in Petroleum Geoscience.

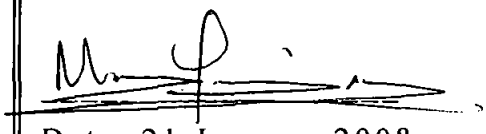

Date: 21 January 2008

Signature 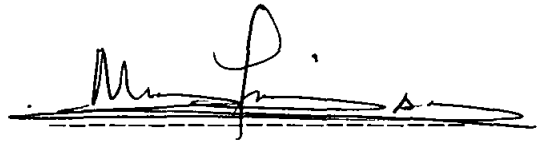

Main Supervisor : M Firdaus B A Halim

Date : 21January 2008

Co-Supervisor : M Renal K Sengupta

Abstract

X Field is located in the west-central Malay Basin, offshore Malaysia. The X field main reservoirs are aligned on a stacked pattern within an anticline structure. Seismic attributes will be utilized to understand the faults distribution and extension of hydrocarbon sand of the E34 reservoir within the X field. The E34 interpreted horizon on seismic and the faults interpretation are incorporated to extract the hydrocarbon sand in the reservoir. The E36 reservoirs are characterized by massive bodies of sand. The attribute extraction shows that the distribution of sand bodies ties well with the structure map. Three different amplitude related attributes were utilized to determine the hydrocarbon sand extension. Crucial assumptions made in this project were the E34 reservoir is homogenous throughout the X field and the amplitude within the hydrocarbon sand zone does not show any anomalous change. The amplitude variation on several exploration and deviated wells are studied by observing the amplitude values given within the hydrocarbon zone. The well markers and related well logs are used to verify the hydrocarbon zone at each location. The hydrocarbon zone observed on well logs is approximately 36 ms. Therefore, the attribute extraction are conducted on a window basis. The minimum distance from E34 horizon showing hydrocarbon presence is 4 ms. The windows are extracted between 4ms to 36 ms below the E34 horizon, which apparently give the amplitude values for the hydrocarbon sand. First, the attributes are extracted for a wider range of amplitudes observed on seismic sections at the well location. Later these values are compared between windows of different depths to get the nominal value for hydrocarbon sand. The attribute analysis in this report was conducted for the entire X field. The main concentration was given to the Unit area where wells are available. Therefore, users may be able to determine expected possible hydrocarbon distribution at particular depth (ms) within the E34 reservoir. More wells need to be drilled in the Western and Eastern areas to understand the amplitude variance. These results can be incorporated to change the current amplitude limits for each attribute and define a new range for the Eastern and Western areas.

Acknowledgement

I would like to thank my two supervisors M Firdaus & M K Sengupta for their guidance and support on this project.

I would be grateful to PRSB staffs especially from Geoscience Group and all my IFP/UTP lecturers for their kind assistance.

TABLE OF CONTENTS

LIST OF FIGURES:

LIST OF TABLES:

CHAPTER ONE: INTRODUCTION TO X FIELD

X Field is located in the west-central Malay Basin, offshore Malaysia and belongs to ADD oil company. The field was discovered in 1981. It is situated about 130km from Terengganu Crude Oil Terminal (TCOT) with an average water depth of 76m (Figure 1.0).

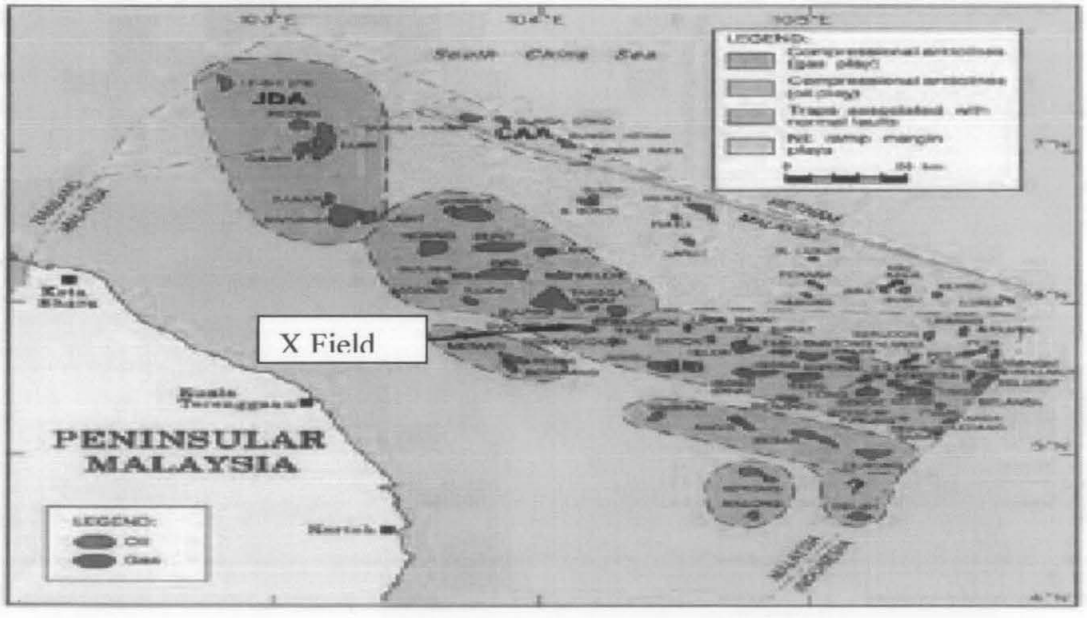

Figure 1.0: Location of X field, offshore Peninsular Malaysia

The X field can be divided into 3 major areas (Figure 1.1) namely Unit Area, Western Area and Eastern Area. Currently, the X field produces from four (4) platforms, three (3) within the Unit area and a single platform in the western area. The first production from X field was on 15 March 1991 and the highest production of approximately 54Mstb/d was in October 1994.

These units are located within an anticline structure where each unit is separated by major faults. Past studies have shown that not all the faults show sealing capacity and therefore the general overview of the field needs to be studied to understand the fluid movement associated with the geological structures present in the field. In order to achieve the objective of this project, general seismic interpretation on the entire field is conducted with focus on the X field Unit area.

1.1 Problem Statement

X field shallow reservoirs has been explored extensively by ADD Oil Company. A very limited exploration work been carried out on deeper reservoirs below the E34 reservoir.

This project and the study carried will provide assistance to understand the hydrocarbon distribution within the X field. The attribute analysis using the common seismic amplitude approach will be used on this study considering the time limitation for this project. The introduced method can be considered as a preliminary approach to define the hydrocarbon sand distribution. This method will be tested on E34 reservoir and several blind well tests with be carried out to prove that the introduced method works at this vicinity. Therefore, further research and exploration work may add value to reservoir E34 study.

1.2 Objectives

Objective of this study is to utilize the seismic attributes to understand the Faults distribution and extension of hydrocarbon sand within the Unit zone of X field below the E34 horizon window.

Prior to attribute extraction, a detailed interpretation was conducted on E34 horizon to understand the horizon extent and horizon termination due to faults.

1.3 Scope of Work

1. Well and Seismic data loading of different vintages
2. Well – Seismic correlation/calibration
3. 3D Seismic Interpretation – E34 horizon interpretation
4. 3D Seismic Attributes analysis – Fault and Hydrocarbon determination

Logs from 135 wells were made available in the database. The most crucial part of this project was to interpret the E34 horizon as accurate as possible on the final migrated seismic data. For this purpose, the well data was utilized fully to tie the seismic with well markers. The well markers interpreted from well logs and core cuttings were made available in this project. Any seismic mis-interpretation of the E34 reservoir will lead to

erroneous identification of hydrocarbon the sand extension. This is because the reservoirs in this field are stacked reservoirs and the separation within the reservoirs varies are very small.

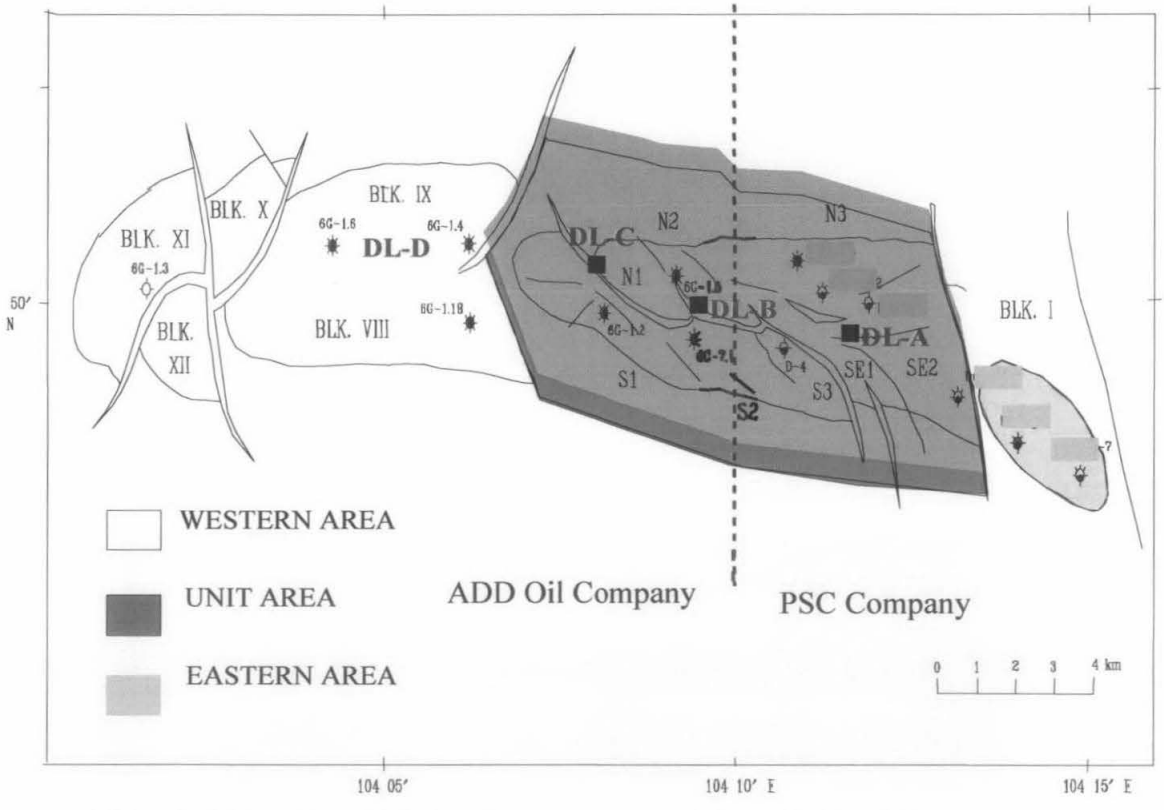

Figure 1.1: X field can be divided to three (3) main units as displayed above.

The seismic attributes that can be extracted using Landmark Seiswork Poststack software were utilized. The attributes studies will focus on identifying faults and later extracting the hydrocarbon sand extent. The faults in the field were over laid on seismic to conduct the E34 horizon interpretation taking into consideration the complexly faulted anticline structure of the X field.

The seismic attributes extractions were done by using horizon E34 as the guide horizon and defining windows within the E34 layers. Amplitude based attributes were utilized to observe the hydrocarbon distribution within an area or window of extraction. **For the study, key assumption is that the E34 reservoir distribution has no drastic amplitude values change within the hydrocarbon sand zone throughout the field.** The vertical wells are used to classify the amplitude values within the hydrocarbon zone.

The amplitude values are later crosschecked with blind wells to determine the reliability of this method.

The final step was to verify and determine the amplitude variation method on various amplitude attributes does work within the X field. Therefore, several blind wells were tested on the amplitude attribute maps and the results were used to prove the method.

CHAPTER TWO: STRUCTURAL GEOLOGY AND DEPOSITIONAL ENVIROMENT

2.1 Structural Geology

The X field is located off the east coast of Peninsular Malaysia, approximately 125 kilometers northeast of Kuala Terengganu, as noted on Figure 1.0. The field is associated with an anticline structure located approximately 1,200 meters sub sea. The water depth in the area is 74 meters. The X field is a complexly faulted anticline structure. The structure is approximately 4 kilometers wide and 24 kilometers long with a closure of approximately 100 meters as measured from the E-8 sand oil water contact to the crest of the structure. The field has been subdivided into three primary areas: the Western area, the Central area (Unit area) and the Eastern area.

The X field is located in the Malay Basin. The Malay Basin is a major structural feature that lies to the northeast of Peninsular Malaysia. Regionally, the X field is one of the many hydrocarbon-bearing structures in the Basin. The axis of the basin is oriented approximately in a northwest-southeast direction between Peninsular Malaysia and the Khorat Swell south of Vietnam.

The X field structure is an elongated westward plunging anticline with three (3) major faults sets that dissect the structure into a number of fault blocks. The major fault display a typical negative flower structure and are the product of deep-seated wrench movements, probably related to the regionally extensive X field fault zone. Almost 220 faults were mapped but only the strike-slip faults are believed to be sealing at all level. These sealing faults have generally has divided the X field into compartments and classified as units in this project (Figure 1.1). The seismic and isochore data demonstrate that fault in the X Field were active during deposition. Evidence for fault movement during the deposition were noticed and studied on Isochore of pseudo horizon from well control by X field geologist previously.

2.2 Depositional Environment

X field is interpreted to be most likely located on a coastal plain in the depositional environment on Figure 2.0. The shoreface interpretation shows that the most marine-influenced unit is E14 and older sequences like E34, E36 and E40 shows an increasingly fluviatile imprint. The reservoir facies associations were recognized as shoreface, channels and mouth bars while the non-reservoir paleoenvironments were dominantly bayfill and peat swamp. This erosional event was followed by the E14 sand itself, which has been interpreted as a shallow marine, shoreface deposit that was deposited as either a forced regression or transgressive sand. Generally, the X field can be classified as fluvial in nature.

The X Field reservoir section contains repetitive cycles of interbedded sandstones and shales that are often terminated by coals. Study done from the available core photographs, the wireline logs, available special geological studies, and data derived from drilling, the overall groups of noncoal clastic sediments in the area of the X field have been subdivided into three primary lithologic facies: sandstones, mixed sandstone/shale sequences, and mudstones. The sandstone facies includes sand accumulations varying from massive sandstones that are either cross-bedded or even bedded to thin nonbedded layers of sandstone. These various sand units have, by definition, a sand-to-shale ratio between 0.9 and 1. Therefore, most of the sandstones in this category represent very good quality reservoir units. A second distinct lithofacies is the mudstones. By definition, the mudstones have a sand-to-shale ratio between 0.1 and 0, they represent the pure mud facies (shale) and are nonreservoir units. The majority of the noncoal clastics in the X field fall between these two lithologic end members and can be grouped into a general mixture of alternating lenticular sands and interbedded shales. These interlaminated sands and shales vary from simple alternating thin beds of sand with minor shale known as flaser beds (having a sand/shale ratio of between 0.75 and 0.9) to the wavy-bedded lenticular sands (having a sand/shale ratio between 0.25 and 0.75). The thin-bedded flaser sands are often two to three centimeters in thickness with veneers of mudstone between the separate sand accumulations. Occasionally, there are some organic

materials distributed within the mudstone partings and some intraformational clay clast conglomerates within the intermediate shale partings.

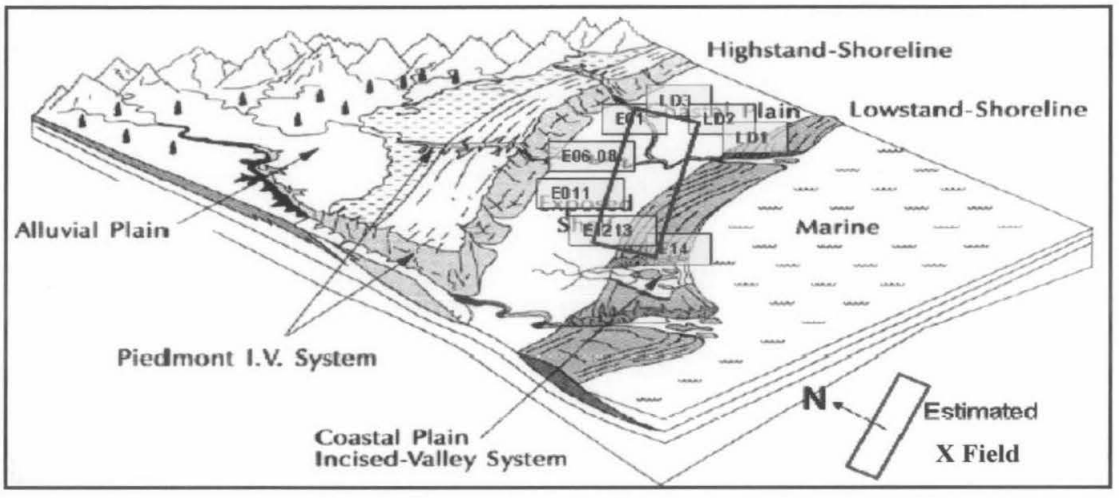

Figure 2.0: Depositional Environment of X field

The primary hydrocarbon-bearing reservoirs in the X field are in the Upper Miocene portion of the offshore geologic section. In the area of the X field, the reservoir section is approximately 400 meters thick and consists of alternating sands and shales with some intercalated coal beds. The various hydrocarbon reservoirs occur below a 3 to 4 meter thick coal marker that forms both the key seismic reflector and the primary correlation level within the field. This coal unit has been classified as the "E marker." Four dominant hydrocarbon-bearing intervals comprise the X field. The uppermost interval is a gas-bearing zone within the lowermost sands of the Group D zone that immediately overlies the E marker. The primary oil-bearing reservoirs in the X field are the field wide sand of the E8 trough E14 interval. The other two intervals occur between the E marker down to the top of the E8 sand and the E14 sand down to the E50 sand. These two intervals comprise a series of lenticular and channel sands that are probably discontinuous.

The X field was subdivided into three primary sections or blocks. In addition to the fault control, the Western Block had a different apparent E14 oil/water contact than that found in the Central Block. In addition, the fault separating the Central and Eastern

blocks was considered to be sealing since it separates oil in the Central Block from gas in the Eastern Block with no apparent fluid contact.

As conclusion, the E34 reservoir is delineated throughout the X field with sandstone facies. Therefore, the amplitude extracted within the E34 reservoir will show the hydrocarbon in the sandstone facies.

CHAPTER THREE: SEISMIC INTERPRETATION

3.1 3D Horizon Interpretation & Well-Seismic Correlation

The X block consisted of approximately 26,481 km of 48 fold data, which was recorded in year 2002 with a dual source - six streamers configuration. There were 5895.68 km of undershoot data around the platforms area. A total of 12 subsurface lines were recorded in one pass using this configuration.

The seismic-well correlation was conducted on the vertical and selected deviated wells considering the crucial part of the attribute extraction is to make sure the E34 horizon interpretation was conducted as correct as possible. In this project, the horizon interpretation was conducted on the final migrated seismic data using Landmark Seiswork software. The first step taken was to analyze the waveform characteristic of the seismic horizon E34 on the acquired seismic data. The water bottom was verified to be peak amplitude (SEG negative polarity convention). Well logs from 135 wells are available in the database.

In this project, 13 vertical Exploration wells were taken as the main reference to conduct E34 horizon correlation. All the 13 wells were analyzed using SynTool seismic synthetics software. Synthetics were created for all the wells and the markers from each well were overlaid on seismic before conducting the horizon interpretation. Prior to generating the synthetics, all the displayed well logs were check shot corrected.

In order to create synthetic traces, the software first uses the densities and/or velocities in the well logs to calculate acoustic impedance and reflectivity in the earth at the well. The Syntool generates synthetic traces that simulate the behavior of a wavelet traveling trough the earth. A filter was adopted to create Ricker model wavelet, which convolves the wavelet with the reflection coefficient series to produce one-dimensional (1D) synthetic traces (Figure 3.0).

The generated synthetic traces were correlated with the seismic data to identify the best fit of the seismic behavior at the well in the zone of interest (Figure 3.0 & 3.1) mainly the E34 horizon. On most of the wells, time shifts between 8 to -15ms were done to get the best fit between the synthetics and the seismic data.

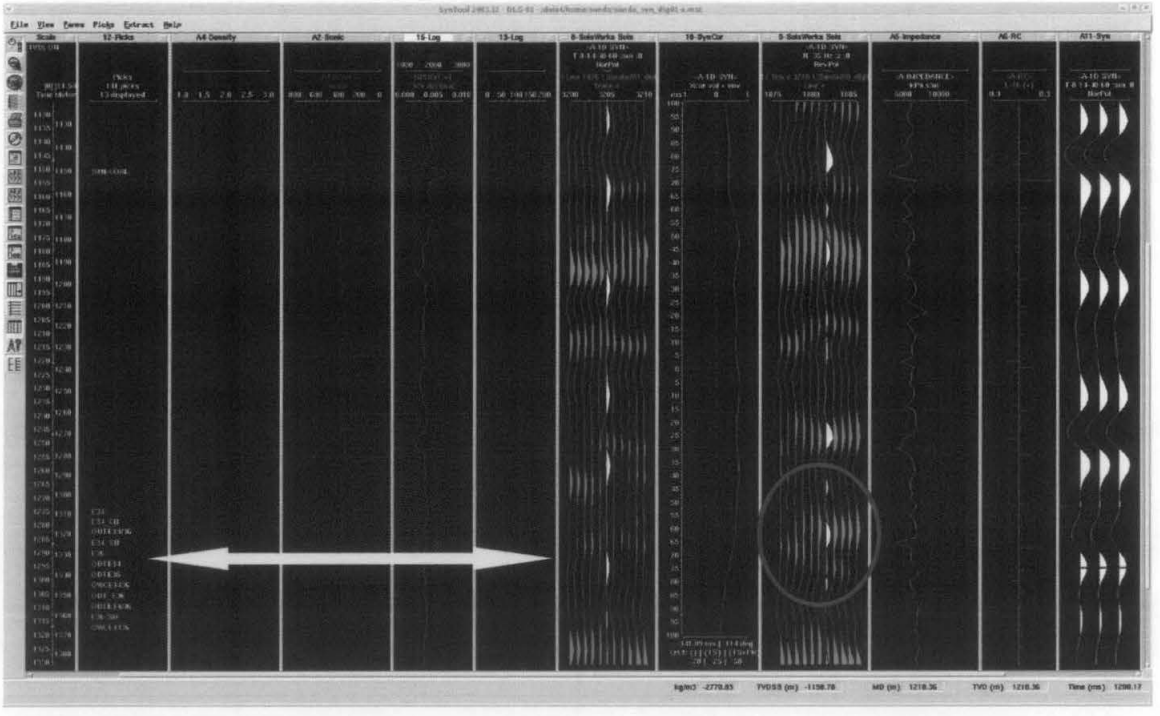

Figure 3.0: D_01 well correlation results and synthetic produces from modal based Ricker wavelet. Red circle shows the reverse polarity synthetic ties with seismic data. The red circle shows the tie between seismic and reverse polarity synthetic wavelet. The yellow arrow shows the E34 horizon referring to the well markers.

The synthetic and real seismic correlation on all the studied wells shows that the E34 horizon ties with the reverse polarity synthetic (Figure 3.2). Therefore, the E34 horizon is interpreted as trough on this project. During the horizon interpretation, the synthetics and the well markers were overlaid on the seismic as a point of reference and calibration. Both the vertical and deviated well markers were overlaid on the seismic section to enhance the horizon interpretation accuracy.

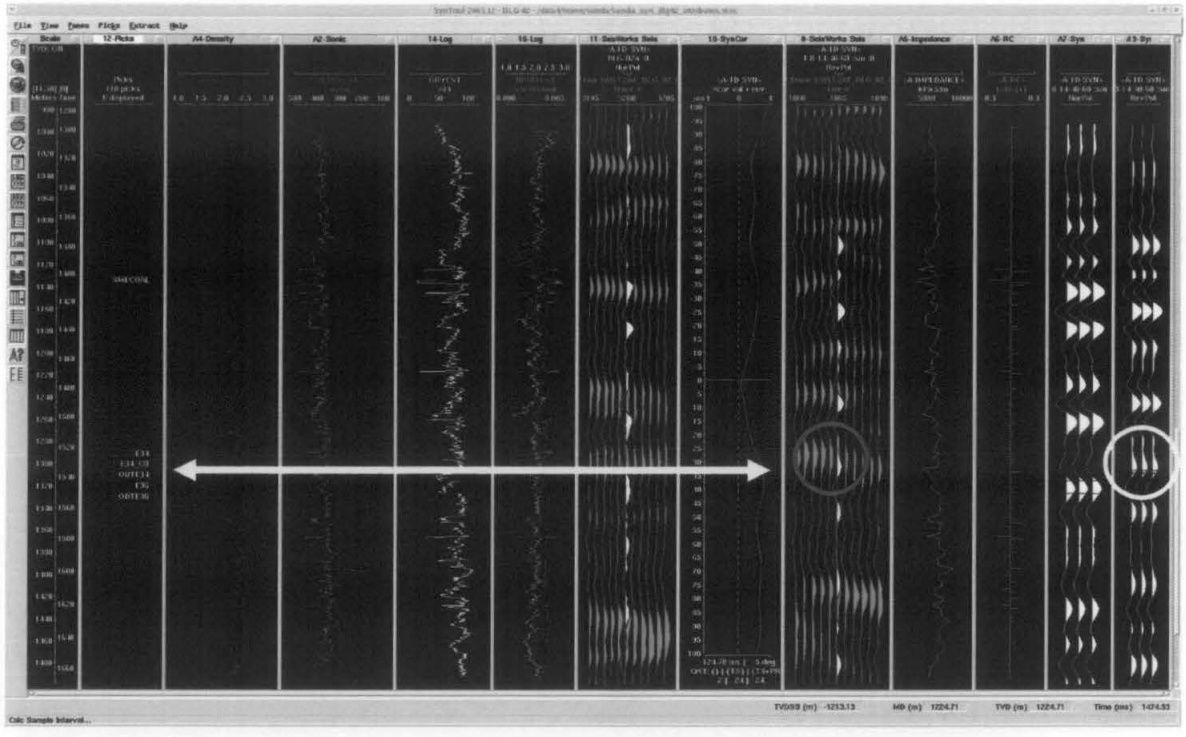

Figure 3.1: D_02 seismic well correlation results. The red circle shows that reverse polarity synthetic ties with the seismic data, whereas the yellow circle shows the reverse polarity synthetic. The yellow line shows the level of E34 horizon.

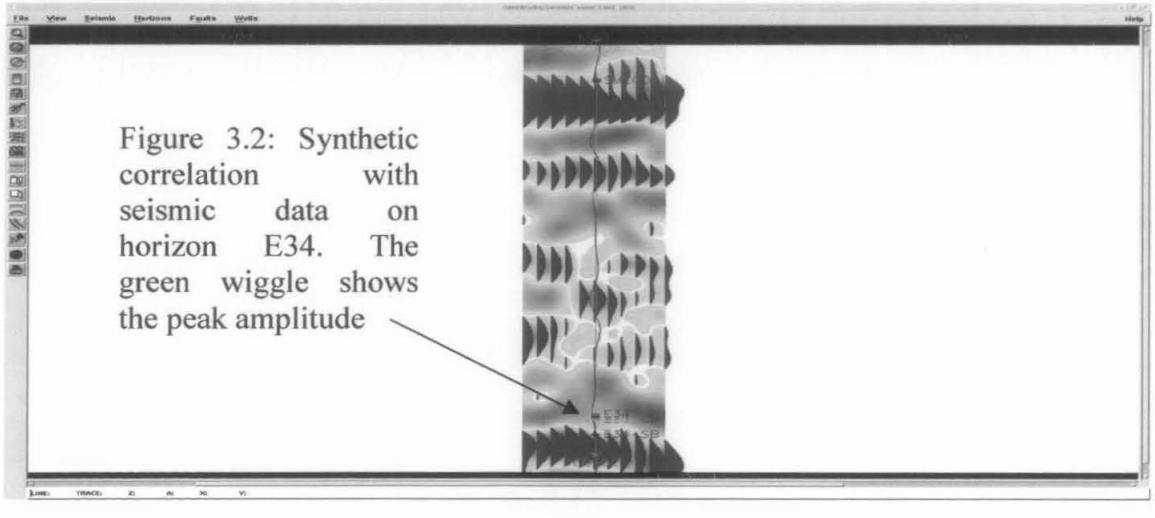

For the D-02 well correlation, the top of E34 layer ties well with the sonic, neutron porosity and formation density logs. The E34 layer is probably associated with coal because the Gamma Ray and resistivity logs show a kick (anomalous) reading. The details will be discussed in the attribute analysis section later. The synthetic on the

reverse polarity ties with the seismic record. The SMECoal layer shows an anomalous reading on both formation density and sonic logs (Figure 3.0 & 3.1).The SMECoal layer is taken as reference layer together with E34 layer for interpretation. On the seismic, the E34 horizon is interpreted on a trough and the synthetic on reverse polarity ties well with the seismic (Figure 3.3). All the available synthetics and well markers (Figure 3.4 & 3.5) were overlaid on seismic line and trace sections to interpret horizon E34.

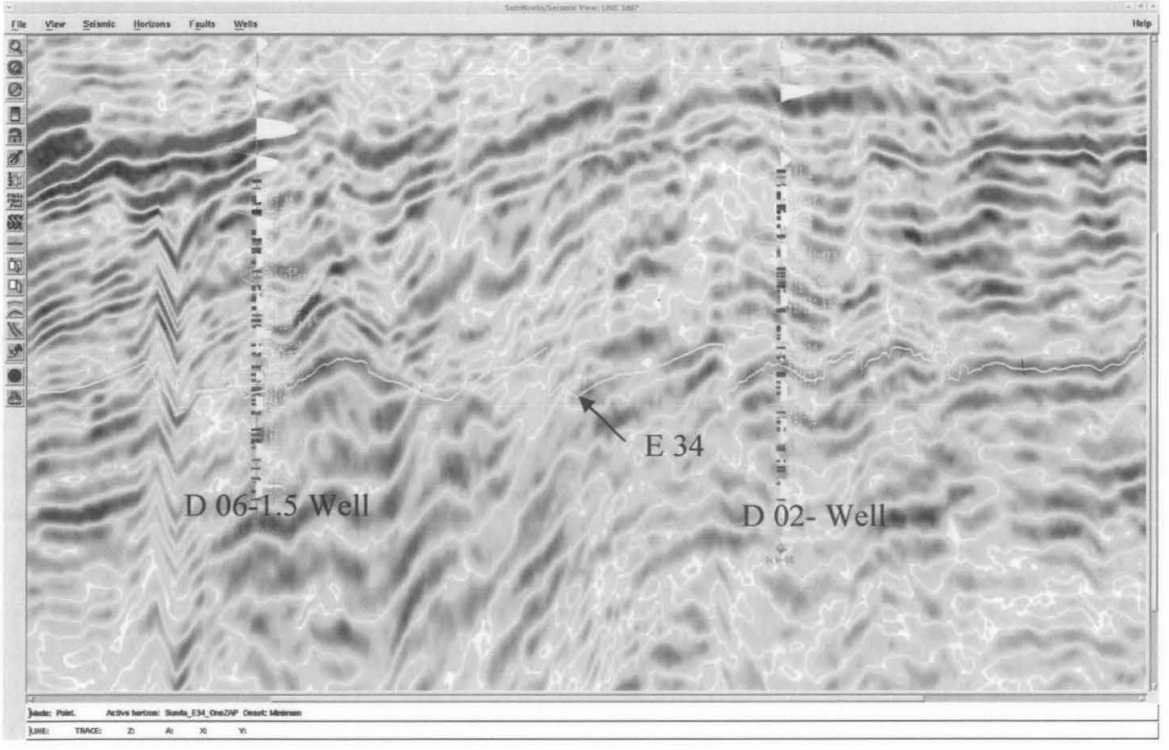

Figure 3.3: The Synthetic correlation with seismic data and well markers. Line 1887 with wells D_02 and D_06_1.5

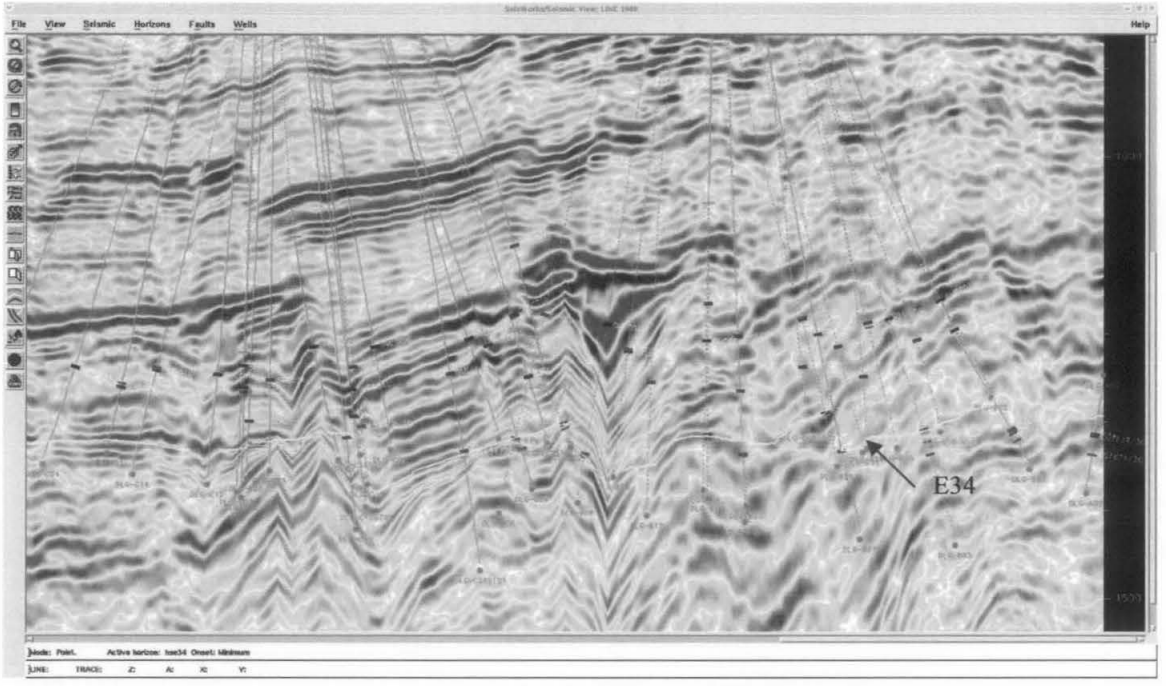

Figure 3.4: Horizon E34 interpreted on seismic with well markers taken into consideration

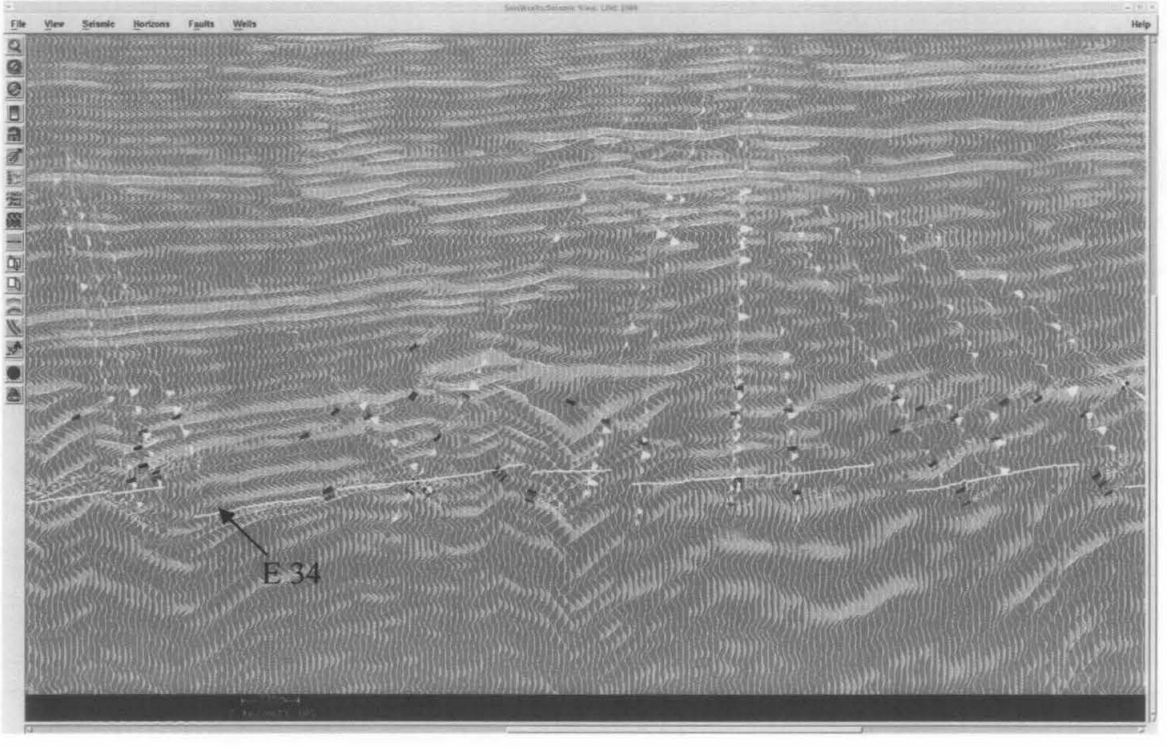

Figure 3.5: Horizon E34 interpretations, with synthetics from different wells were overlaid on seismic (wiggle, variable area).

The horizon interpretation was conducted on a 50 inline interval and 50 trace on cross line (trace) interval. Later, the horizon was interpreted on every 20 lines interval and crosschecked between trace-line directions. The adjacent horizons such as E36 and SMECoal were also observed carefully.

The major faults and any identifiable small faults were interpreted within the seismic resolution on the seismic sections (Figure 3.6). The fault delineation was done on every 50 metres followed by 20 meters interval along line and trace direction. Horizon E34 was auto-tracked to obtain a clear outline of the horizon before performing the attribute analysis. Post stack attribute analysis work well if the entire survey area or mainly the area of interest have continuity on reflector delineation. In order to achieve this, E34 horizon was auto tracked using ZAP. ZAP is Landmark's interactive auto-tracking product for 3D seismic projects. To ensure the interpreted horizon is delineated smoothly, the E34 horizon was interpolated with a smoothing factor. The result of ZAP and interpolation of E34 horizon is shown on Figure 3.7, which shows the structure map for the E34 horizon.

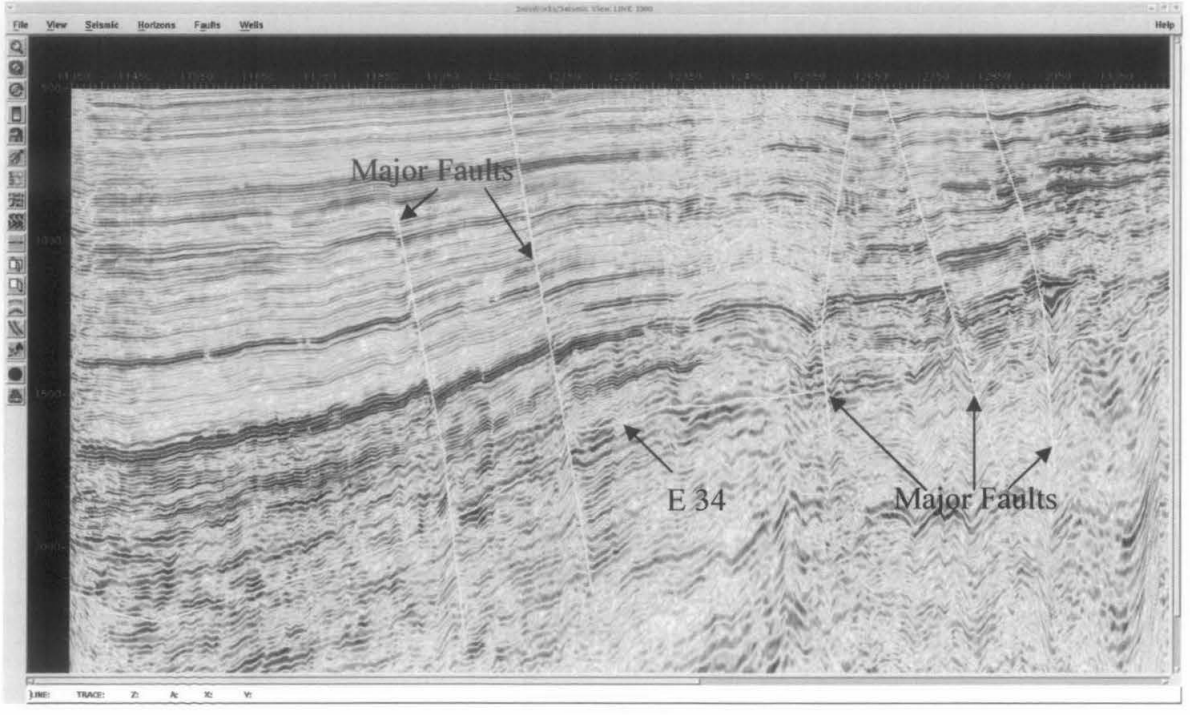

Figure 3.6: Major faults and E34 horizon interpretation on line 1900

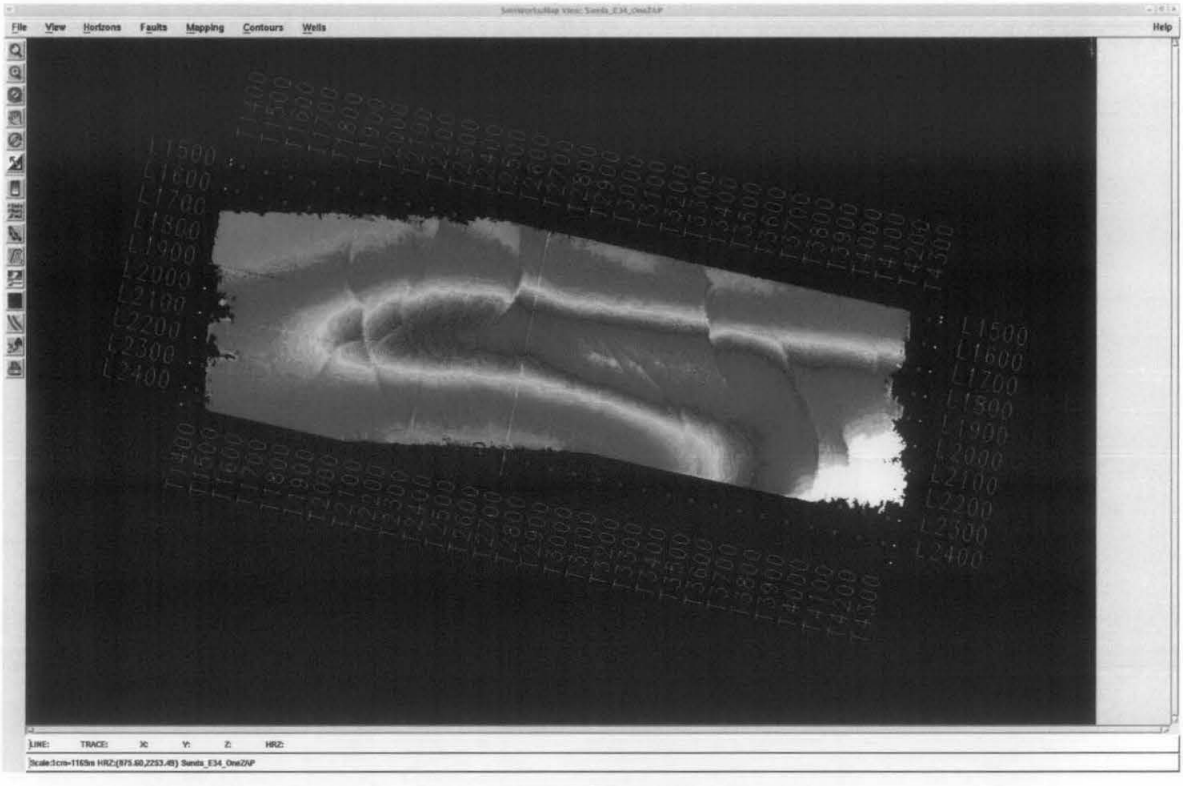

Figure 3.7: Structure map of E34 horizon after ZAP (one iteration)

CHAPTER FOUR: FAULTS IDENTIFICATION USING SEISMIC ATTRIBUTES

4.1 Methodology

Mapping of geological features at reservoir level is important to achieve an optimal field development. Due to the limited resolution in the seismic, it is difficult to map smaller scale discontinuity in seismic sections. Consider the importance of geological features such as faults having displacements less then ~20-30 m in a reservoir and these data are tracked down using relevant seismic attributes. Identification and determination of fault information can be achieved from a physical and theoretical understanding of the relation between faults and seismic attributes. Therefore, the seismic processing should be amplitude preserving. Further, it will be important to understand which seismic attributes or combinations that gives the most successful interpretation of faults close to seismic resolution.

The faults distributions are studied prior to determine the hydrocarbon sand extent in X field. This information is crucial because the attribute will be extracted below the E34 interpreted horizon. Therefore, the event terminations along E34 reservoir are pre-determined to enhance the hydrocarbon sand distribution analysis accuracy using seismic attributes.

There are mainly two objectives on this subject. Firstly, to select the right attribute that is capable to identify the faults interpreted on seismic sections. Secondly is to locate any new faults, which are visible on attribute maps and add to the existing volume of faults in X field. In this report, the clearly identified faults from previous interpretation in the database were used to select the type of attribute. The identified attribute on the later stage was used to detach any new discontinuity events that are probably faults.

The major faults were identified on the widely spaced vertical section namely, 20 to 50 line/trace intervals on both line and trace sections. The major faults and other identified faults are correlated on seismic sections (Figure 4.0). The 220 faults from previous interpretation are present within the X field location. These faults are interpreted on

final migrated seismic sections. The interpreted faults were overlaid on each created attribute maps to study the correlation and further identify any new faults.

The conventional method to detach faults was implemented to identify any missing faults by studying the alignment of event termination. Even termination is visible at the faults because any horizontal section alignments indicate the strike of a feature. If there is a significant angle between structural strike and fault strike then the event will terminate. For cases where structural strike and fault strike are parallel, the event will not terminate but will be parallel with the faults.

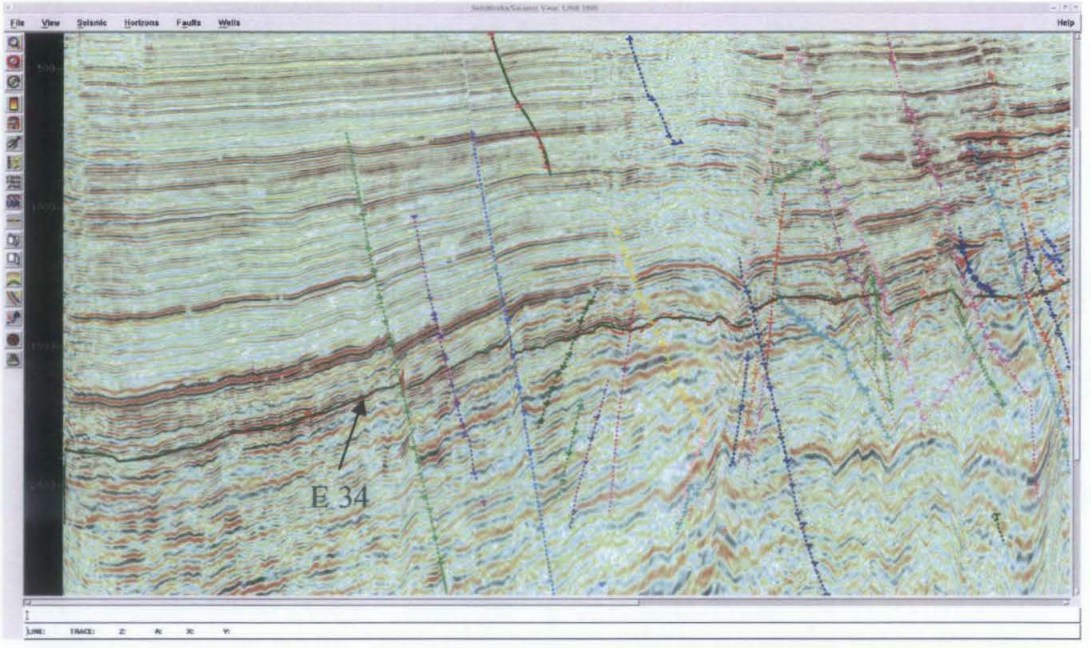

Figure 4.0: Fault interpretation conducted on seismic line 1900 that can be observed via event termination.

Mainly for attribute analysis, Landmark Post Stack attributes were used to understand and analyze the fault prediction. Because the layers are broken by faults where mis-alignment or discontinuity occurs, the attributes proposed are based on measuring the loss of local coherence or pointing out a local disorder in seismic signals. Post Stack 3D ESP (Event similarity prediction) method was adopted to study the fault delineation and identification along the E34 horizon within the Unit area specifically and X block generally.

The interpreted features were defined as probable faults because the 3D ESP method will identify various features such as fault, levees, channels and anomalous discontinuity events. Therefore, the curvature attribute were used to crosschecked and define the features identified on ESP maps. The Post Stack Curvature method using weighted average attributes was adopted. The positive and negative curvature values were used to confirm the fault and channel existence.

4.2 Post Stack 3D ESP (Event similarity prediction) Methods

Landmark Post Stack Seiswork provides the Event similarity predictions (ESP) 3D attribute analysis. The X field 3D final migrated data were utilized to conduct the analysis. This attribute is taken into consideration because of the capability to identify similarity and dissimilarity along adjacent and surrounding traces that are calculated and calibrated mathematically.

ESP 3D utilized both Semblance and Manhattan distance to predict the similarity between traces. ESP 3D scans from one to eight nearest neighbor traces (Scan Pattern) using semblance to determine the minimum or maximum (Evaluation Statistic) similarity. ESP 3D has two methods to determine which windows on the neighbor traces to use in the semblance calculations. On this project both the option were taken into consideration. The first option uses unconstrained semblance (Figure 4.1 to Figure 4.10, Option 1) which scans of the center trace to each neighbor trace as per sliding window. The second option uses planner constrain (slant, or dip-scan) stacks (Figure 4.11 to Figure 4.24, Option 2) to compute a best-fit plane orientation. The dip scan method uses eight traces, which were generated over a range of dip in two perpendicular directions, and the semblance similarity is calculated.

The best semblance value calculated and retained for each neighbor trace will then be the target trace for Manhattan distance dissimilarity evaluation which optionally be the one with the highest semblance (Evaluation Statistic - Maximum) with the center trace, or the

one with the lowest semblance with the center trace (Evaluation Statistic - Minimum). Generally, high semblance is captured when the geology is flat and continuous whereas low semblance or similarity occurs when the geology is dipping and continuous. A very anomalous reading of semblance is shown for a case of discontinuity. For both the evaluation method, the Manhattan distance dissimilarity value is computed using the center reference trace, the target neighbor trace, and the value output at the middle sample of the center trace window.

A dataset of Manhattan distance dissimilarity values has a range of 0 to 1. These values are then scaled by multiplying by 100 facilitate display in Seisworks. High values are areas of highest dissimilarity that can indicate areas of rapid change such as faults. Average or median values give you a view of the representative data similarity in the area. Low Manhattan distance values indicate a very uniform (low dissimilarity) geology.

Several attempts were made with various parameters before executing the 3D ESP attributes. The two (2) main options identified are unconstrained and dip slant semblance method were taken into consideration.

4.2.1 Maps analysis

4.2.1.1 Unconstrained Method (Option 1)

The Unconstrained option measures data similarity via a two-trace semblance analysis. For each center trace, data within a fixed time window is compared to data in a sliding time window on a neighbor trace. The best semblance value computed during the sliding process is retained for that neighbor. This process is repeated for each selected neighbor.

The scan pattern compares the current existing trace with two adjacent with one from in-line and other from cross-line direction (Scan Pattern – Ell -2 Trace scan). A window length between 1000ms and 2500ms were adopted considering the horizon is interpreted to be within the specified range. The major faults are interpreted from seismic and compared with the ESP 3D result. The result of ESP 3D were studied on each lines and

traces. The faults interpreted and visible on seismic sections are overlaid on the ESP attribute maps. The purpose is to make sure that the created attribute map can detect these faults. The observation shows that the unconstrained method does not show clear image for faults delineation especially on deeper time slices.

Time slices are taken at 1200 ms (Figure 4.1), 1400 ms (Figure 4.2), 1400 ms with fault display (Figure 4.3), 1800 ms (Figure 4.4), 2200 ms (Figure 4.5), 2400 ms (Figure 4.6) and at 2400 ms with fault display (Figure 4.7).

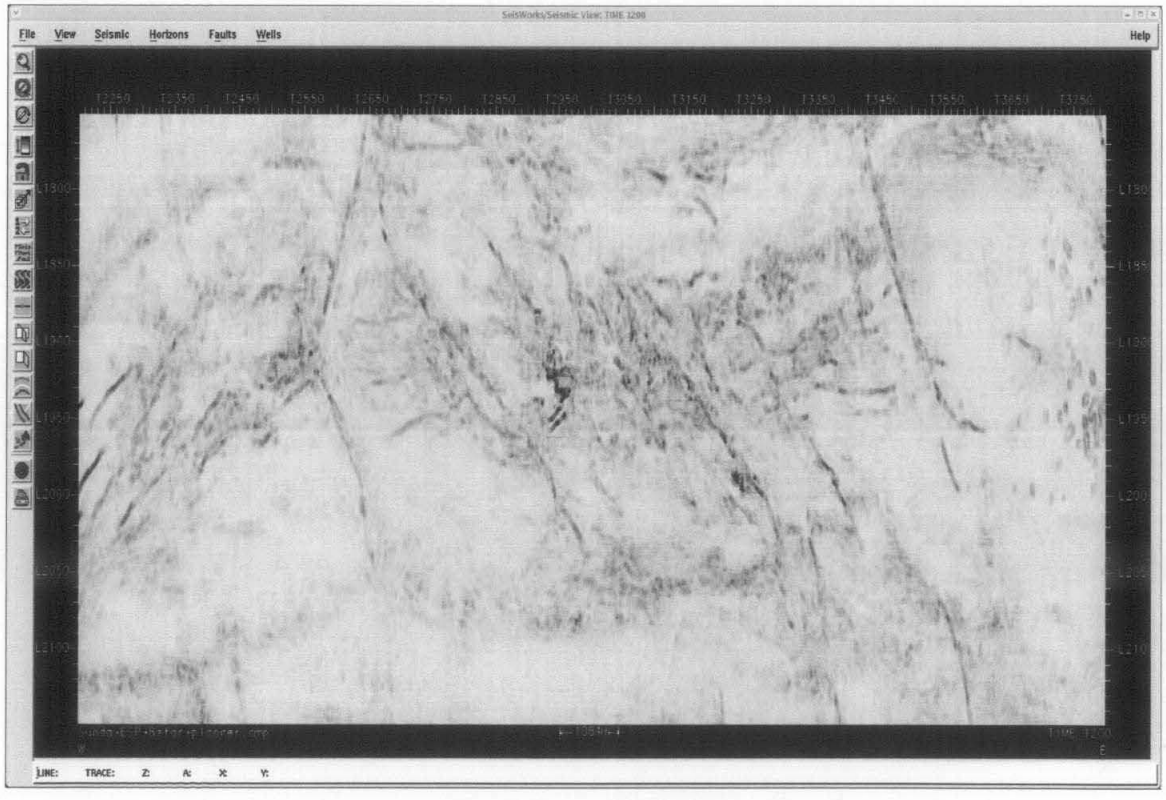

Figure 4.1: ESP Unconstrained method along slice 1200ms

The displays of ESP unconstrained method are studied along a trace line and its capability to identify faults along the anticline feature is shown on Figure 4.8, Figure 4.9 and Figure 4.10. Further discussions on these seismic lines are on section 4.3 Summary: Attribute Selected for Fault Detection.

Figure 4.2: ESP Unconstrained method along slice 1400ms

Figure 4.3: ESP Unconstrained method along slice 1400ms with fault display

Figure 4.4: ESP Unconstrained method along slice 1800ms

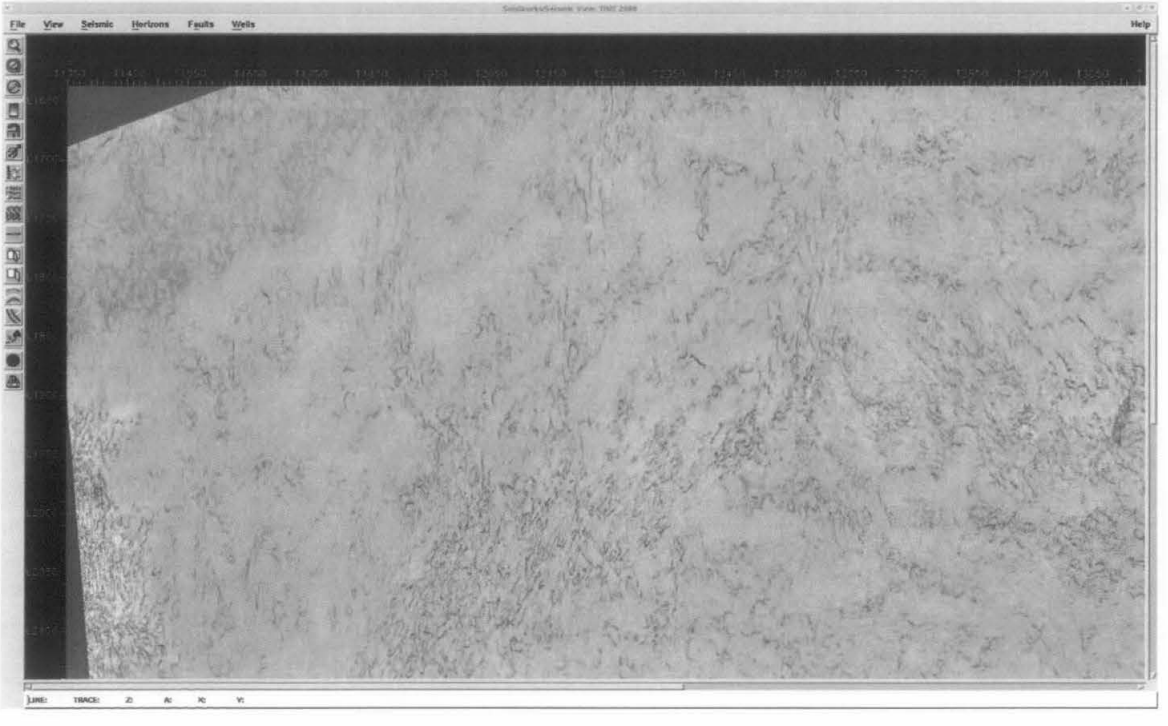

Figure 4.5: ESP Unconstrained method along slice 2200ms

Figure 4.6: ESP Unconstrained method along slice 2400ms

Figure 4.7: ESP Unconstrained method along slice 2400ms with fault display

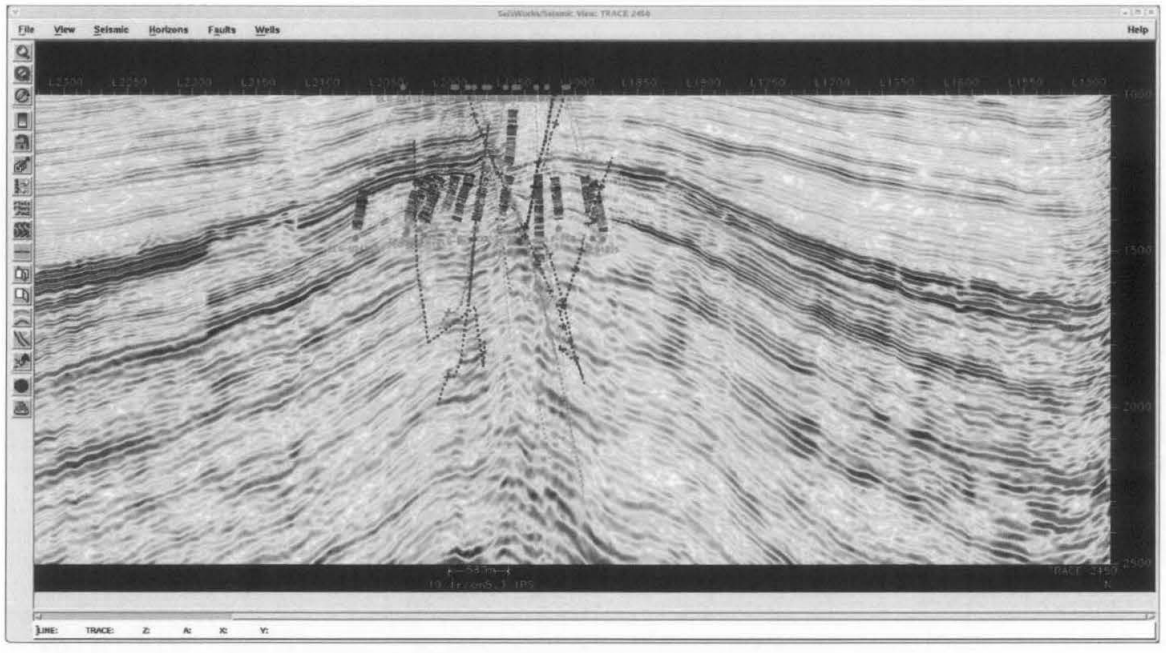

Figure 4.8: Seismic display observed on trace 2400 with fault and well display

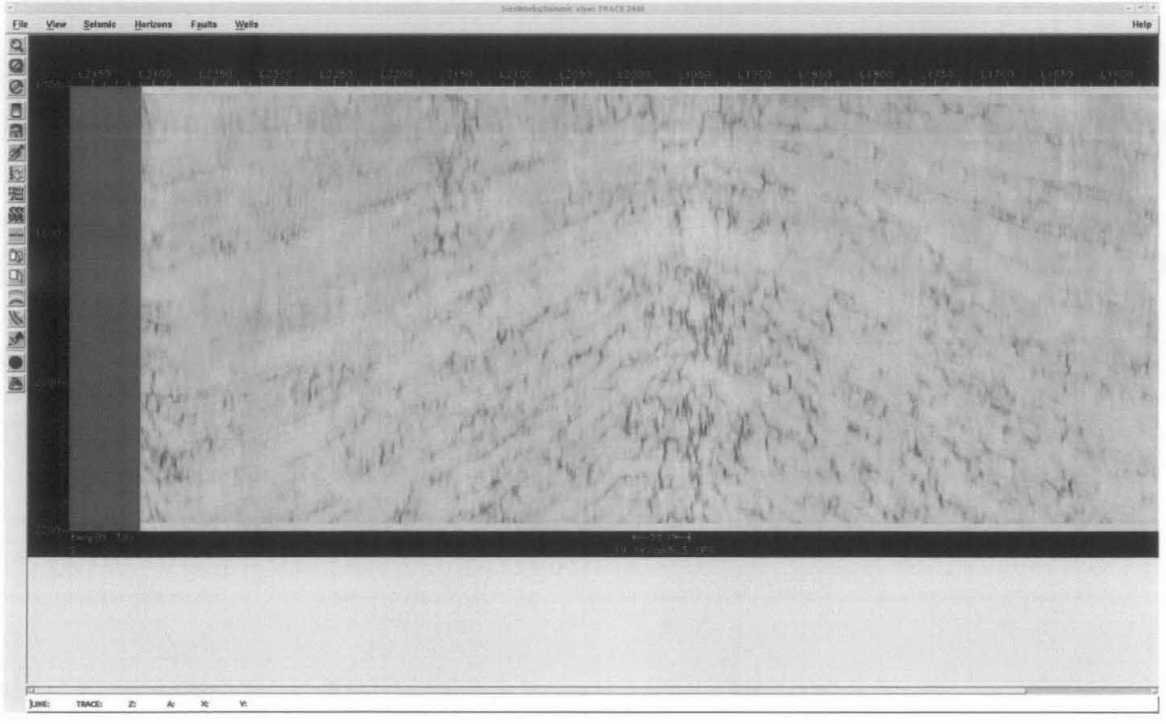

Figure 4.9: ESP Unconstrained method along trace 2400ms.

Figure 4.10: ESP Unconstrained method along trace 2400ms with fault display

4.2.1.2 Planar Dip Constrained method (Option 2)

The Planar Dip Constrained option uses semblance analysis to perform dip scan. Dip-scan uses eight neighbor traces to generate over a range of dips, in two perpendicular directions, and the semblance values are calculated. Analysis of these semblance values yields the best orientation of a plane. Where this plane intersects the neighbor traces, defines the center of the window of samples used for each trace. Semblance, using the fixed window on the center trace and the newly defined fixed window on each selected neighbor trace, is computed and retained.

This method is used to compare the centre trace with all eight surrounding traces (Star - 8 Method). A window length between 1000ms and 2500ms were adopted considering the E34 horizon is interpreted to be within the specified range. The planner ESP method with 8 star scanning method with maximum evaluation statistic shows clear lateral traces changes and provides better dissimilarity prediction with event or horizon termination.

In this project, the X field data seems to be clearly identifiable for shallower range of 500ms to 2000ms as compared to deeper targets below 2000ms. There are probably two reasons for the attributes to show this characteristic. Firstly, the data acquired below the SMECoal layer seems to be low energy and poor penetration of seismic signal due to absorption. Secondly, the deeper data seems to be unclear due to signal distortion. The seismic acquisition was acquired using a 4800-meter cable length and the target expected during that period of acquisition was shallower.

Two main areas were located for determine which attribute to utilize for faults identification. The red circle and the black circles show event termination characteristic on time section as shown on Figure 4.11, Figure 4.12, Figure 4.13, Figure 4.14, Figure 4.15 and 4.16. Therefore, these two areas are compared on different time slices to determine the right attributes to be used. Detail discussion of these areas is given on section 4.3 Summary: Attribute Selected for Fault Detection.

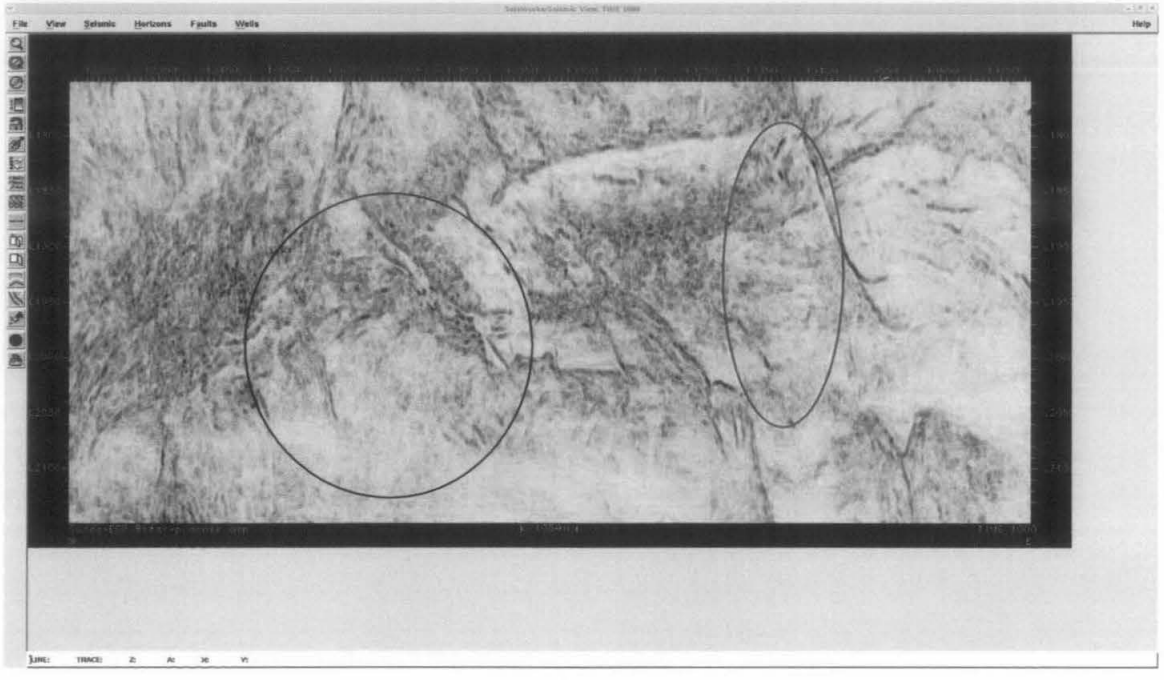

Figure 4.11: Time slice showing at 1000 ms with ESP Planner Dip method

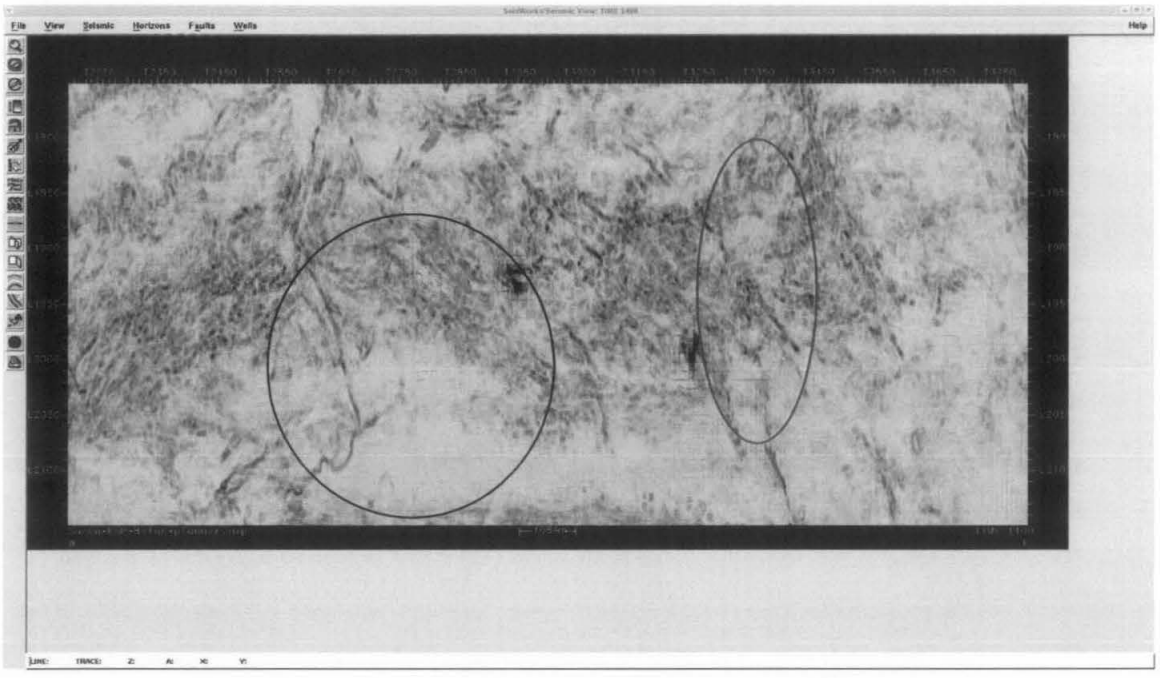

Figure 4.12: Time slice showing at 1200 ms with ESP Planner Dip method

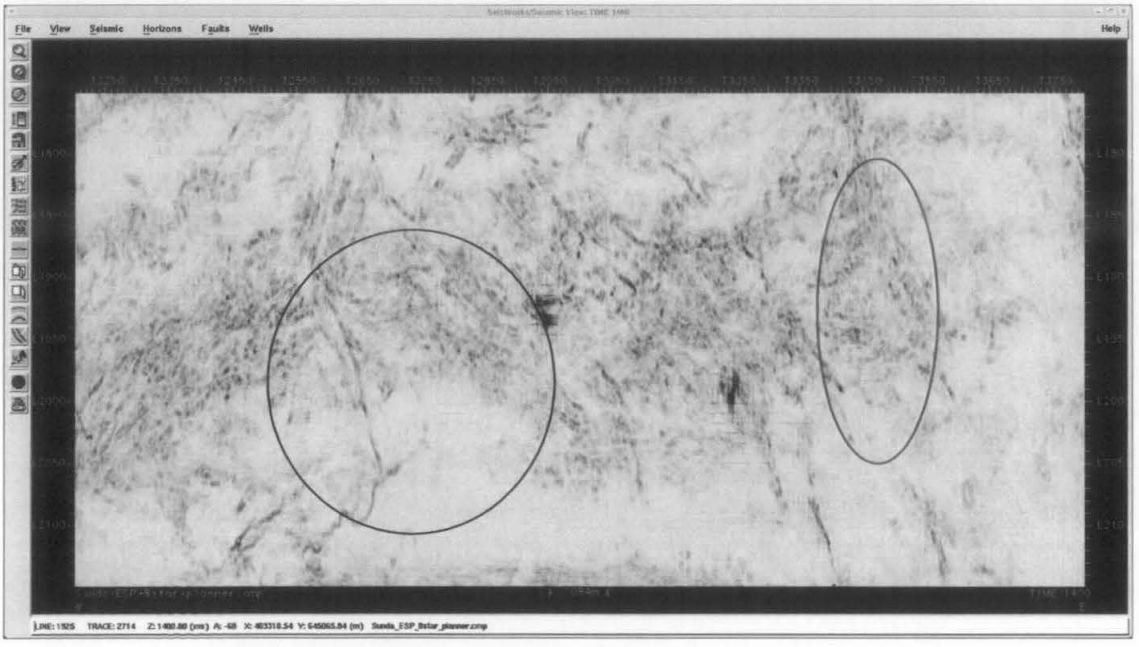

Figure 4.13: Time slice showing at 1400 ms with ESP Planner Dip method

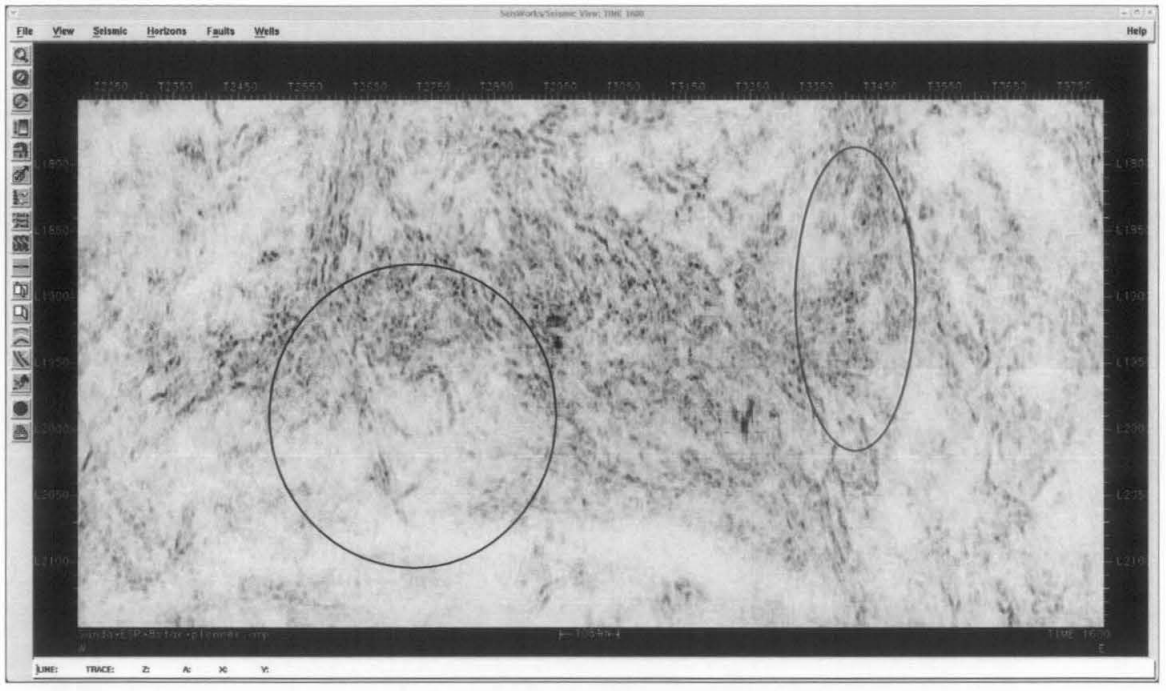

Figure 4.14: Time slice showing at 1600 ms with ESP Planner Dip method

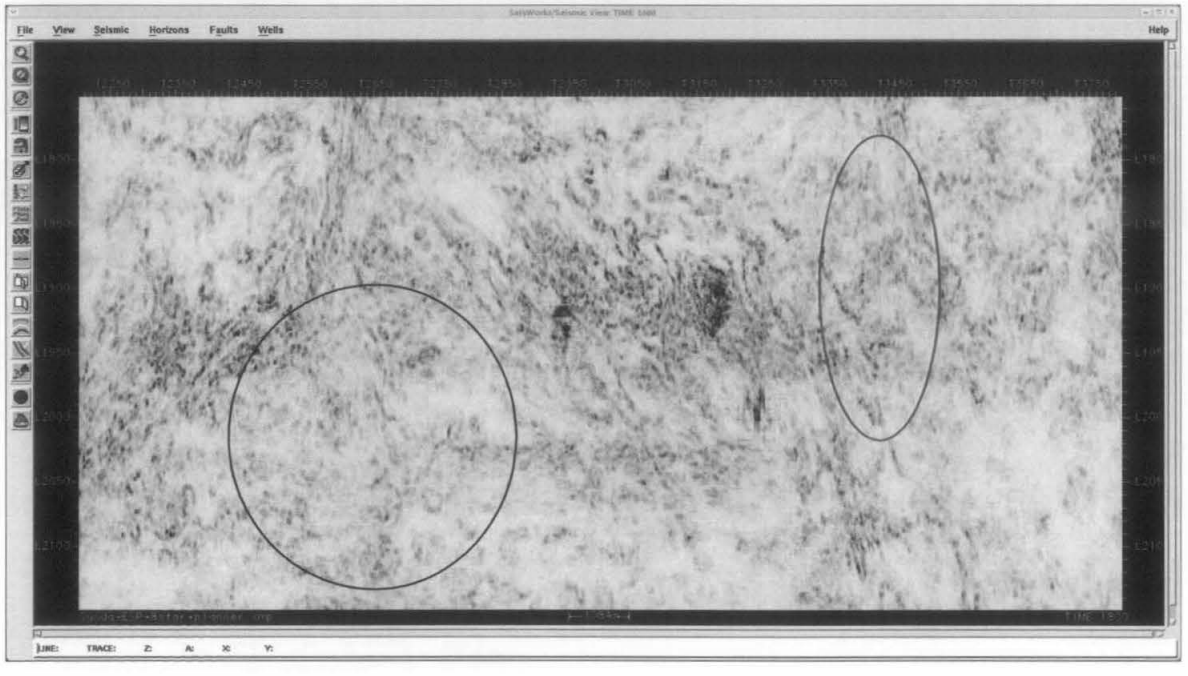

Figure 4.15: Time slice showing at 1800 ms with ESP Planner Dip method

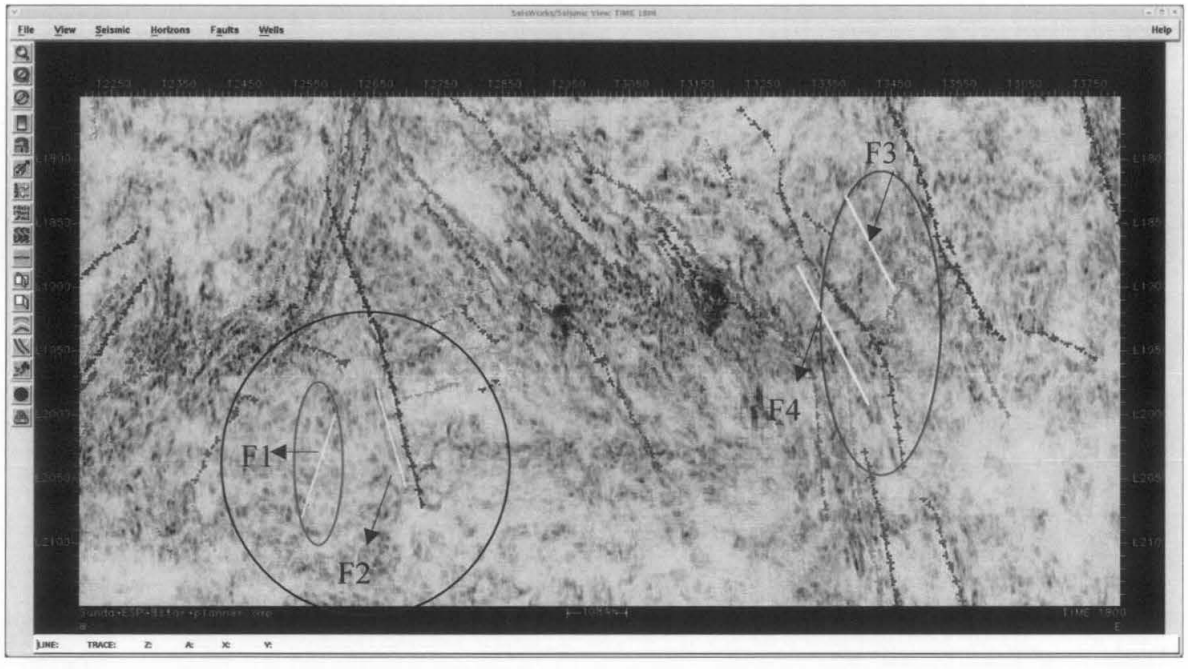

Figure 4.16: Time slice showing at 1800 ms with ESP Planner Dip method with fault display

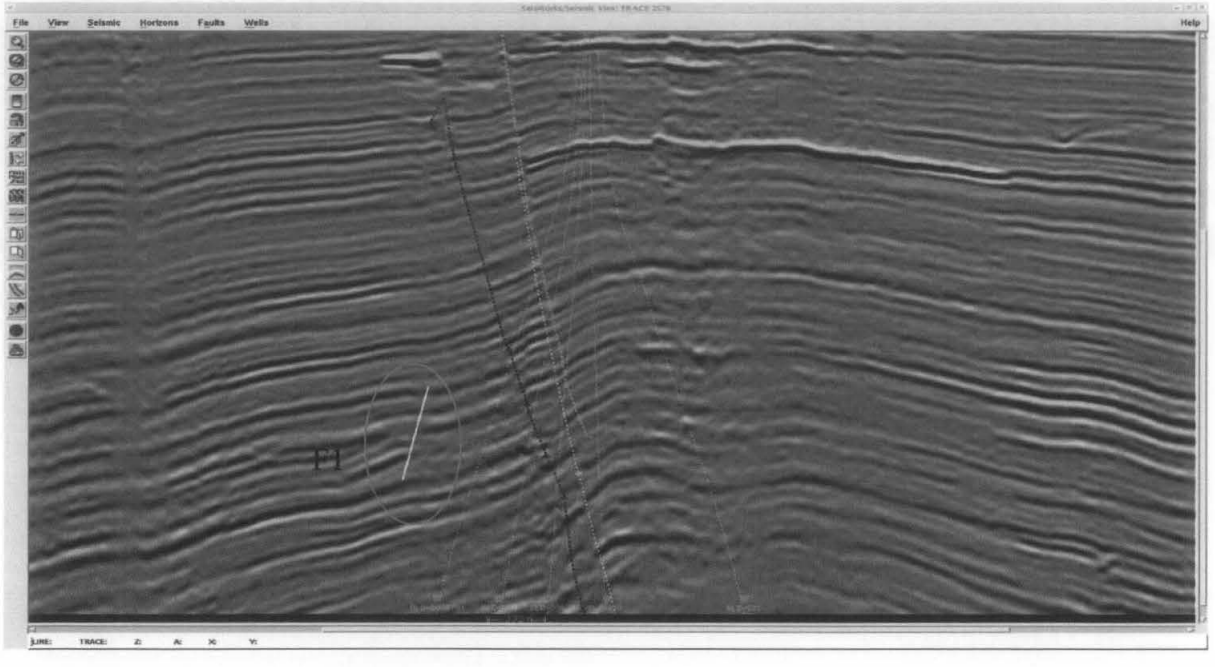

Figure 4.17: Fault F1 identified on seismic line delineated from ESP attributes map on trace 2570.

4.3 Summary: Attribute Selected for Fault Detection.

The seismic interpreted faults delineation can be observed on the shallower time slice for Option 1 unconstrained method, on 1200 ms (Figure 4.1), 1400 ms (Figure 4.2), 1400 ms with fault display (Figure 4.3) and 1800 ms (Figure 4.4). The deeper target is not very clear as at 2200 ms (Figure 4.5), 2400 ms (Figure 4.6) and at 2400 ms with fault display (Figure 4.7).

The comparison at slice 1400 ms shows that the faults interpreted on seismic are better identifiable on the attribute time slice maps. The result of ESP 3D were studied on each lines and traces. The fault map is overlaid on the ESP result to understand the correlation between seismic attribute and fault delineation. The display of ESP unconstrained method is studied along a trace line and its capability to identify faults along the anticline feature is shown on Figure 4.8, Figure 4.9 and Figure 4.10. The faults are not shown clearly along the anticline features on seismic sections compare to ESP vertical sections. The faults interpreted on ESP vertical section on Figure 4.16 and Figure 4.17 show that the faults present are clearer and provide better fault identification on Planner Dip Method.

The overall observation shows that the unconstrained method does not show clear image for faults delineation especially on the deeper targets. The unconstrained method is suitable for shallow non-complex geological area. The benefit of the unconstrained method is the duration taken to run the process is much shorter as compared to the ESP dip method.

Comparisons conducted on both ESP 3D method shows that the planner dip method shows better maps and visible faults delineation attributes as compared to unconstrained method. The ESP planner method adopted eight traces scan method, which scan the eight adjacent traces trough a specified window to get the result. Whereas the unconstrained method only scan two adjacent traces and could not provide better similarity comparison than the planner dip method. Both ESP Planner dip method and unconstrained method do not show good fault delineation for data below 1900 ms. There are probably two reasons

behind this observed case. Firstly the X field Unit is located along a anticline geological features with a flank observed approximately from 1900 ms. Therefore the data observed below the anticline are not smooth and added with massive faults occurs at the X field. Secondly, the seismic data below the anticline layer shows energy loses probably due to the SMECoal layer above the E34 horizon.

The ESP slant/dip method was selected for faults analysis in this project. The four (4) existing faults on the database namely F1, F2, F3 and F4 are used to determine on the reliability of ESP planner dip method to identify faults.

As shown in Figure 4.16, the circled area shows event dissimilarity and able to identify the four existing faults. The faults are also checked on seismic sections (Figure 4.14) to understand the fault extent. The faults observed on time slice 2800 ms on Figure 4.16 are compared on time slice 1000 ms (Figure 4.11), 1200 ms (Figure 4.12), 1400 ms (Figure 4.13), 1600 ms (Figure 4.14) and 1800 ms (Figure 4.15 & 4.16). The similar observation is done between line 1900 to 2150 and trace 2350 to 2850 ms (Black Circle area), line 1850 -2053 and trace 3355 - 3455 (Red Circle area)(Figure 4.17).

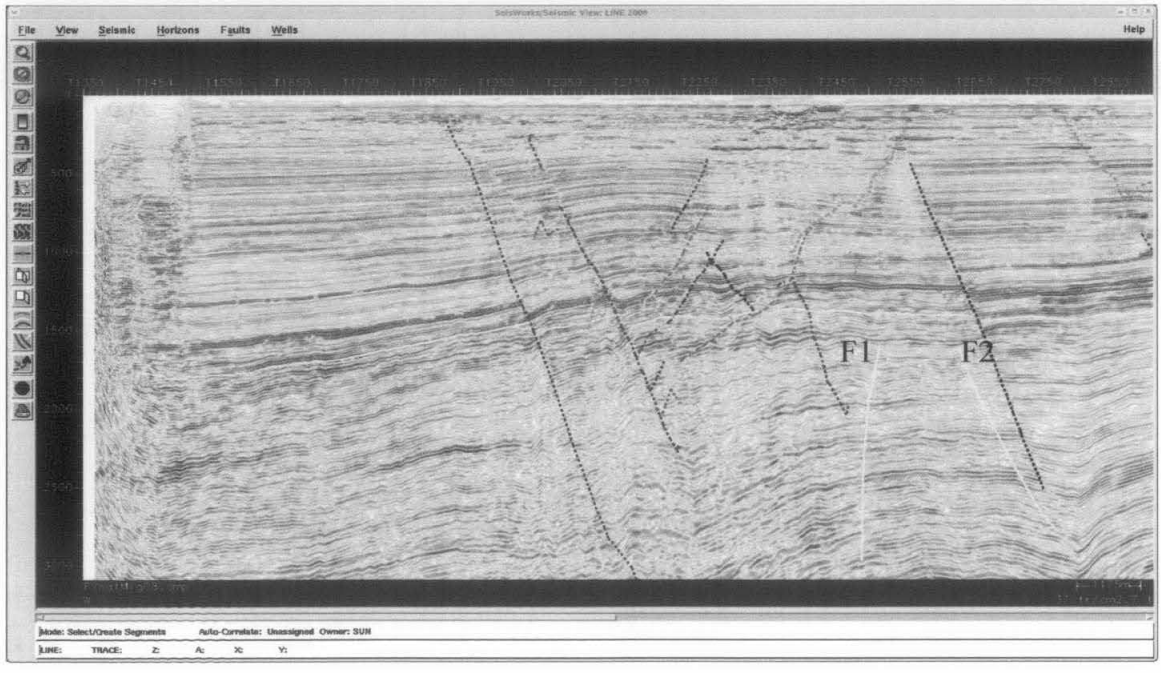

Figure 4.18: Fault observed on ESP attribute map around the Black circle were delineated on line 2000

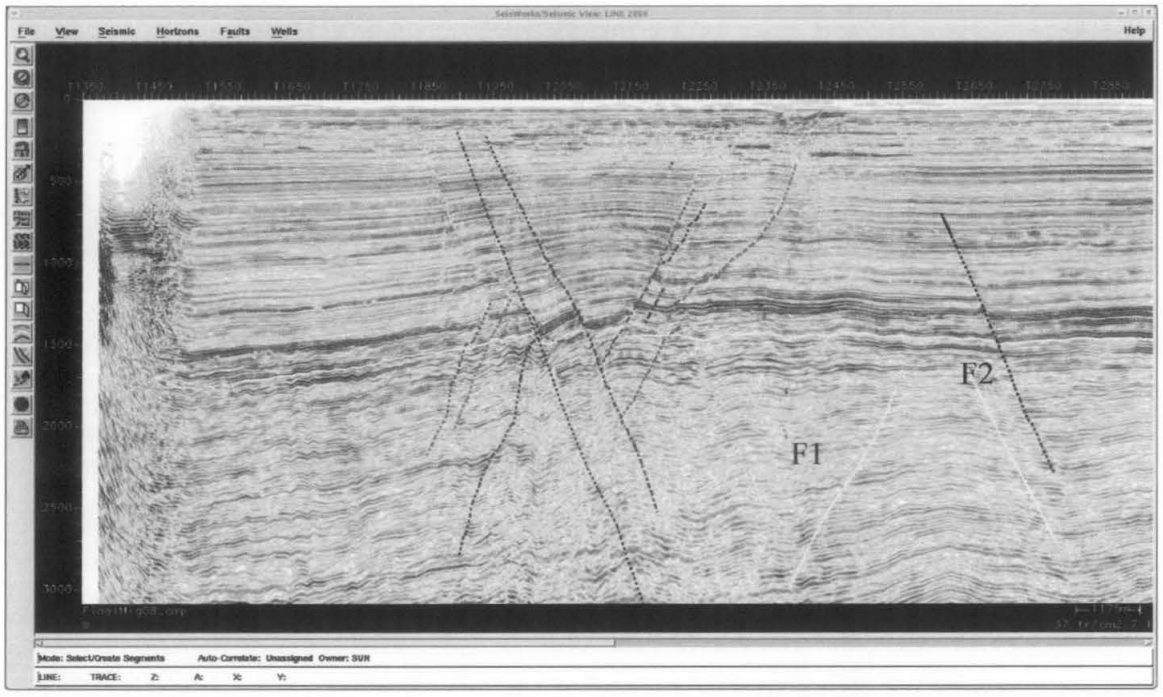

Figure 4.19: Fault observed on ESP attribute map around the Black circle were delineated on line 2150

Figure 4.18 and 4.19 shows that the fault delineation in the area of dissimilarity observed around the black circle area is been interpreted on both lines 2000 and 2150. The similar event termination is also observed on trace 2570 (Figure 4.17). The dissimilarity effect on ESP as mentioned earlier are not very transparent for time slice below 2200 ms. Therefore the interpretation of the faults below timeline 2200ms are more based on event termination on seismic rather than the attributes map.

Faults F3 and F4 were both determined on attribute map Figure 4.16 were also visible on lines 1850 to 2053 (Figure 4.20). Figure 4.20 shows the fault delineation observed on line 1850.

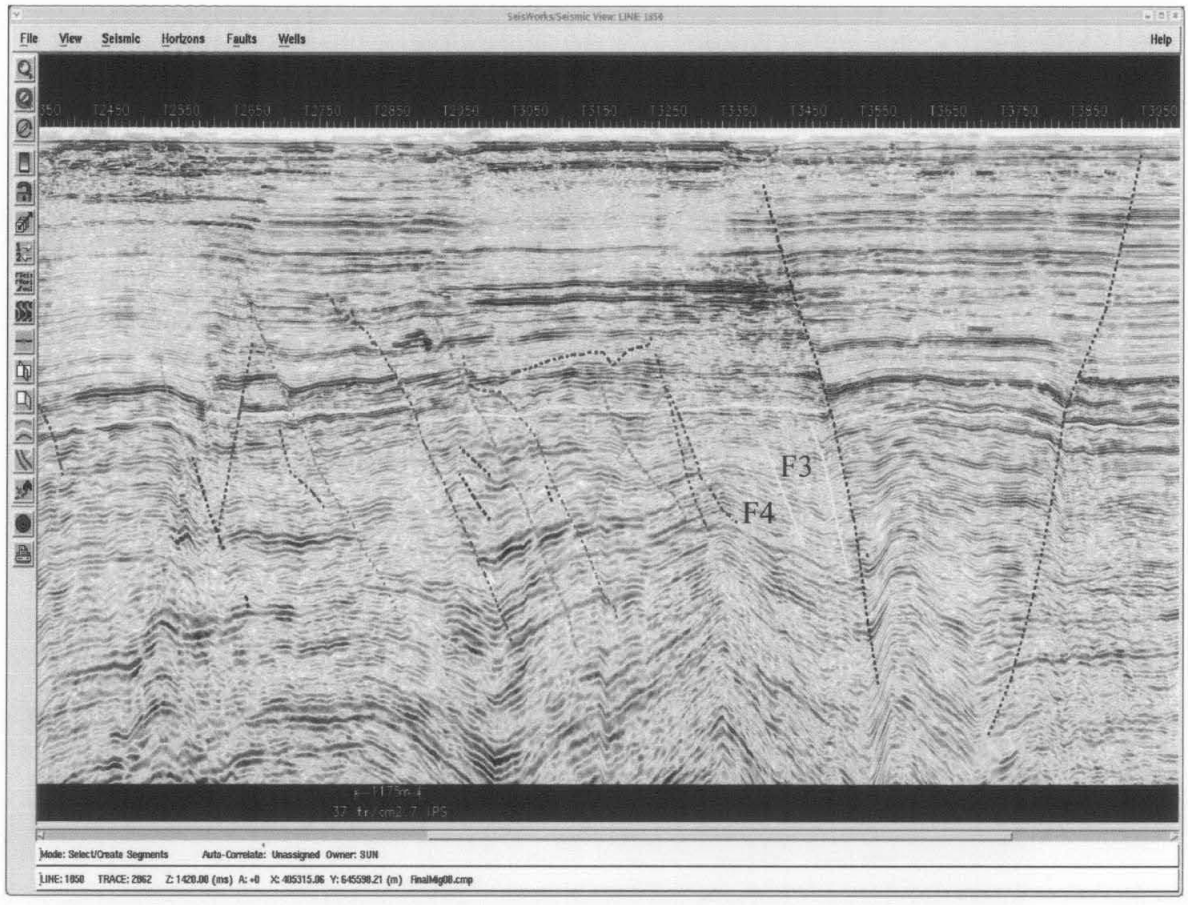

Figure 4.20: Fault observed on ESP attribute map around the Red circle were delineated on line 1850

The F1, F2, F3 and F4 faults are visible on both seismic and attributes map. In conclusion, the Planner dip method gives results that are more reliable. Therefore, this method was adopted to study the fault distribution.

4.4 New faults identification

4.4.1 ESP Planner/Dip on new faults identification

The next step on the fault analysis is to observe features that probably can be interpreted as faults. Fourteen (14) features are identified on the ESP attribute maps. These features are crosschecked with seismic and classified as probably faults or channel related.

Details of these discontinuity features will be discussed further on the following paragraph with associate figures. Figure 4.21 and Figure 4.23 shows the newly interpreted features on ESP time slices at 1200 ms. These features are crosschecked on vertical seismic sections. The features are detached at the point where ESP shows geological non-similarity between the traces on the specified window. Total faults in the database and the identified features are shown in Figure 4.22 and Figure 4.24 on time slice 1600ms.

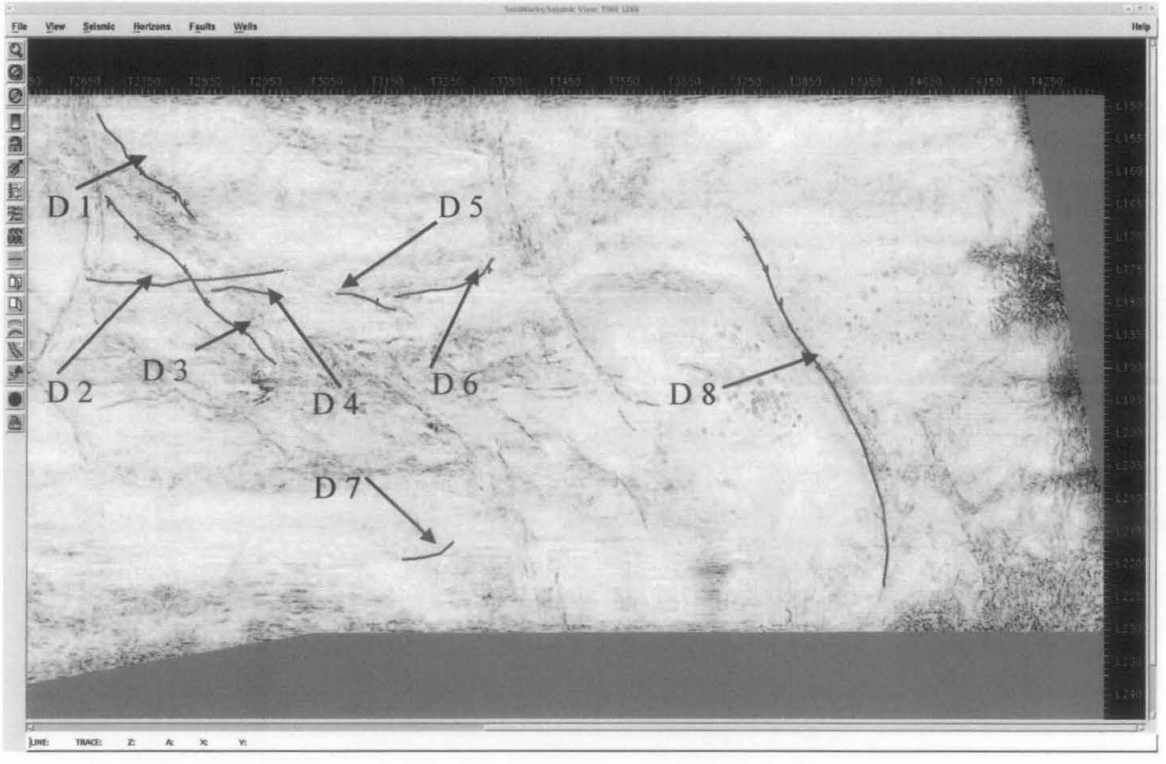

Figure 4.21: Discontinuity events (D1 to D8) identified on time slice 1200ms at Eastern and Unit zones

Figure 4.22: Total faults (together with probable faults) identified on time slice 1600ms at Eastern and Unit zones

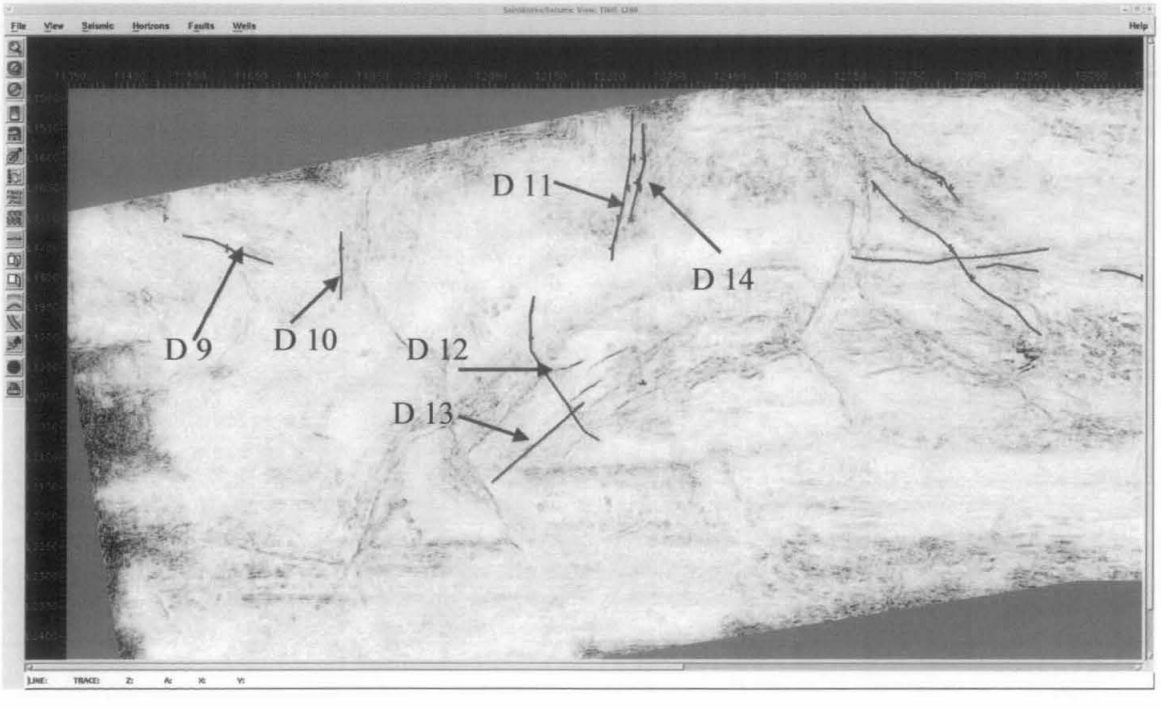

Figure 4.23: Discontinuity events (D9 to D14) identified on time slice 1200ms at Western and Unit zones

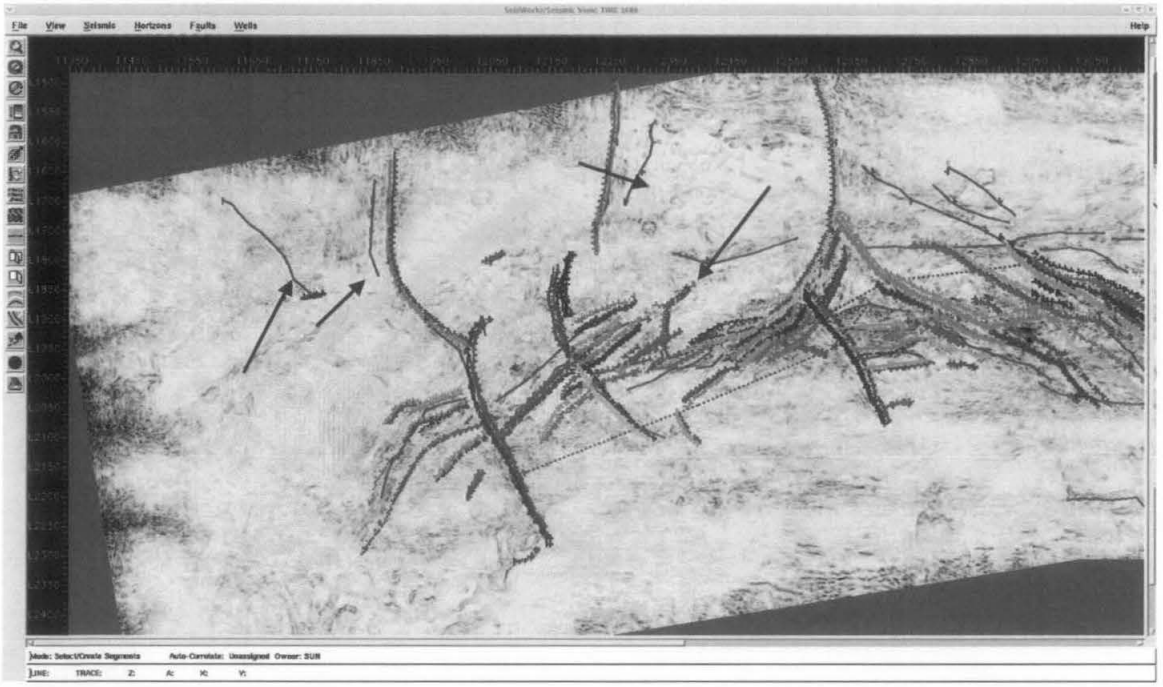

Figure 4.24: Total faults (together with discontinuity events) identified on time slice 1600ms at Western and Unit zones

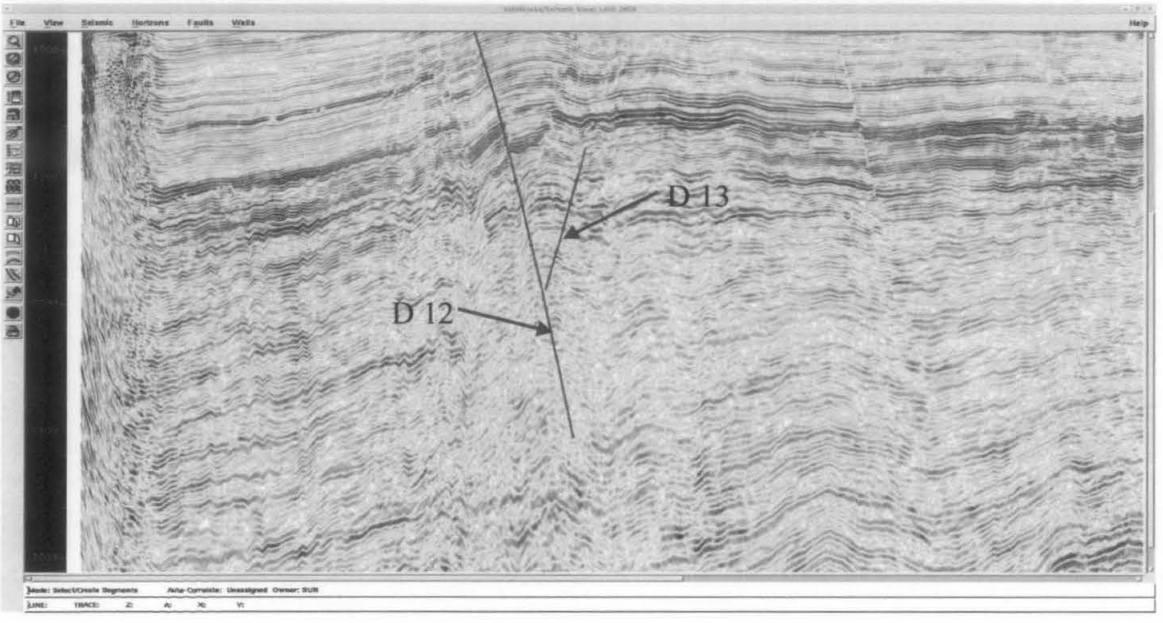

Figure 4.25: Two discontinuity events that can be classified as probable faults identified on line 2050

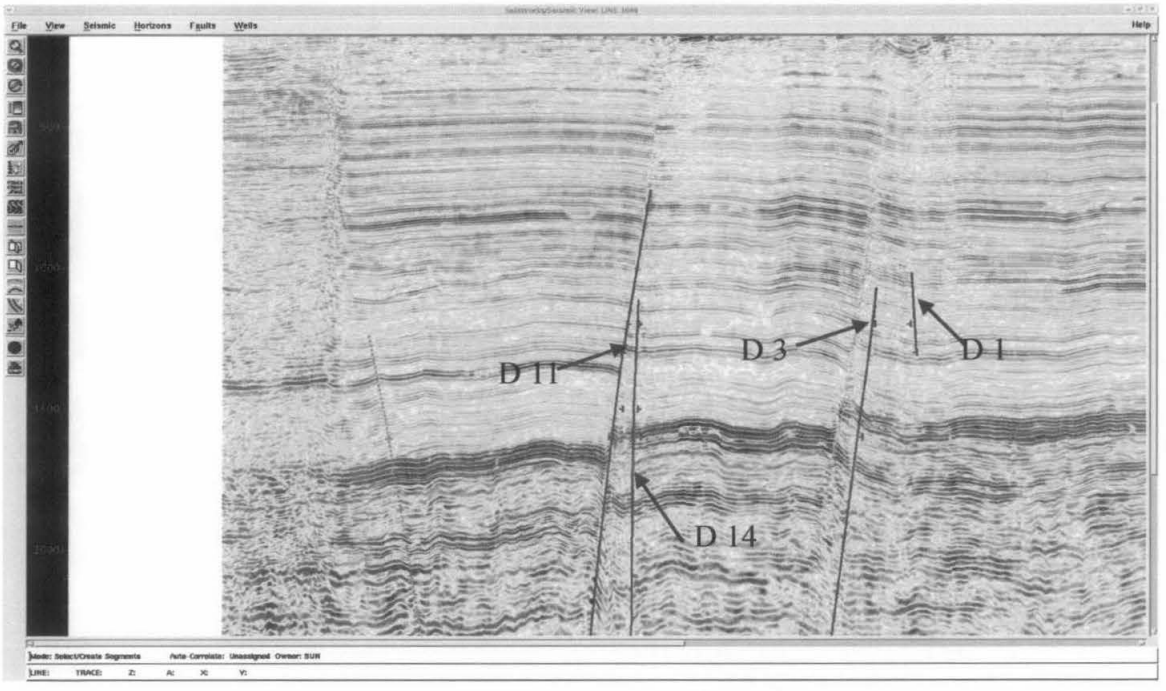

Figure 4.26: Four discontinuity events that can be identified as probable faults on line 1640

The features studied on ESP attribute slices are studied on seismic lines and traces as shown on Figure 4.25 and Figure 4.26. Some events are observed on seismic lines but are still not very promising. The displacements of reflectors are not very transparent. Few features that noticed on seismic are D1, D3, D8, D12, D13 and D14. The features observed on ESP are studied on other attribute such as curvature to confirm their existence and classify their identity either as faults or as other geological events.

4.4.2 Curvature attribute on new faults identification

4.4.2.1 Methodology

Curvature measures of how bent a surface at a particular point along any horizon or surface. The more bent a surface is, the larger its curvature. Curvature analysis refers to the study of subsurface strata deformed under stress, to predict the presence of fault and fracture lineaments, which are formed because of the deformation. The X field main

geological feature is the heavily faulted anticline formed to tectonic compression. The other features seen on curvature display are channel and reefs.

Mathematically, for a curve, curvature is defined as the reciprocal of the radius of a circle that is tangent to the given curve at a particular point (Figure 4.27). This implies that curvature will be large for a curve that is bent more and will be zero for a straight line, whether horizontal or dipping. Definition of curvature in a two-dimensional curve can be described as anticline surfaces are assigned a positive sign for curvature and a negative sign for synclinal surfaces.

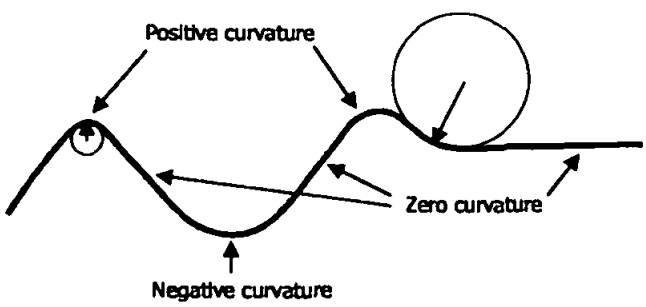

Figure 4.27: Positive curvature on syncline features and negative curvature shown on anticline features.

The 2D concept explained above is extended to define the 3D curvature concept .Cutting any surface with a plane will make a curve which enable us to calculate the curvature. If we cut this surface with an orthogonal plane, we obtain what is known as normal curvature. From any two sets of orthogonal normal curvature values, we can calculate other curvature attributes such as mean curvature.

In this project, the Post Stack software calculates the mean curvature. The curvature computation is based on a simplified formula that employs second derivatives to differ the curves on both X and Y directions. The derivative results are weighted averagely to conduct curvature computation. Attribute computation considering the weighted average attributes tend to be cleaner and easier to interpret, though they have less resolution, depending on the length of the averaging window.

The curvature attribute is extracted on a window basis below the E34 interpreted horizon. The window of 500 ms above and 500 ms below the E34 horizon is used. Landmark

software provides a built-in color bar that varies between +128 to 0 to -128. This range shows a combination between minimum and maximum curvature value. In this report, the two positive and negative curvatures are displayed separately to show the changes. The good color map with an appropriate range of values can enhance discontinuities, even if they are subtle. The color ramp and the color spectrum must be selected carefully because too many base colors may make us lose some definition. Therefore, the positive curvature with a range between 0 to +128 is ramped from dark to light on black color tone. Whereas, the negative curvature from 0 to -128 is ramped on red color tone.

4.4.2.2 Map Analysis

The displayed maps are on time slices from the horizon-based extraction. These comparisons were done in such a way to compare the ESP maps with Curvature results because the features identified on ESP Planner method are displayed on time slices. Eastern, Western and Unit areas are displayed on the positive curvature (Figures 4.28, 4.29, 4.30 and 4.31), negative curvature (Figures 4.32, 4.33, 4.34 and 4.35) and combination of both positive and negative curvature together (Figure 4.36, 4.37, 4.38 and 4.39).

The most positive and most negative curvature defines the lateral change on the waveform as shown on Figure 4.27. These changes are most probably due to differential on compaction, which may also be interpreted as potential deposition of the levees, the most-positive curvature defines the flanks of the channels and potential levees and overbank deposits. On the scale bar, 32 to 84 represent the probable channel related whereas 85 to 126 represent probable faults. The most negative curvature, highlight the channel axis. Similarly, the scale bar between -32 to -84 represent the probable channel related whereas -85 to -126 represent probable faults. Detail interpretation of the fault delineation will be done on section 4.5 Summary: Results of Fault Delineation.

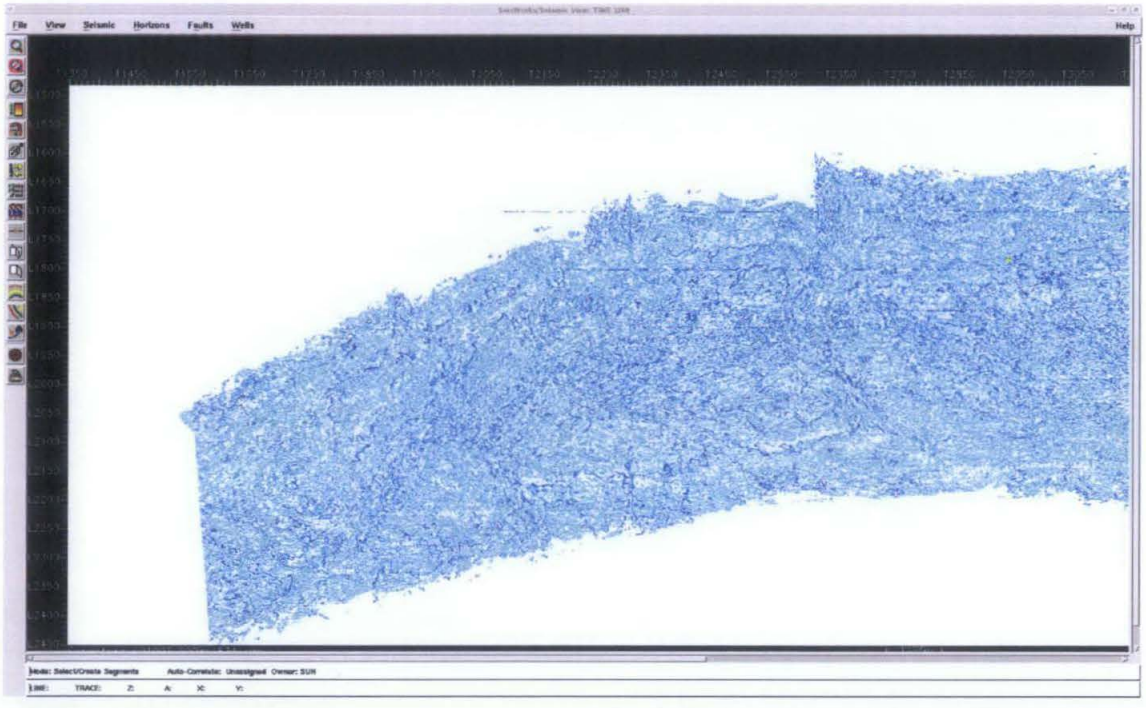

Figure 4.28: The positive Curvature display on time 1200ms without faults display at Eastern and Unit zones

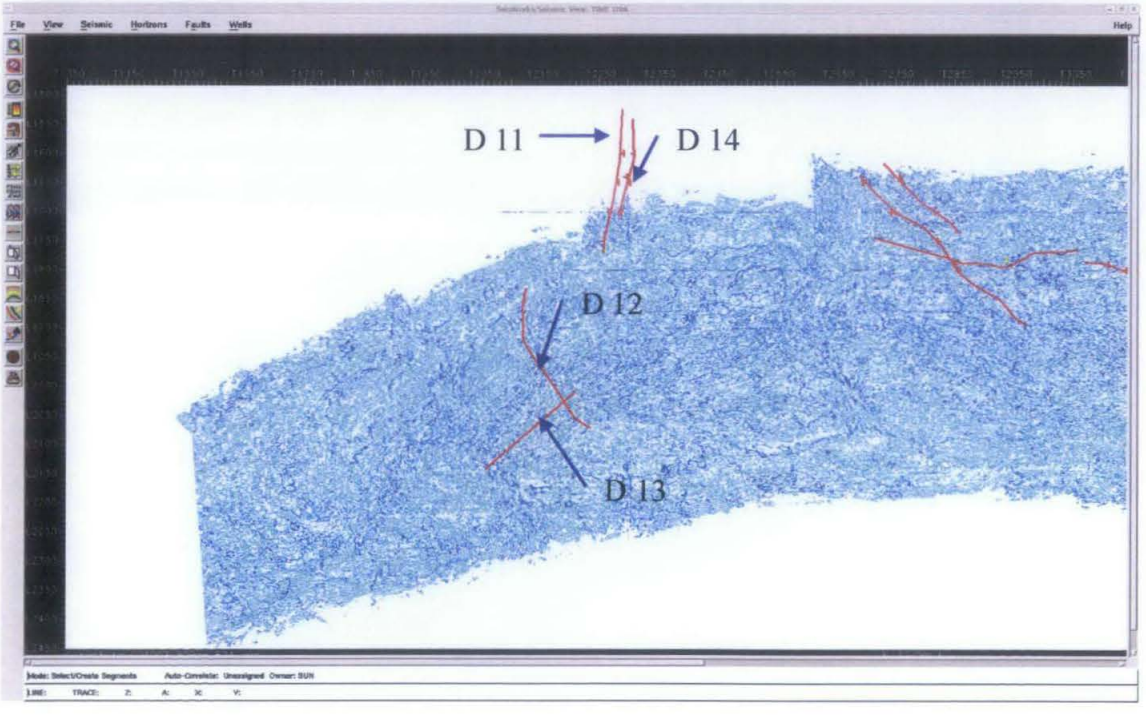

Figure 4.29: The positive Curvature display on time 1200ms without discontinuity events display at Eastern and Unit zones

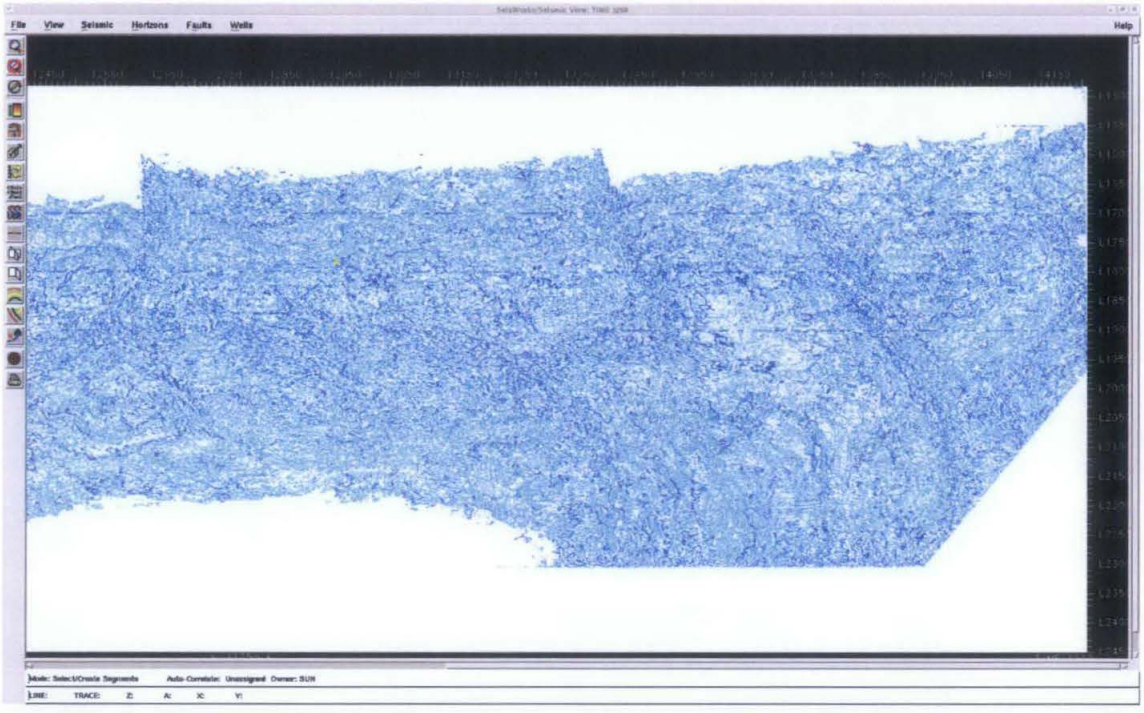

Figure 4.30: The positive Curvature display on time 1200ms without faults display at Western and Unit zones

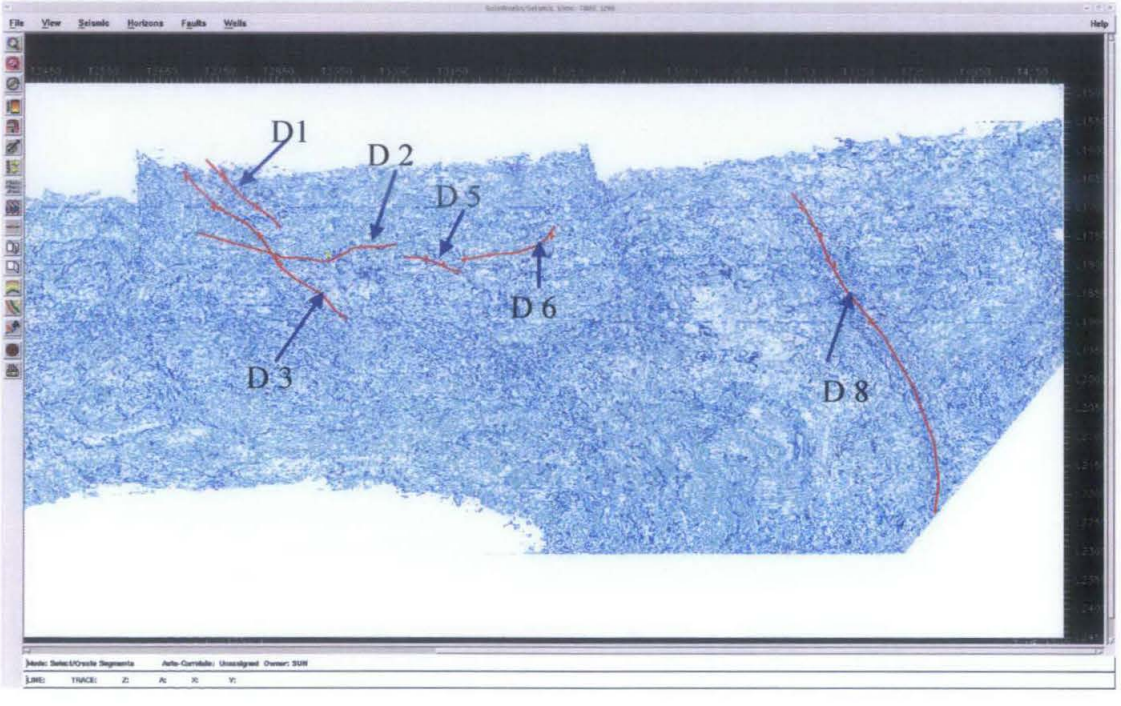

Figure 4.31: The positive Curvature display on time 1200ms without faults display at Western and Unit zones

Figure 4.32: The Negative Curvature display on time 1200ms without faults display at Western and Unit zones

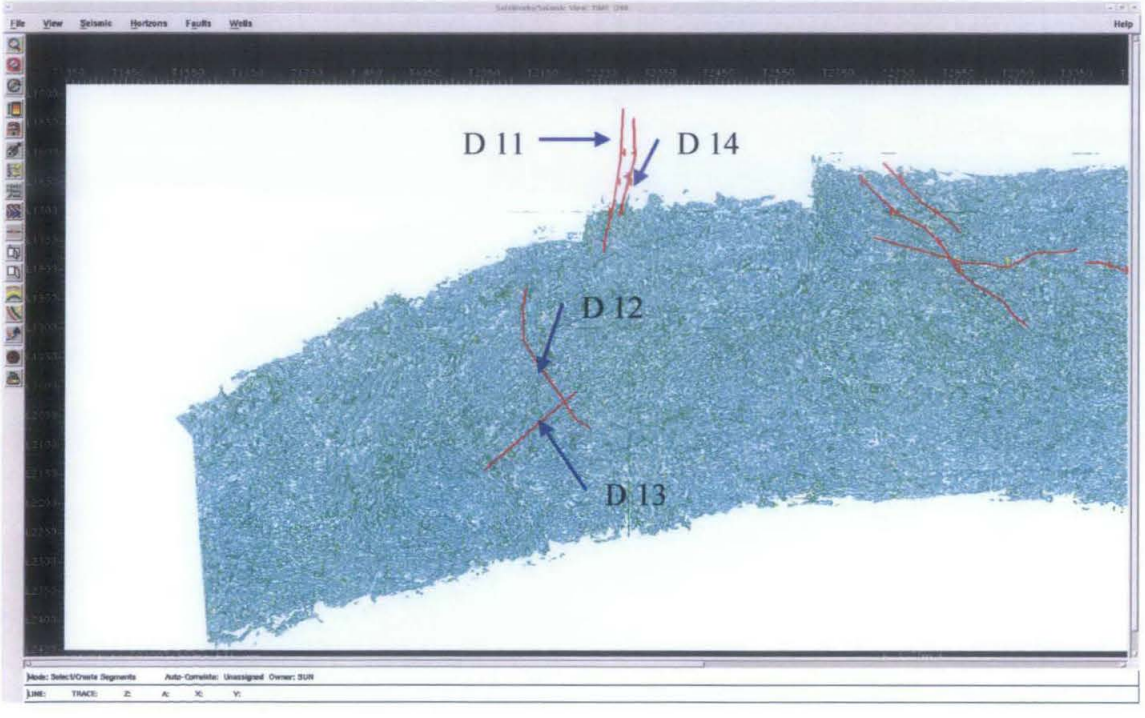

Figure 4.33: The Negative Curvature display on time 1200ms without faults display at Western and Unit zones

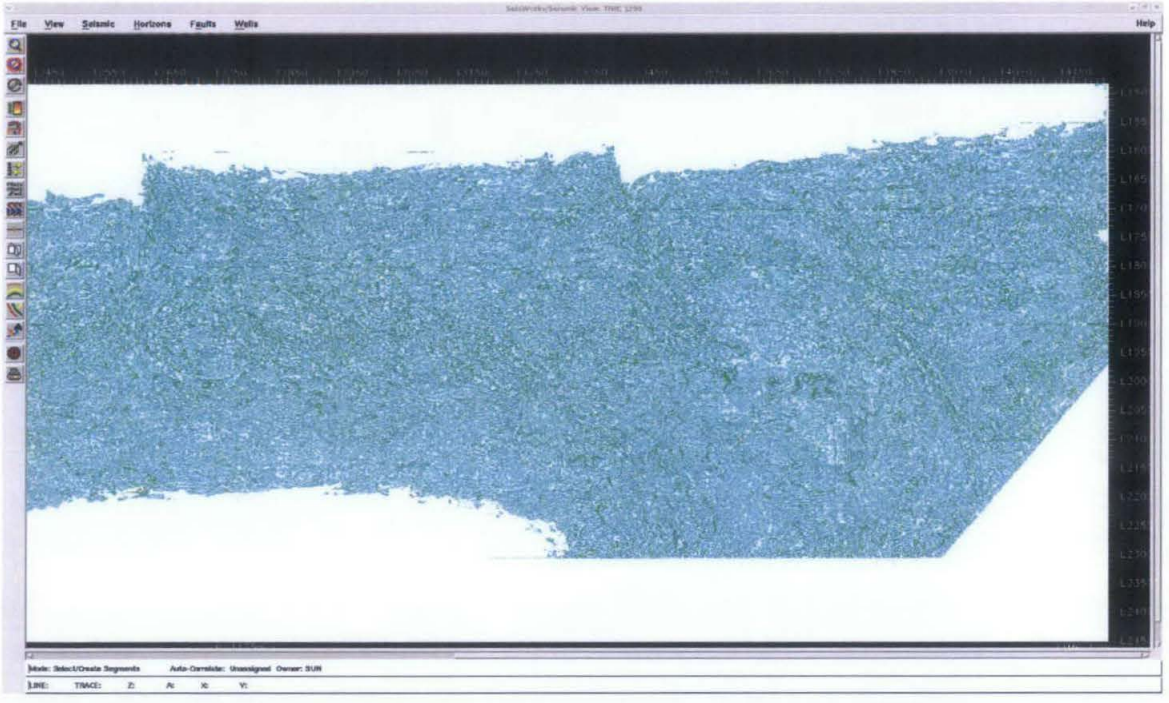

Figure 4.34: The Negative Curvature display on time 1200ms without faults display at Eastern and Unit zones

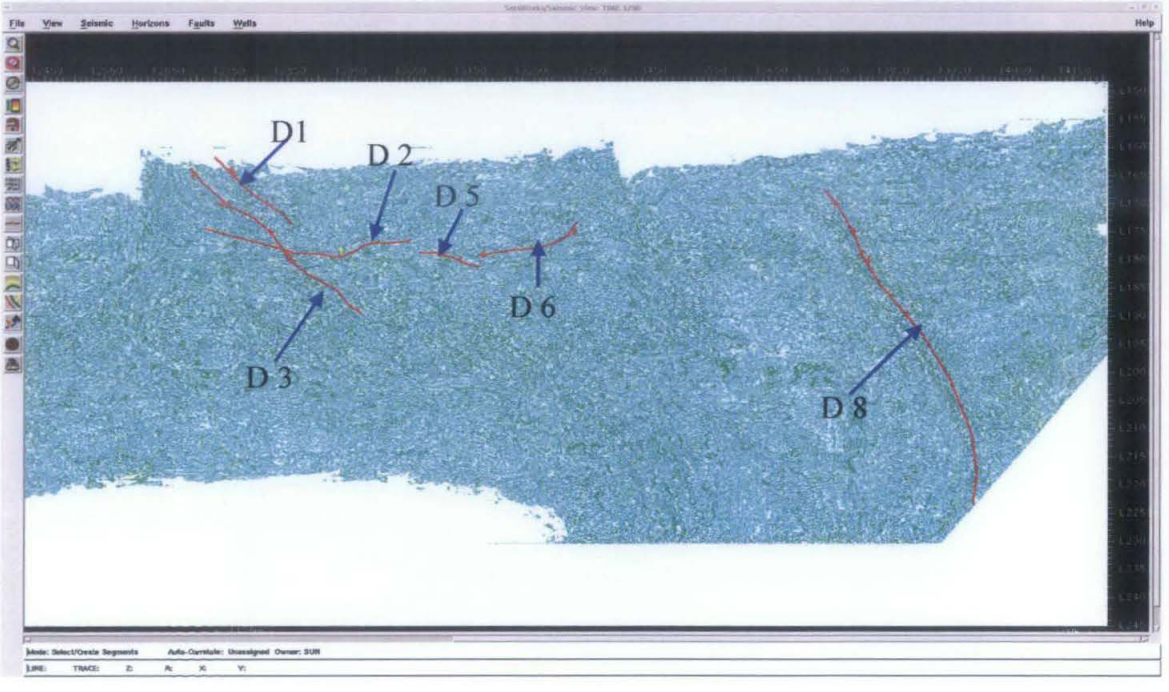

Figure 4.35: The Negative Curvature display on time 1200ms without faults display at Eastern and Unit zones

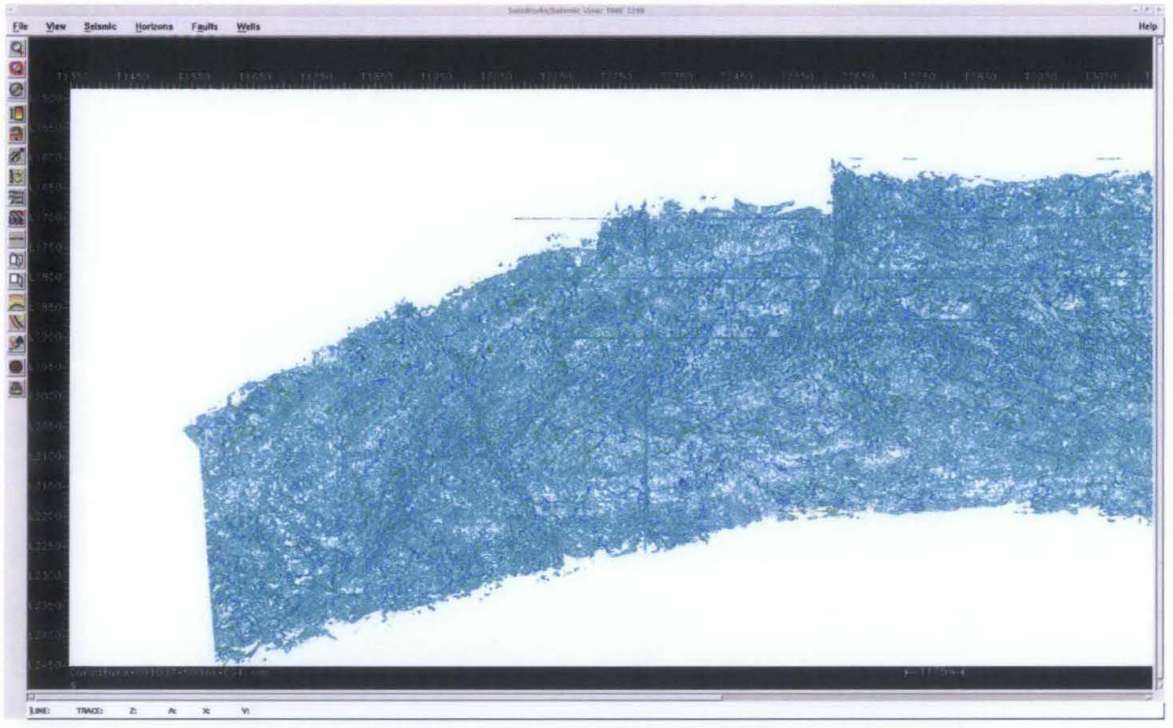

Figure 4.36: Combination of both Positive and Negative Curvature display on time 1600 ms without faults display at Western and Unit zones

Figure 4.37: Combination of both Positive and Negative Curvature display on time 1600 ms with total X field faults display at Western and Unit zones

Figure 4.38: Combination of both Positive and Negative Curvature display on time 1600 ms without faults display at Eastern and Unit zones

Figure 4.39: Combination of both Positive and Negative Curvature display on time 1600 ms with total X field faults display at Eastern and Unit zones

4.5 Summary: Results of Fault Delineation

There are 220 number of faults from previous interpretation exist in the database. The presences of these faults are crosschecked on ESP planner Dip attribute analysis. An additional fourteen (14) features are identified on the ESP Planner Dip attribute maps and seismic sections (D1 to D14).

The features, D1, D3, D8, D11, D12, D13 and D14 are seen on both ESP and Curvature attribute maps as shown in Figure 4.21, Figure 4.23, Figure 4.31 and Figure 4.33. These events reflectors termination are moderately recognizable on seismic sections. Therefore, these events can be classified as possible faults.

The features, D2, D4, D5 and D6 are noted both on ESP and Curvature attribute maps. These events are not recognizable on seismic section. These features are interpreted as channel related features. The locations of these features are at the edge of the anticline, which are seen clearly on structure map on Figure 3.7. Furthermore, the most-positive curvature on Figure 4.30 and Figure 4.31 shows high positive curvature readings at this location. The high readings on most-positive curvature define the flanks of the channels.

The D7, D9 and D10 features are seen on ESP (Figure 4.23). These events are not clear on seismic as shown on Figure 4.25 and not seen on Curvature maps. These events can probably be classified as artifacts cause by acquisition footprints.

Therefore, total faults identified and exist in the database are 227 (220 on the database and 7 newly found). These faults are overlaid on seismic to re-define the interpreted E34 horizon. These faults are auto tracked using the FZAP software.

CHAPTER FIVE: HYDROCARBON EXTEND ON SEISMIC ATTRIBUTES

5.1 Methodology

The hydrocarbon extent was studied referring to potential sand distribution that contain hydrocarbon below the E34 horizon generally and E34E36 reservoirs particularly.

The fluid type (gas, oil and water) and the fluid levels (oil up to, oil down to, gas up to and gas down to) were identified on most of the exploration wells in X Field blocks, which comprise X Unit area (platform A, B and C), Western X (platform D) and Eastern X field (Figure 1.1). This report will focus more on the Unit area because most of the vertical and deviated wells are located within this vicinity. Furthermore, the ADD oil company is currently active on Unit area whereas both Eastern and Western areas are still under study. However, in this report, the amplitude extractions were conducted for the larger area, which includes Unit, Eastern, Western, and the outside areas. The amplitudes extraction is expected to give similar range for hydrocarbon sand if we assume that no drastic amplitude variation are presence within the E34 reservoir throughout the studied areas.

Primarily, occurrence of hydrocarbon sand and it's level were studied on attribute maps extracted below horizon E34 and later crosschecked with logs (well markers) available in the database particularly from vertical exploration wells. There were 135 wells with logs in the database. The results of the hydrocarbon depth from the well markers were used to determine the hydrocarbon window.

The extracted attributes below E34 horizon were adjusted accordingly within the window to observe changes on the amplitude characteristic of each displayed attributes. The window determination is crucial on this study because the X field comprise of few-stacked reservoirs on top and bottom of the E34 horizon. Any mis-define of the window may lead to wrong interpretation of the hydrocarbon below the E34 horizon. For

instance, the E32 and E40 reservoirs located above and below the E34 reservoir respectfully are been identified to contain hydrocarbon sand.

X field contains continuous stacked reservoirs below the anticline trap with thickness of approximately 400 metres. On this project, the focus will be on the E34 reservoir, which mainly contains oil with intermediate gas zones as per well information. The well studies show that E34 reservoir in X field has a common hydrocarbon contact with E36 reservoir on several wells. The distance between these two reservoirs varies from 10 to 20 metres that can be considered as thin. Therefore, in this project, studies were carried out considering E34 and E36 as a combine reservoirs. The attribute extraction will be considering E34 as top and the level where the hydrocarbon down to is identified as bottom. On most of the cases, the oil down to for E34 horizon was located below the E36 horizon. These observations were clearly identified on well markers.

Both E34 and E36 reservoirs are characterized by massive bodies of sand. The attribute extraction shows that the distribution of sand bodies ties well with the structure map extracted along E34 horizon. This report will define the hydrocarbon sand distribution on window basis below E34 horizon. Users may able to determine expected possible hydrocarbon distribution at particular depth (ms) within the E34 reservoir by referring to the interested target window. The details will be discussed on following sections.

5.2 Horizon Interpretation and Window Determination

5.2.1 Horizon Determination

The most crucial part of the attribute extraction is to make sure the E34 horizon interpretation was conducted as correct as possible. In this project, the horizon interpretation was conducted in final migrated seismic data.

The first step taken was to analyze the waveform characteristic of the horizon on the acquired seismic data. The water bottom was check to be peak amplitude (SEG reverse convention) (Figure 5.0). As mention on the well correlation chapter earlier, the well markers are tied with the seismic data to confirm the correlation. The synthetic for each wells are created from modal based Ricker wavelet. The model based created synthetic ties with the seismic on reverse polarity synthetics and applied time shift between 8 ms to -15 ms for all the exploration wells. The synthetic was time shifted to get a best tie at the E34 horizon and associate well markers. The E34 horizon was picked at the trough and adjusted to tie with the reverse polarity synthetic trace.

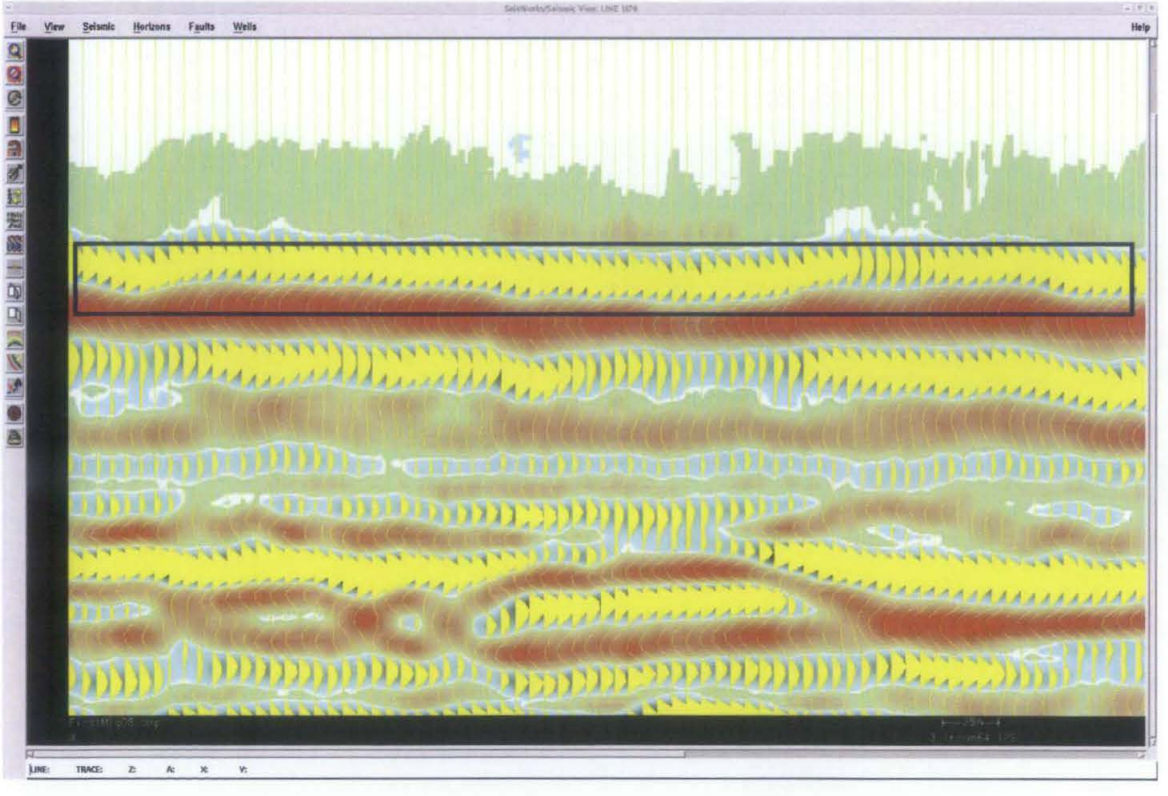

Figure 5.0: Water bottom showing a positive (peak) wiggle trace on Trace 2750. The positive wiggle is filled on yellow color. The blue box above shows the water bottom reflection.

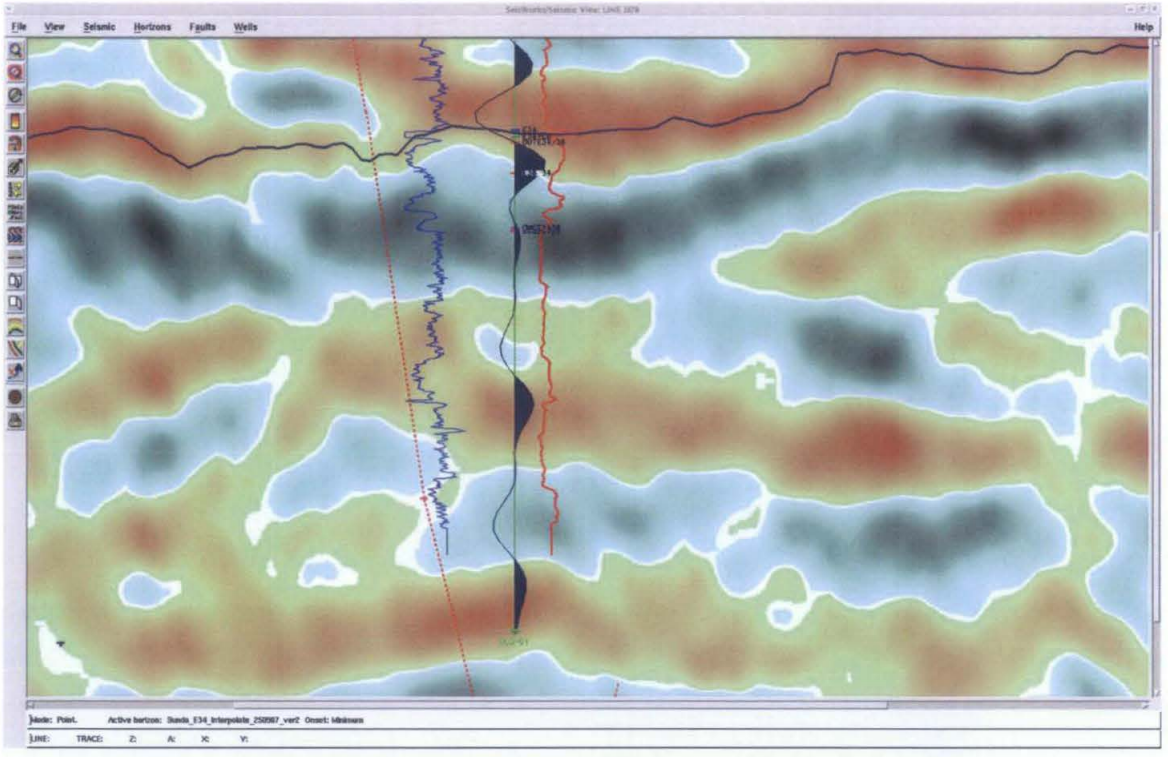

Figure 5.1: Synthetic (dark blue), Gamma Ray (red) and Resistivity (light blue) curves overlaid on seismic line 1870 at well D 01 location

The synthetic seems to tie well with horizons on the shallow part of the seismic and does not fit very well with the deeper reflectors especially below the SMECoal layers. The well synthetic seismic tie were done for all the vertical wells and crosschecked with other nearest deviated wells where the synthetics are available in the database. The interpreted horizon was interpolated and one time ZAP (autocorrelation) conducted using Landmark Seiswork software.

Figure 5.1 show that the synthetic overlaid on seismic to check the tie in for E34 horizon and the hydrocarbon extents on the markers. The hydrocarbon zone is generally noticed on peak amplitude on high variable area section as above. In order to double check the markers, other well logs curves such as Gamma Ray and Resistivity were overlaid on seismic.

The E34 horizon, which is believed to be associated with coal, shows a spike reading on both Gamma ray and resistivity logs. Similar responses are also noticed in Formation density and Neutron porosity logs as shown in Figure 5.2 & 5.3. The impedance curve shows an increase whereas the reflection coefficient shows a spike reading of 0.3 at E34 horizon marker. Therefore, the E34, E36 and SMECoal layers are easily interpreted on well logs. The markers can be calibrated accordingly to meet the requirement if any mis-tie encountered between the well markers and seismic data.

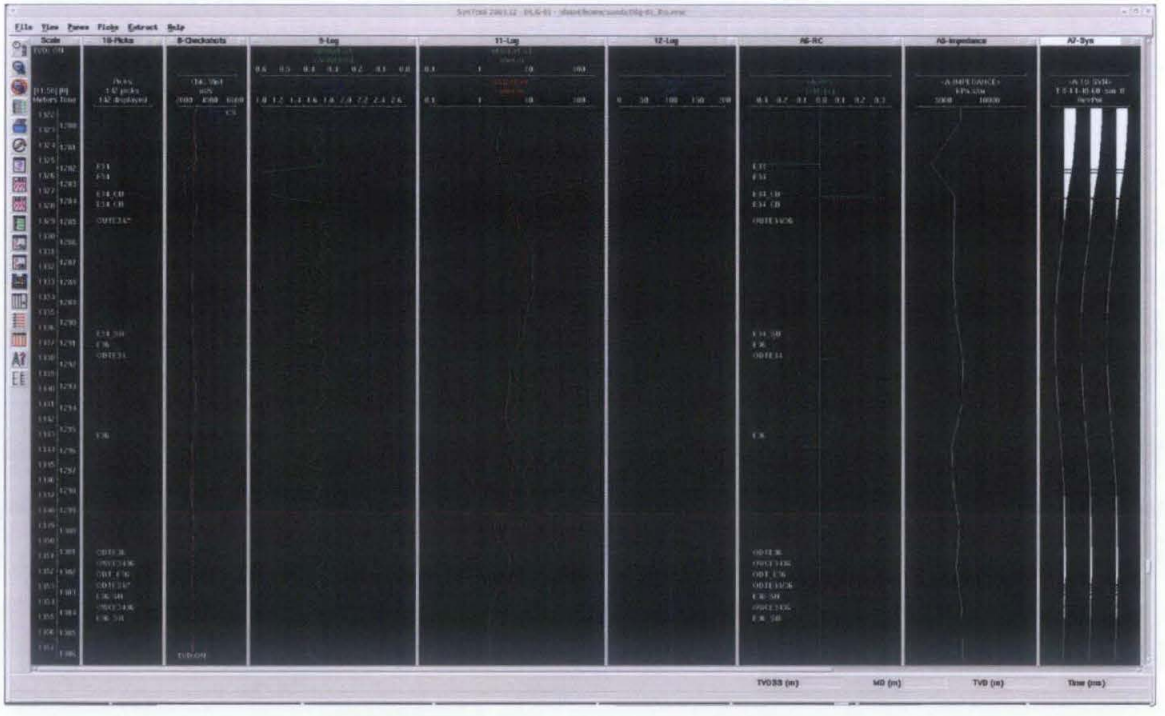

Figure 5.2: D-01 Neutron-Porosity, Formation Density, Reverse Polarity Synthetic, Resistivity (ILD, MFSL), Gamma Ray, Reflection Coefficient and Impedance curves.

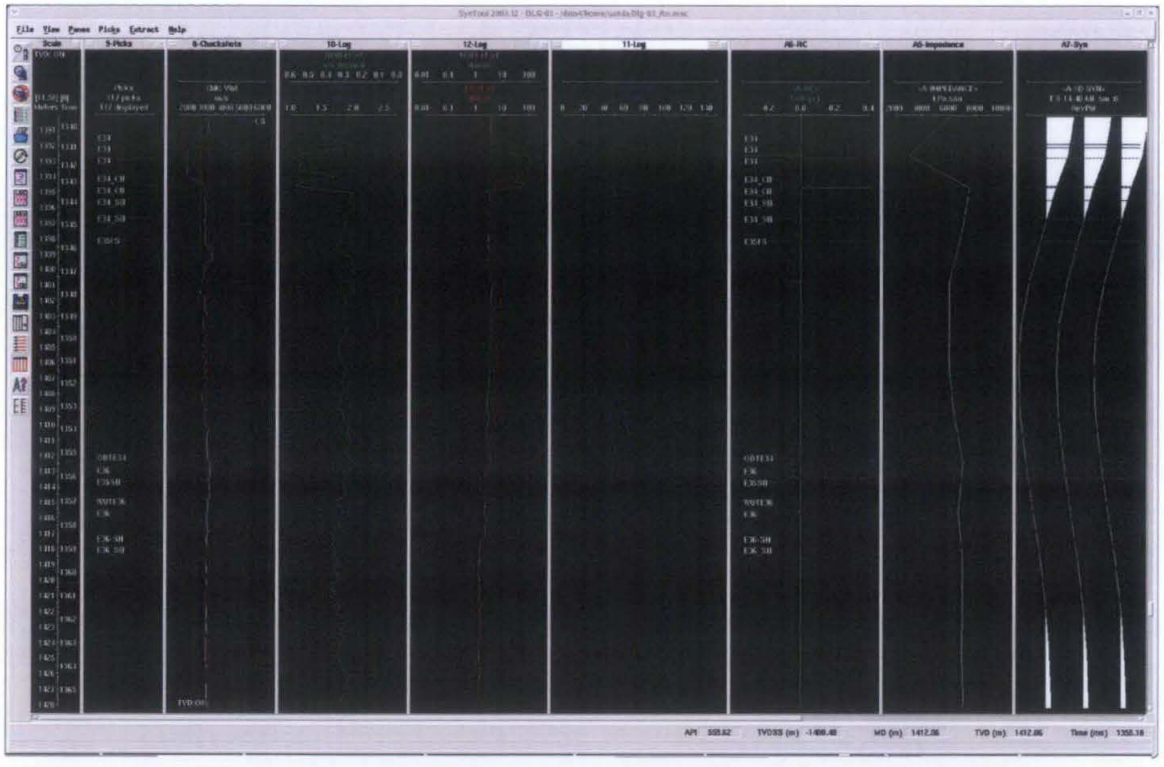

Figure 5.3: D-03 Neutron-Porosity, Formation Density, Reverse Polarity Synthetic, Resistivity (ILD, MFSL), Gamma Ray, Reflection Coefficient and Impedance curves.

5.2.2 Window Determination

The Hydrocarbon sand associated windows were determined once the E34, E36 and SMEcoal layers are determined from well markers and crosschecked with available well logs.

The next step taken was to understand the hydrocarbon window and depth (m and ms) which is noted on exploration wells and other nearby wells (deviated wells). The hydrocarbon indicated markers were notice on five vertical Exploration wells namely D-02, D-01, D-07, D-03 and D-08. Other deviated well D-A03 is also taken into consideration considering the gas sand observed on this well.

Two methods were used to determine the hydrocarbon extent. The synthetic and well markers were laid on seismic sections (Wiggle trace variable area sections) to check were the hydrocarbon and are expected. The hydrocarbon zone is generally noticed on peak amplitude on high variable area plot as shown in Figure 5.1. The second method is by referring the well markers and the depth/time of hydrocarbon sand on Landmark Syntool software. The second method will be discussed later on this chapter.

Observation was done by overlaying the hydrocarbon indicated wells synthetic with the seismic section to notice the correlation. The wiggle density trace seismic data shows that the hydrocarbon extents match with the well markers as shown in Figure 5.4 and 5.5. The combination of results from well correlation and seismic density wiggle map shows that the hydrocarbon extents to approximately 20 ms on well D-03 and D-02. Similar observation is done on other wells that indicate hydrocarbon presence. Details on available wells with hydrocarbon presence are studied from X field Full Field Review (FFR) report.

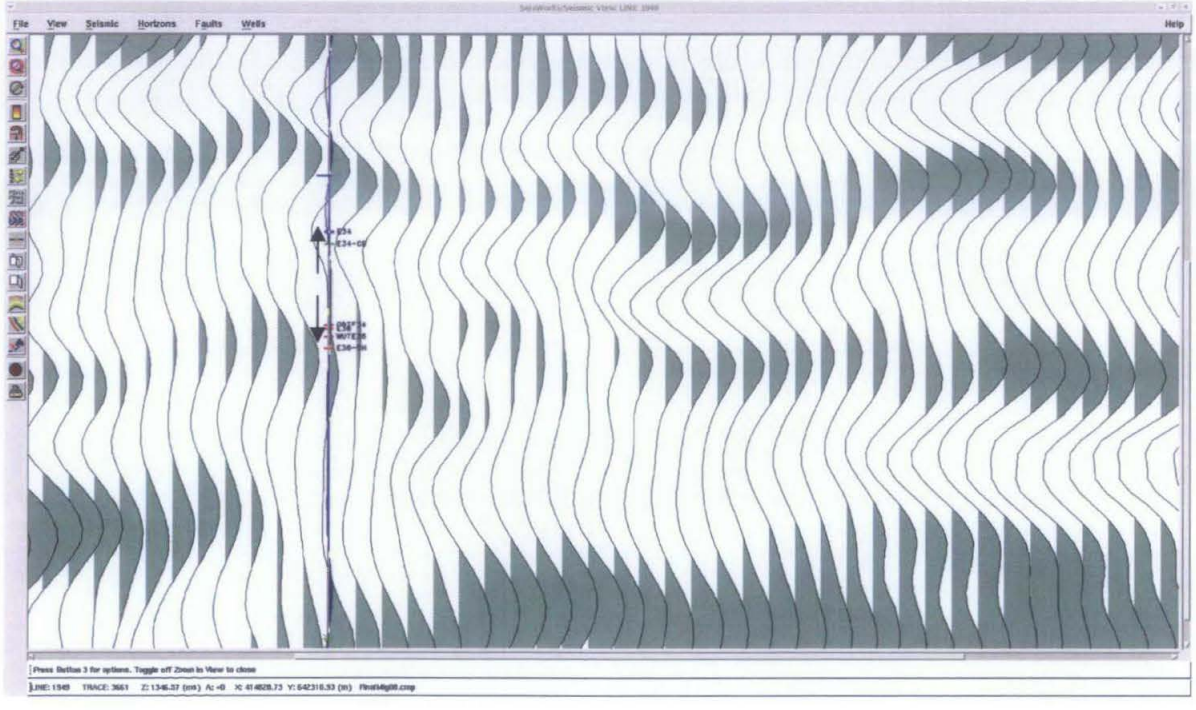

Figure 5.4: Well D-03 synthetic and well markers overlaid on variable density seismic plot of line 1887. The arrow indicate the hydrocarbon extent of 15 ms.

The similar observation is done on other vertical wells to observe the hydrocarbon extent markers. The purpose of getting the hydrocarbon extents is to extract attributes based on the right window. These window will act as a sliding limit between below E34 horizon to the extent of hydrocarbon.

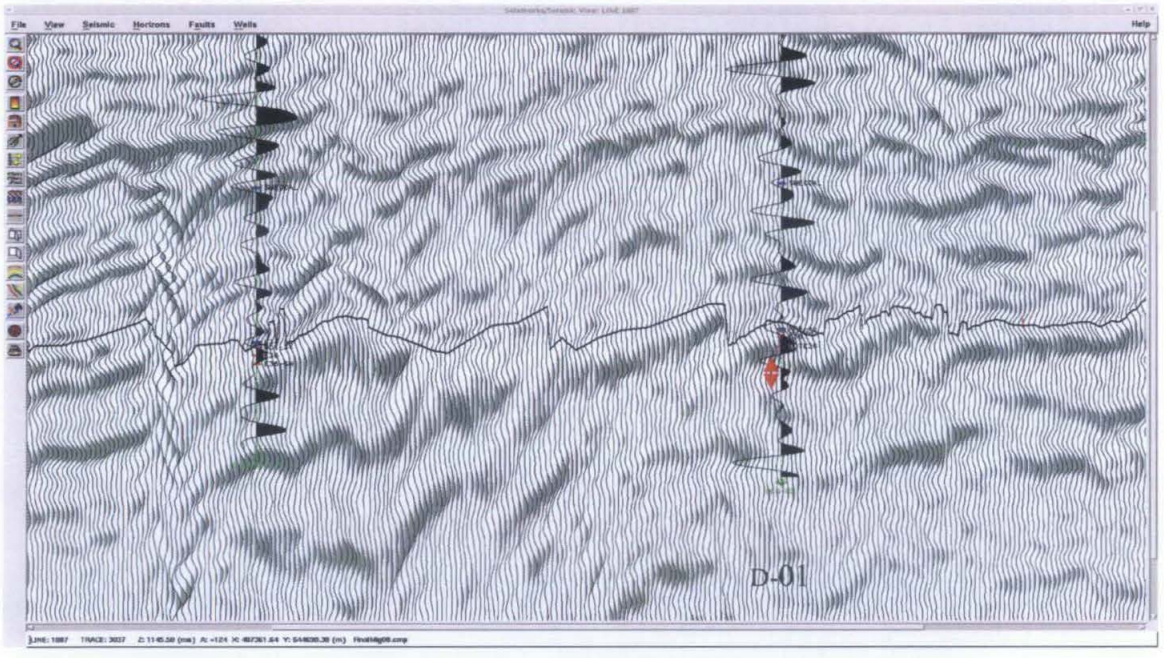

Figure 5.5: Well D-02 and D-6G-1.5 synthetic and well markers overlaid on variable density seismic plot of line 1887. The arrow indicate the hydrocarbon extent of 17 ms on D-02.

In order to double check the hydrocarbon depth, the well markers were displayed again on Syntool. The hydrocarbon intervals were checked again on the time-depth and check-shot corrected well logs. The results are displayed on Table 1. The results are compared with the Full Field Review Report (FFR) done by the ADD oil company as shown on Figure 5.6. The report was released on year 2002. Observation on the vertical wells showing hydrocarbon presences are distributed at X field unit and eastern area. Considering the distribution, all other deviated wells around the mention area were studied to notice any indication of hydrocarbon troughout the X field. Therefore, similar observations as on vertical wells are conducted on deviated wells. Referring to available information on the FFR report, five vertical Exploration wells namely D-02, D-01, D-07, D-03 and D-08 and one deviated well D-A03 is taken into consideration. These wells are

proven to show hydrocarbon trace on well logs and core cuttings. The deviated wells with hydrocarbon presence were studied and the results are shown on Table 2.

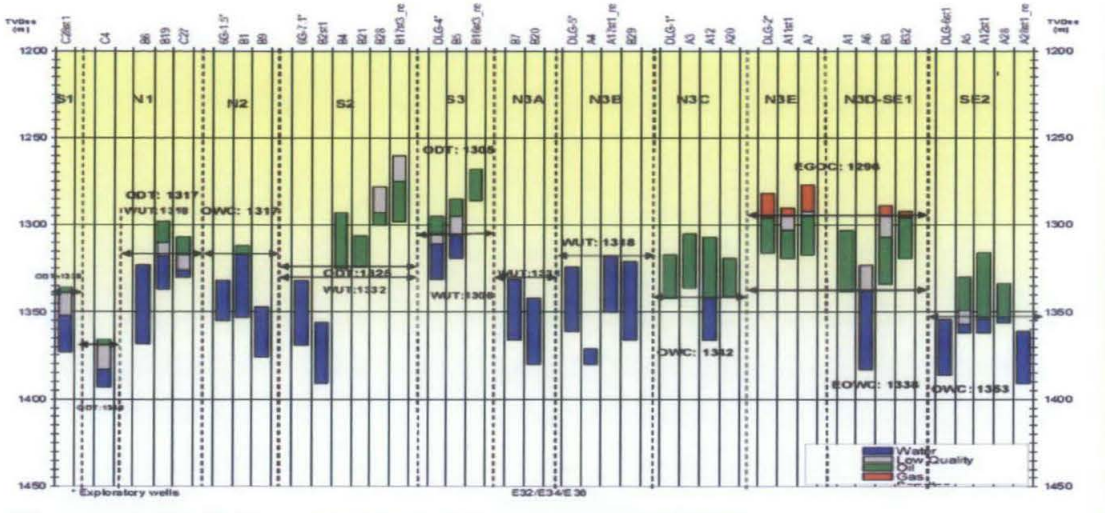

Figure 5.6: Stick Plot of X field Unit area at E32/E34E36

The complete observation on Table 1 is used to determine the hydrocarbon window. Most of the wells are showing oil presence. The gas presences are noticed on wells D-08 and D-A03 with thickness of 6 ms and 4 ms respectively.

There are two important consideration made prior to window length determination. Firstly, the window length selected must be within the sampling rate of the seismic data. The acquisition data was obtained on four (4) ms sampling rate and therefore the window length must be a multiple of four (4) ms. Secondly, due to the stacking reservoir pattern in X field, the hydrocarbon that presence above and below the E36E34 reservoirs should not be included in the window range. The top of the reservoir can go maximum up to the E34 layer. Whereas the bottom of the reservoir is normally, the Oil Down To (ODT) extents of E36 or E34E36 layers. The reservoir below the E34E36 reservoir is E40 reservoir with average depth of 1408 ms. The Oil Water Contact (OWC) of E40 reservoir is approximately at depth 1449 ms. The distance between E36 horizon and E40 OWC is approximately 41 ms. The distance between the E36 ODT to E40 OWC is approximately 80 ms.

The average depths for expected hydrocarbon are determined from the well information as stated on Table 1 and Table 2. Distance between E34 and E36 varies from 10 to 23 ms. Distance between E34 and top hydrocarbon or Oil Up To (OUT) varies from 3 to 9 ms. Distance between E34 and the bottom of the hydrocarbon extent or ODT E36E34 varies from 17 to 28 ms. Therefore, the average depth between top to bottom oil presence varies between 7 to 23 ms and average depth between top to bottom gas presence varies from 6 to 15 ms. The window determination has to consider the sampling rate of 4 ms and the variable hydrocarbon thickness observed from logs and seismic. The maximum thickness of hydrocarbon in E34 reservoir is 34 ms. The minimum depth where hydrocarbon can be detected from E34 horizon is 3 ms. Therefore, the window are design for a range of 4ms to 36ms which gives a thickness of 32ms.

Hydrocarbon identification within the vertical wells/ SynTool _ From well markers										
	Dlg-01/Chksht		Dlg-07/Chksht		Dlg-03/Chksht		Dlg-08/Chksht		Dlg-02/Chksht	
	Time/ms	Depth/m	Time/ms	Depth/m	Time/ms	Depth/m	Time/ms	Depth/m	Time/ms	Depth/m
E34	1317.00	1313.91	1370.20	1388.41	1341.02	1380.55	1357.15	1376.89	1296.00	1294.00
OUTE34/36	1319.71	1317.46	1376.00	1394.00	1346.00	1387.00				
ODTE34	1325.87	1325.72			1356.00	1400.00			1299.00	1298.00
OWC			1382.82	1403.58						
GUTE36							1361.00	1381.00		
GDTE36							1366.64	1389.22		
WUTE34				1404.00						
E36	1329.98	1331.94	1387.02	1408.62	1356.01	1401.78	1367.36	1390.24	1308.00	1309.00
ODTE36	1337.11	1341.31								
OWCE34/E36	1337.24	1341.48								
ODTE34/E36	1337.50	1341.84							1313.00	1316.00
WUTE36			1390.00	1413.00	1357.12	1403.53	1368.30	1391.58		
WDTE34/E36				1413.00						
Limit/thickness of hydrocarbon extend within the wells										
	Dlg-01		Dlg-07		Dlg-03		Dlg-08			
	Time/ms	Depth/m	Time/ms	Depth/m	Time/ms	Depth/m	Time/ms	Depth/m	Time/ms	Depth/m
Distance between E34 to E36	12.98	18.03	16.82	20.21	18.00	21.23	10.21	13.35	12.00	15.00
Distance between E34 to ODTE34/E36	20.50	27.93							17.00	22.00
E34 to top HC	3.00	3.55	5.00	5.59	4.98	6.45	3.85	4.11	3.00	4.00
Top to Bottom HC/Oil	17.79	24.38	6.82	9.58	10.00	13.00			14.00	18.00
Top to Bottom HC/Gas	1.00	1.00					5.64	8.22		
E34 to Bottom HC	20.79	27.93	11.82	15.17	14.98	19.45	10.00	12.00	17.00	22.00

Table 1: Hydrocarbon depth observed on vertical well markers and associated logs.

In this report, the attribute analysis will determine the hydrocarbon sand extent. As mention earlier on the depositional environment chapter, X field consist of mainly shale sand interbedded layer. The lithology between the E34 and E36 is classified as massive sand bodies with E34 and E36 has significant interbedded coal layers. Therefore, the

attribute extracted within the named windows will measure the sand hydrocarbon distribution.

The general window length was determined as 4 ms to 36 ms, which comprise the total hydrocarbon distribution in E34E36 reservoirs. The sliding windows between that ranges is determined by referring to average distribution of hydrocarbon sand on the studied wells. On D-03 well, the distance between E34 to top hydrocarbon is approximately 5 ms and bottom hydrocarbon is 15 ms. Therefore the sliding window between these ranges can be 4 to 8 ms, 4 to 12 ms and 8 to 12 ms. On D-01 well, distance between E34 to top hydrocarbon is approximately 3 ms and bottom hydrocarbon is 9 ms. Therefore the sliding window between these ranges can be 4 to 8 ms.

On D-01 well, distance between E34 to top hydrocarbon is 3 ms. The distance between E34 and bottom hydrocarbon (ODTE34/36) is 21 ms. Therefore the sliding windows are determined to cover a range between 4 to 20 ms. The windows will be 4 to 8 ms, 4 to 12 ms, 4 to 16 ms, 4 to 20 ms, 8 to 12 ms, 8 to 16 ms, 8 to 20 ms, 12 to 16 ms, 12 to 20 ms and 16 to 20 ms.

Whereas for wells with both gas and oil presences such as on well D-08 and D-A03, both type of hydrocarbons are studied. On D-A03 well, distance between E34 to top hydrocarbon indicating oil is approximately 9 ms and bottom hydrocarbon indicating oil is 12 ms. Therefore the sliding window for oil sand is between the ranges of 4 to 8 ms, 4 to 12 ms and 8 to 12 ms. The gas indication on D-A03 shows a distance of 8 ms between top gas to E34 and 9ms to bottom gas. Therefore, the window 8 to 12 ms will be studied for gas signatures.

In this project, three types of amplitude attributes were taken into consideration namely RMS amplitude, Average peak absolute amplitude and Maximum peak amplitude attributes. All these attributes are able to identify amplitude anomalies or characterize sequences especially along specific zones or reflectors.

5.3 Type of Attributes Selection

Objective of attribute extraction is to determine possible hydrocarbon sand extent that are visible on the maps. The maps are created referring to horizon E34 within a window identified on well logs and seismic data. The attributes are extracted using Landmark Post stack PAL software. In this project, three types of amplitude attributes were taken into consideration namely RMS amplitude, Average absolute amplitude and Maximum peak amplitude attributes. All these attributes are able to identify amplitude anomalies or characterize sequences especially along specific zones or reflectors. The methodology of each mention attributes are explained in the following paragraph. The attribute analysis was performed on Landmark PAL Poststack software. The input data used in this project is the 8-bit final migrated vertical sections.

5.3.1 RMS Amplitude

PAL computes the RMS (root-mean-square) amplitude within the time window specified for analysis. The time window or the hydrocarbon window extracted earlier from well logs is used for his purpose. RMS amplitude is calculated as the square root of the average of the squares of the amplitudes found in the analysis window. As an example, the following is the computation for the trace and interval:

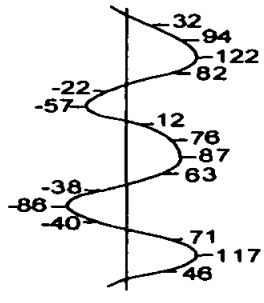

$$RMS = \sqrt{\frac{1}{N}\sum_{i=1}^{N} a_i^2}$$

$$= \frac{1}{16}(32^2 + 94^2 \ldots + 117^2 + 46^2)$$

$$= \sqrt{\frac{1}{16}(83945)}$$

$$= \sqrt{5246.56}$$

$$= 72.43$$

RMS amplitude resembles reflection strength, but is smoother (depending on the window length). The RMS amplitude is computed for every sample from the samples in this

window. However, because amplitudes are squared before averaging, the RMS computation is very sensitive to extreme amplitude values.

5.3.2 Average Absolute Amplitude

Absolute Amplitude replaces all samples with the absolute value of the original sample. For each trace, the absolute values of the amplitudes in the analysis window are added, and then the total is divided by the number of samples in the window to yield the mean. The Absolute Amplitude attribute, will enable zones of high acoustic impedance change become more visible.

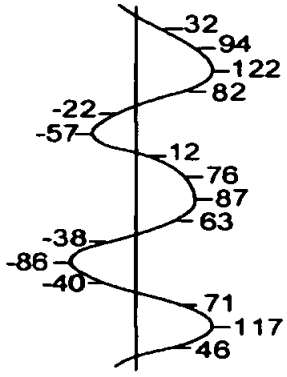

$$\text{Average Absolute Amplitude} = \frac{\text{sum of absolute amplitudes}}{\text{number of samples}}$$

$$= 1045/16$$

$$= 65.31$$

Average absolute amplitude is not nearly as sensitive to extreme amplitudes as is RMS amplitude, which involves squaring of the amplitude values.

5.3.3 Maximum Peak Amplitude

The Landmark Post Stack PAL does a parabolic fit trough the maximum positive amplitude in the analysis window and the two samples on either side of it. As per sample below, the highest amplitude of 125 is taken into consideration.

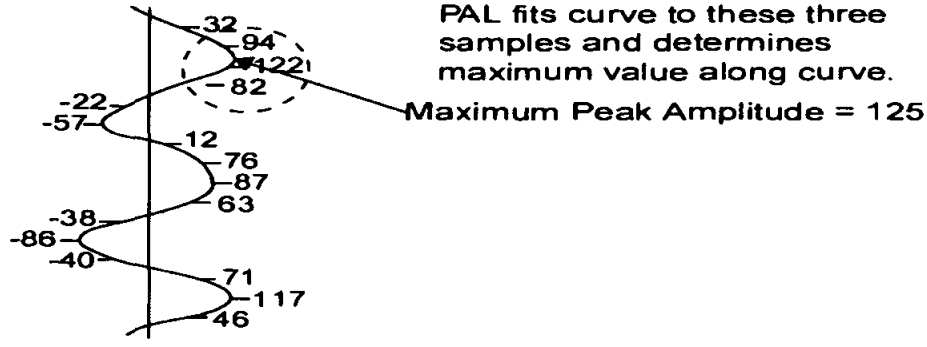

5.4 Attribute analysis methodology

In this project, three types of amplitude attributes were taken into consideration namely RMS amplitude, Average absolute amplitude and Maximum peak amplitude attributes. All these attributes are able to identify amplitude anomalies and able to group or specify the range of amplitudes interested by the users.

These attributes are normally used to detect lateral amplitude changes. The attribute may detach more significantly the amplitude contrasts on a limited analysis window. The selected attribute may focus on a single wavelet and provide accurate information on the characteristic of the window. The attribute maps are created for each window to capture the entire reservoir interval.

The thickness of E34E36 horizon and below the hydrocarbon sand zone is thin which is approximately about 32 ms. The reservoir thickness is not constant troughout the reservoir. This can be observed on the well markers and well logs (both Vertical and Deviated wells). Therefore, the hydrocarbon sand distribution in E34E36 reservoir is studied on windows. The windows are designed as explain on section 5.2.2.

Firstly, the expected highest and lowest amplitudes represent the sand distribution are observed from seismic sections. For this purpose, the well markers are overlaid on seismic section to read the amplitude from Seiswork as shown in Figure 5.7 below.

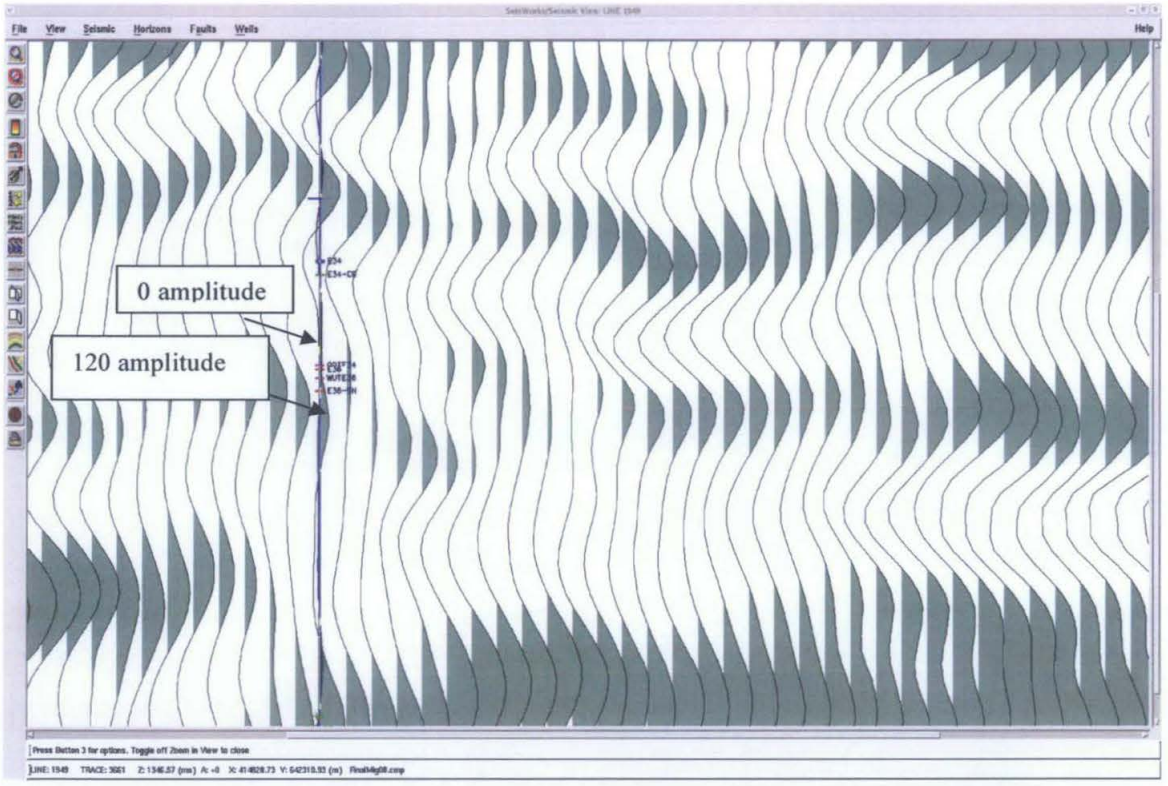

Figure 5.7: Expected amplitude on seismic along the peak wavelet at D-03 well where hydrocarbon is expected to presence.

On D-03 well, the sand layer is expected to be located along the peak wavelet. These phenomena were observed in all the wells overlaid on seismic. The lowest amplitude at the zero crossing is 0 and the highest expected amplitude is 124. The similar observations were done on other vertical and deviated wells. After observing on other wells, the sand layer presences are determined to be within the amplitude range of 0 to 120. **The assumption made here is that the sand layer, which probably contains hydrocarbon, should be present within this range of amplitude. Therefore, the attribute extracted will be set to 0 to 120 amplitude range considering any probable hydrocarbon sand should be within the mentioned range.**

These methods involve few trails and errors stage where different attribute extracted will show different range of amplitudes for the same window. For instants, RMS amplitude will give a lower value at particular point compare to average absolute amplitude. The different are due to the calculation method to compute these attributes. RMS amplitude is

calculated as the square root of the average of the squares of the amplitudes found in the analysis window whereas on average absolute amplitude, the values of the amplitudes in the analysis window are added, and then the total is divided by the number of samples in the window to yield the mean. This is among the main reasons why the amplitude reading varies for each attributes but anyhow, the expected total range will be maintained between 0 to 120 to study the amplitude varying range on all attributes.

The next step taken is to verify the exact expected amplitude that represents the sand value that contains hydrocarbon in the reservoir. Referring to Figure 5.7, the range taken between 0 to 120 is the expected range for sand occurrence. This range shows the sand value along the peak amplitude and does not really shows the hydrocarbon sand. In order to clarify, the wells are overlaid on attributes map to observe the amplitude values given at the hydrocarbon vicinity. Details of this method to determine the hydrocarbon sand range will be discussed on the following map analysis section.

Once the limit of hydrocarbon sand is determined, the attribute maps for different windows are rescaled to the new amplitude limits. The attribute maps created with this scale will represents the hydrocarbon sand distribution at that mention range or depth. Using these attribute maps, user will be able to calculate the expected hydrocarbon that can be acquired at that particular thickness range (window).

5.5 Map analysis

5.5.1 RMS Amplitude Results

The RMS amplitude is computed for every sample in the defined window. As mention earlier, the input data is of 4 ms sample rate. Therefore, the windows are designed on multiple of 4 ms's.

The vertical and deviated wells are overlaid on attribute maps and later used to read the amplitude values the location. For example, on D-03 well the identified distance between

E34 horizon to top hydrocarbon is approximately 5 ms and bottom hydrocarbon is 15 ms. These values are determined from the well markers. The suggested windows are 4 to 8 ms (Figure 5.8), 4 to 12 ms (Figure 5.9) and 8 to 12 ms (Figure 5.10). The RMS amplitude attributes are extracted from 0 to 120 amplitude range for each window and the wells are overlaid on these maps.

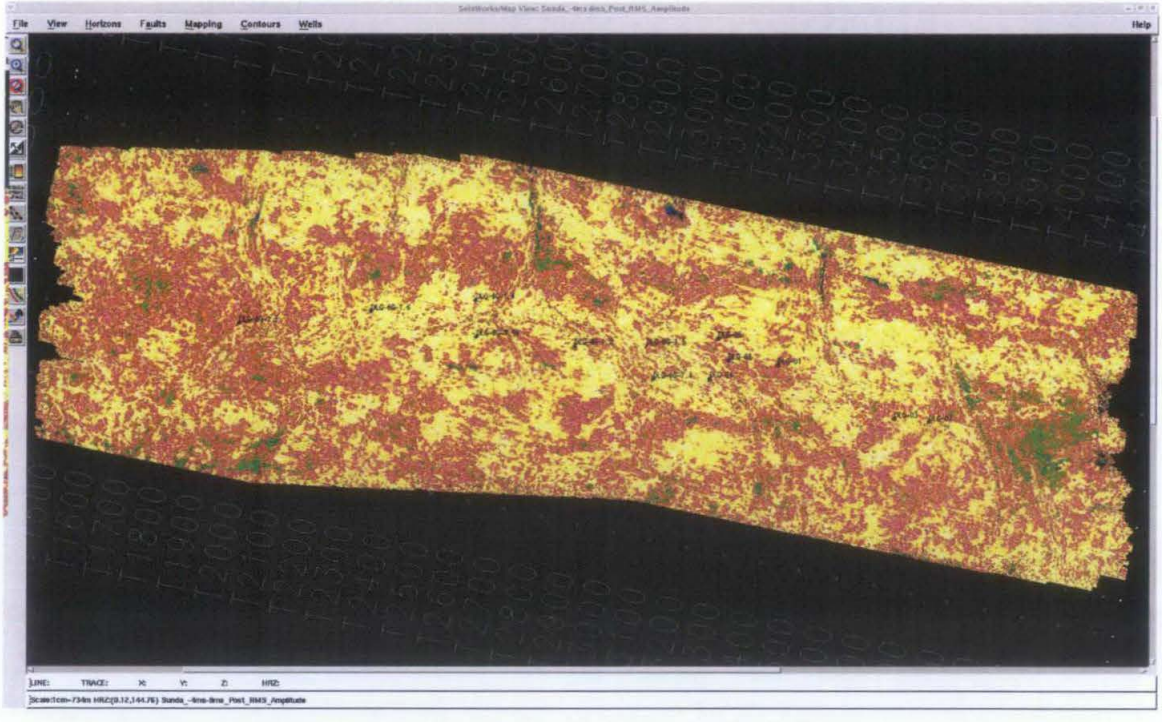

Figure 5.8: RMS Amplitude extracted on 4 to 8 ms window with color scale 0 to 120.

The amplitudes readings are taken directly from each attribute maps displayed on seiswork as shown in Figure 5.8, Figure 5.9 and Figure 5.10. On D-03 well, the OUT on E34E36 reservoir is at 1346 ms and ODT E34E36 is at 1356 ms. The hydrocarbon sand thickness is approximately 10 ms. The marker shows the type off hydrocarbon present at this vicinity is oil sand. Therefore, the amplitude extracted by RMS amplitude at this interval should be the amplitude value for oil sand. The different windows are used to ensure the highest and lowest value for the oil sand is observed. The value of 16.76 is noticed on 4 to 8 ms and 24.76 on 4 to 12 ms. The similar method is done on other wells where the hydrocarbon presences are noticed. Well taken for this analysis are D-02, D-01, D-07, D-03 and D-08 and deviated well D-A03. All studied Exploration wells are vertical and contains check shot information taken at the well vicinity. This is one of the main

reasons for using Exploration wells for amplitude analysis. The results are listed on Table 2.

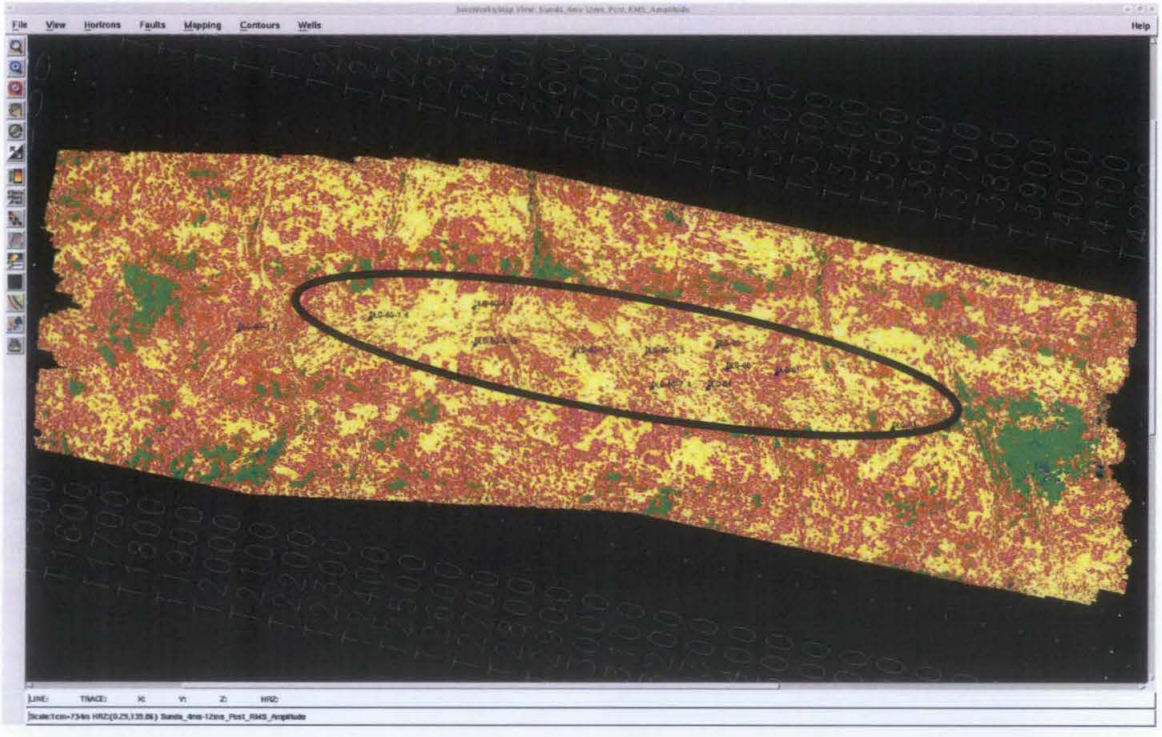

Figure 7.9: RMS Amplitude extracted on 4 to 12 ms window with color scale 0 to 120 ms.

The attribute analyses to determine the hydrocarbon window were conducted for X field Western, Eastern and Unit area as shown on Figure 5.9 ('Black' eclipse). As shown on Figure 5.9, the wells are distributed within the marked area especially around the Unit area as shown on Figure 3.1.

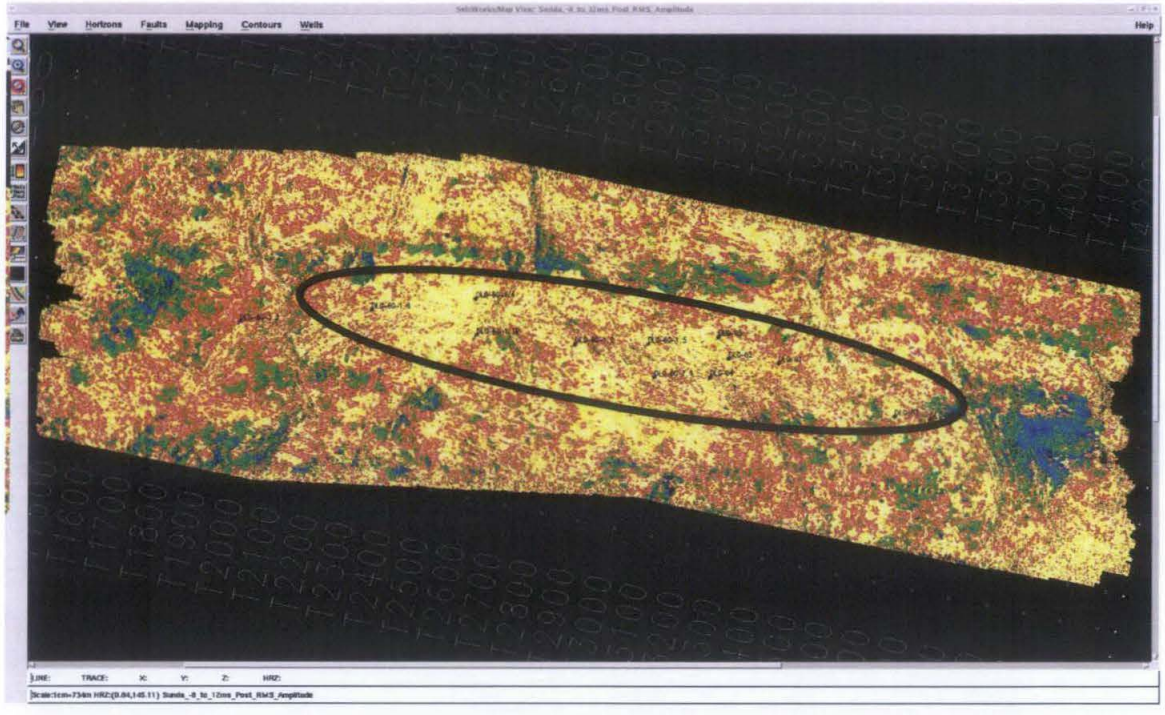

Figure 5.10: RMS Amplitude extracted on 8 to 12 ms window with color scale 0 to 120 ms.

	RMS Amplitude at HC location					
Extraction	D-03	D-08	D-07	D-01	D-02	D-A03
E34 to top HC	5	4	5	3	3	9
E34 to BottomHC	15	10	8	21	17	12
4 to 8 window	25	11.76	36.35	32.85	29.76	28.76
8 to 12 window	30	17.35			30.62	16.76
12 to 16 window	29	55.54			32.38	
8 to 28 window	52.34	56.76				
4 to 20 window				33.6		

Table 2: RMS amplitude extracted at each well location. The 'yellow' highlight the amplitude value for gas sand.

The amplitude values are observed within the vicinity of each wells overlaid on attribute maps at different window ranges. Hydrocarbon sand represents both oil sand and gas sand. The yellow highlighted marker on Table 2 shows the presence of gas sand in E34E36 reservoir in both wells namely D-A03 and D-08. The D-08 well contains gas

sand whereas the D-A03 contains both oil sand and gas sand. Therefore the amplitude showing the gas presence are studied on window 4 to 8 ms and 8 to 12 ms for D-08 well. The D-A03 well has a hydrocarbon thickness of approximately 16 ms. The top hydrocarbon is at 9 ms below E34 horizon. Therefore, the 8 to 16 ms, 8 to 12 ms, 12 to 16 ms windows is used to determine the hydrocarbon sand amplitude.

The Table 3 shows results of amplitude extraction from five (5) vertical wells and one (1) deviated well. On this project concentration were given more on vertical Exploration wells because of the availability of check shot survey on them. The deviated wells have deviation survey data and the check shot were taken from other nearby wells. For instant, the D-B05 and D-B32 uses the check shot from D-02 well whereas D-B28, D-B19, D-B21 and D-B04 uses the D-6G-7.1 check shot data. In order to obtain better accuracy, the amplitude observations are mainly done on vertical wells. The deviated wells are used to crosscheck as blind wells on the attribute map. After studying the available hydrocarbon sand and their amplitude characteristic in X field, the range for the hydrocarbon sand is determined. The amplitude generally varies from 10 to 50 troughout the field. The gas sand shows lower amplitude compare to oil sand that shows higher amplitude. Therefore, the map analysis shows that the hydrocarbon sand is expected to be presence at an amplitude range of 10 to 50 ms. The attribute map are re-scaled as shown on Figure 5.12 to Figure 5.13. The attribute maps show the hydrocarbon distribution that agrees with the structure map retrieved below E34 horizon as shown in Figure 5.11. Various interval were selected to display the hydrocarbon sand distribution within the E34 reservoir as shown from Figure 5.12 to Figure 5.26.

Figure 5.11: X field structure map extracted along E34 horizon

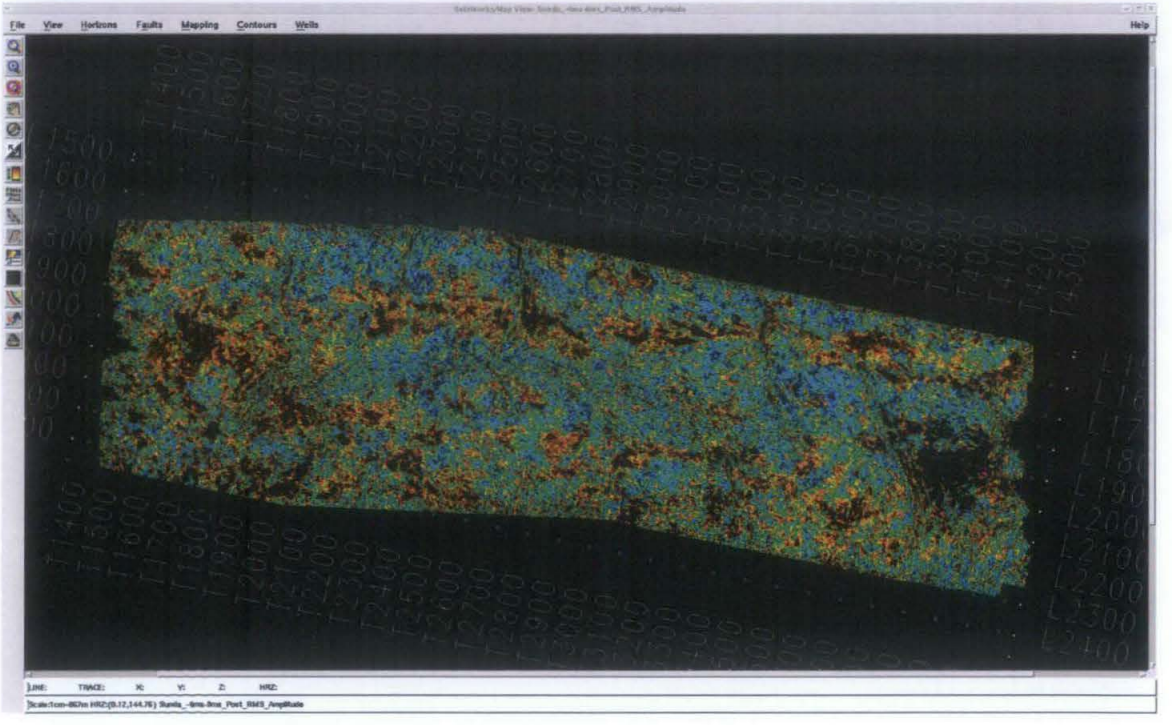

Figure 5.12: RMS Amplitude extracted on 4 to 8 ms window with color scale 10 to 50 amplitude values showing the hydrocarbon sand extent.

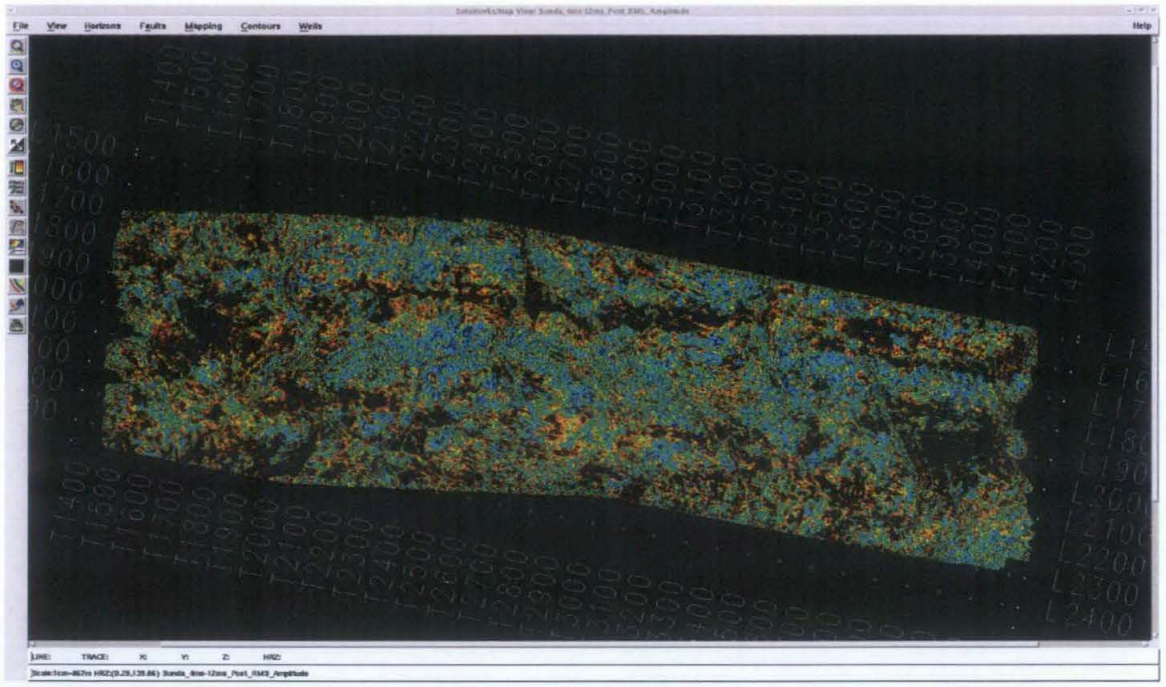

Figure 5.13: RMS Amplitude extracted on 4 to 12 ms window with color scale 10 to 50 amplitude values showing the hydrocarbon sand extent.

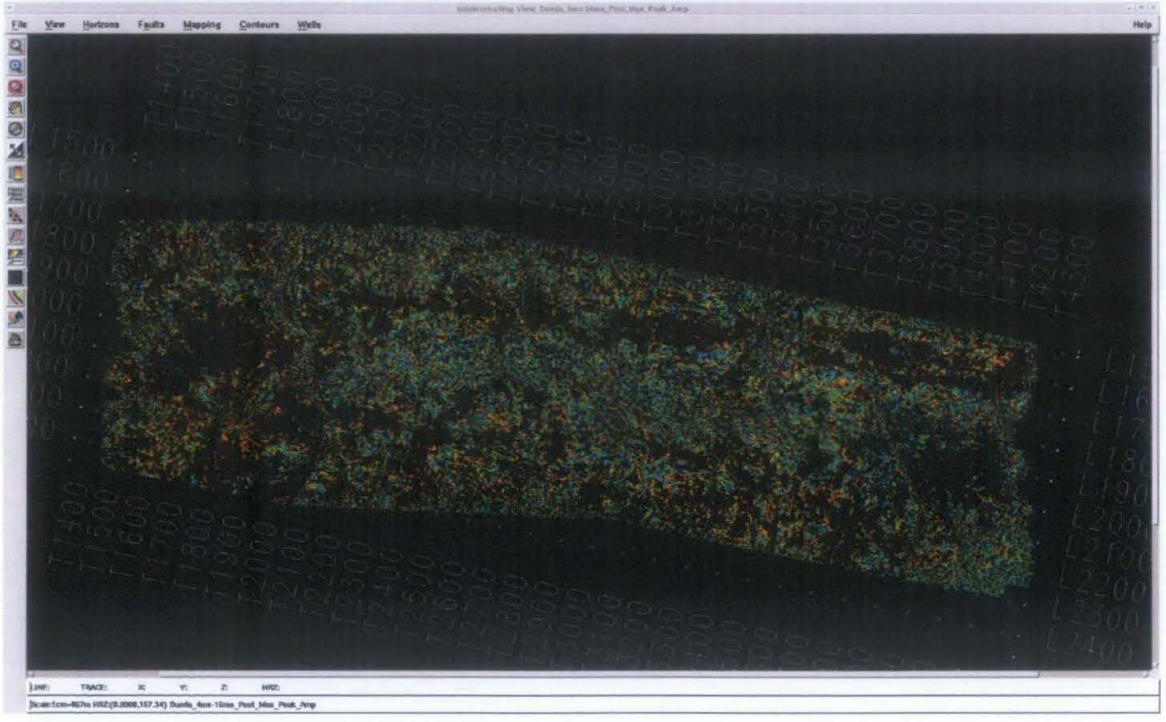

Figure 5.14: RMS Amplitude extracted on 4 to 16 ms window with color scale 10 to 50 amplitude values showing the hydrocarbon sand extent.

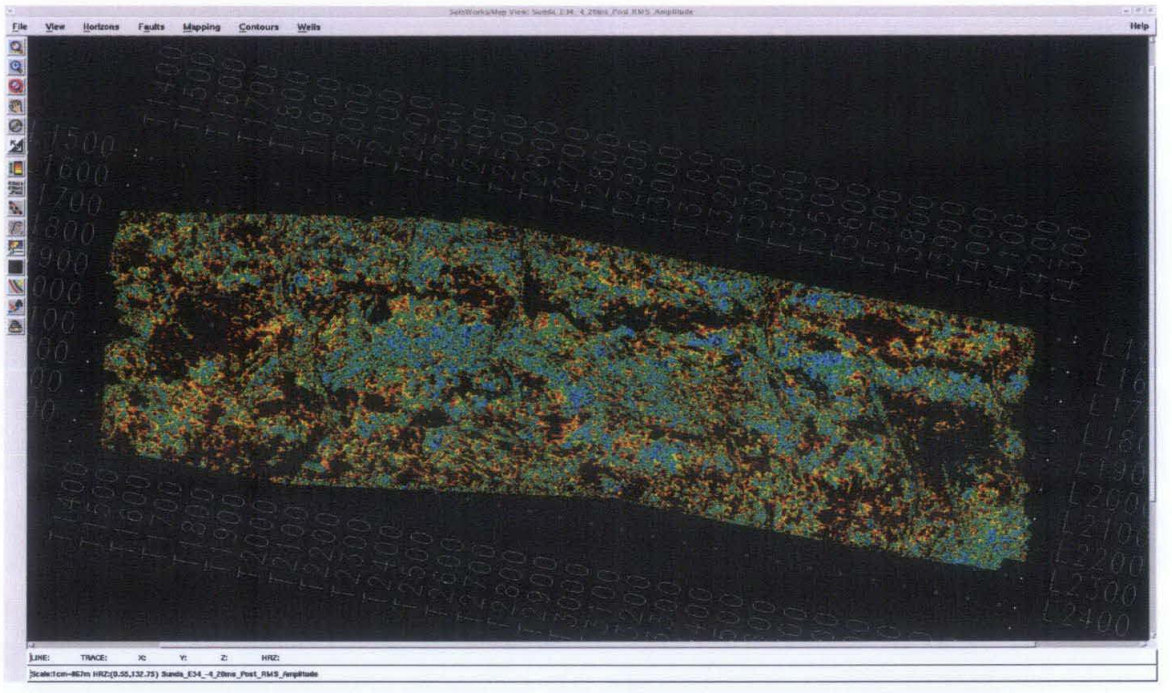

Figure 5.15: RMS Amplitude extracted on 4 to 20 ms window with color scale 10 to 50 amplitude values showing the hydrocarbon sand extent.

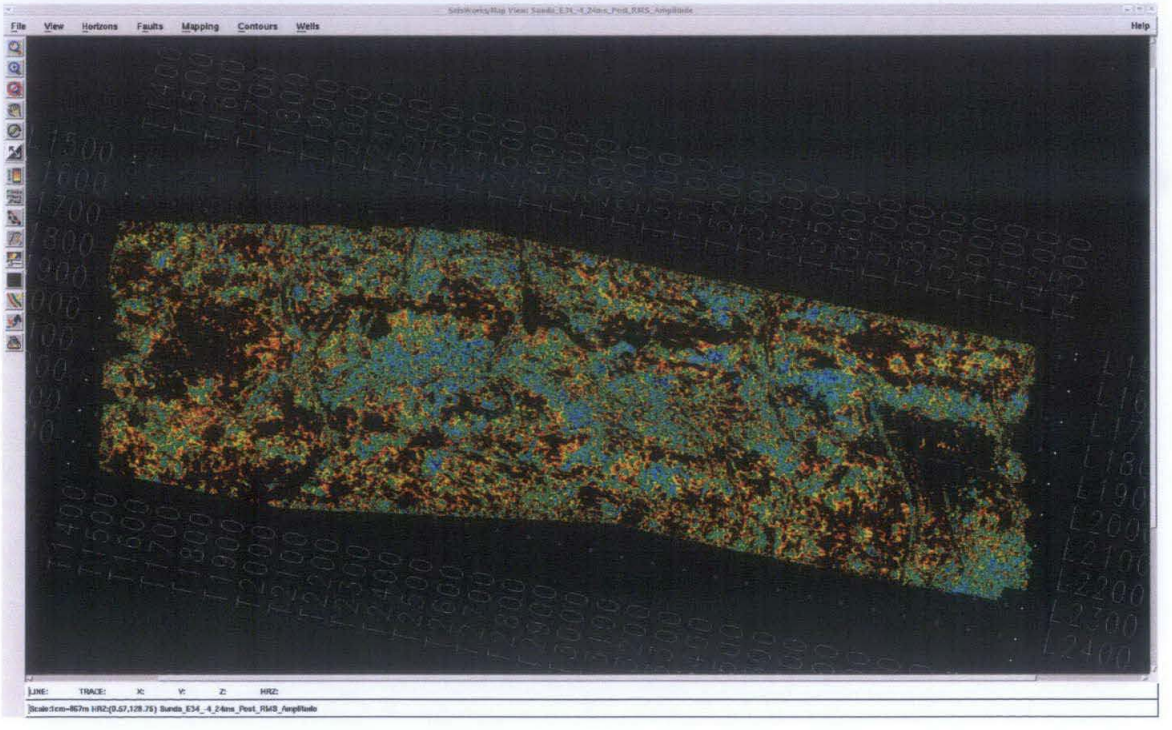

Figure 5.16: RMS Amplitude extracted on 4 to 24 ms window with color scale 10 to 50 amplitude values showing the hydrocarbon sand extent.

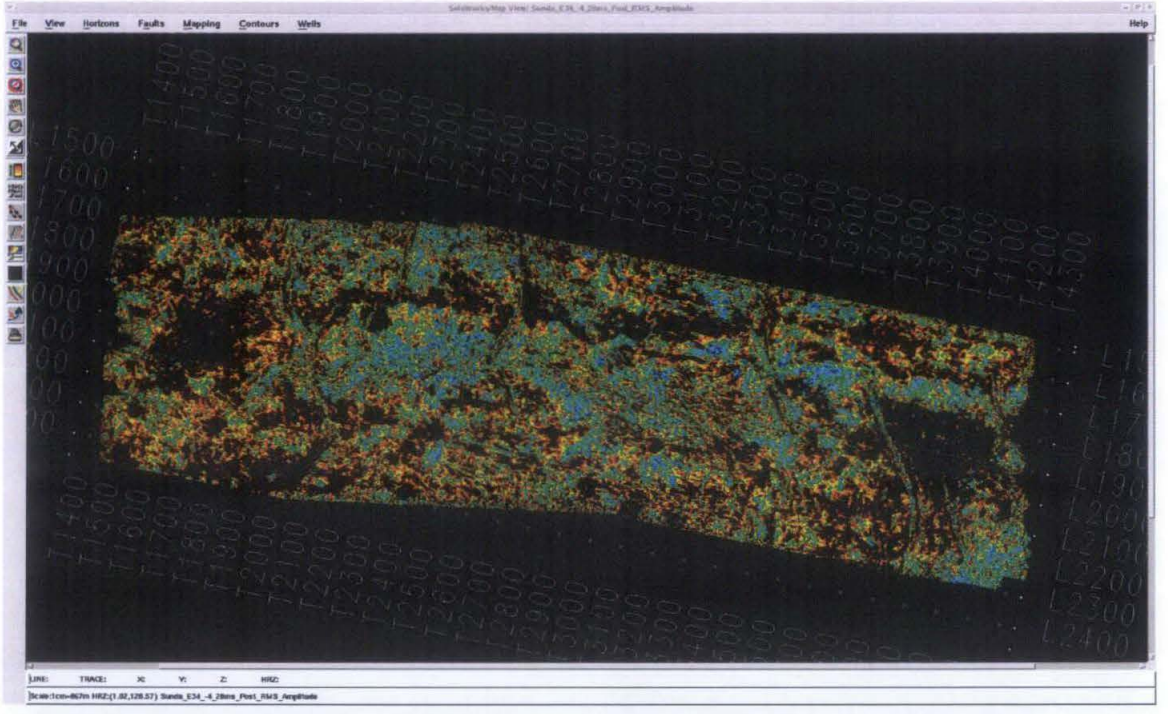

Figure 5.17: RMS Amplitude extracted on 4 to 28 ms window with color scale 10 to 50 amplitude values showing the hydrocarbon sand extent.

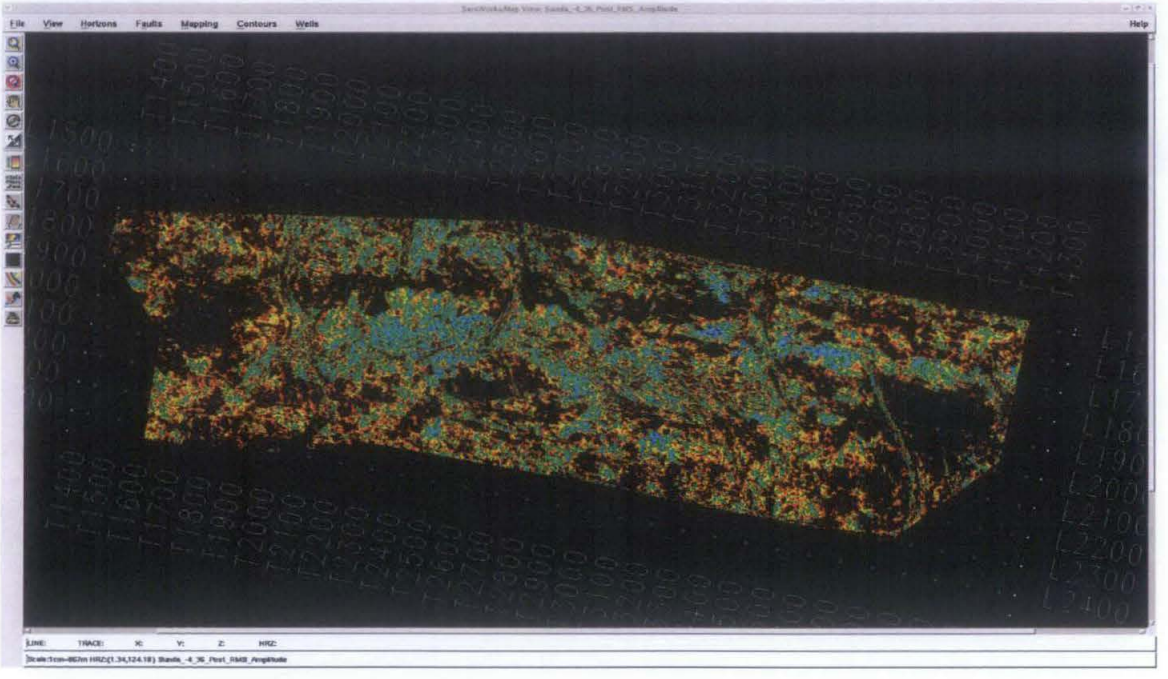

Figure 5.18: RMS Amplitude extracted on 4 to 36 ms window with color scale 10 to 50 amplitude values showing the hydrocarbon sand extent.

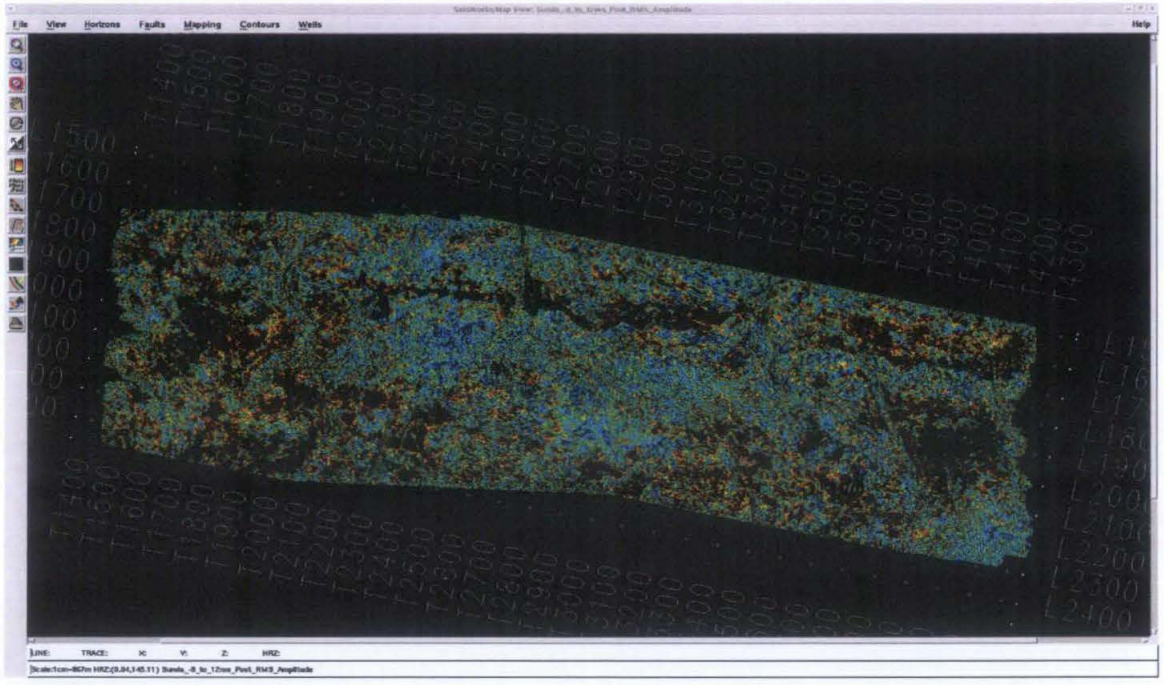

Figure 5.19: RMS Amplitude extracted on 8 to 12 ms window with color scale 10 to 50 amplitude values showing the hydrocarbon sand extent.

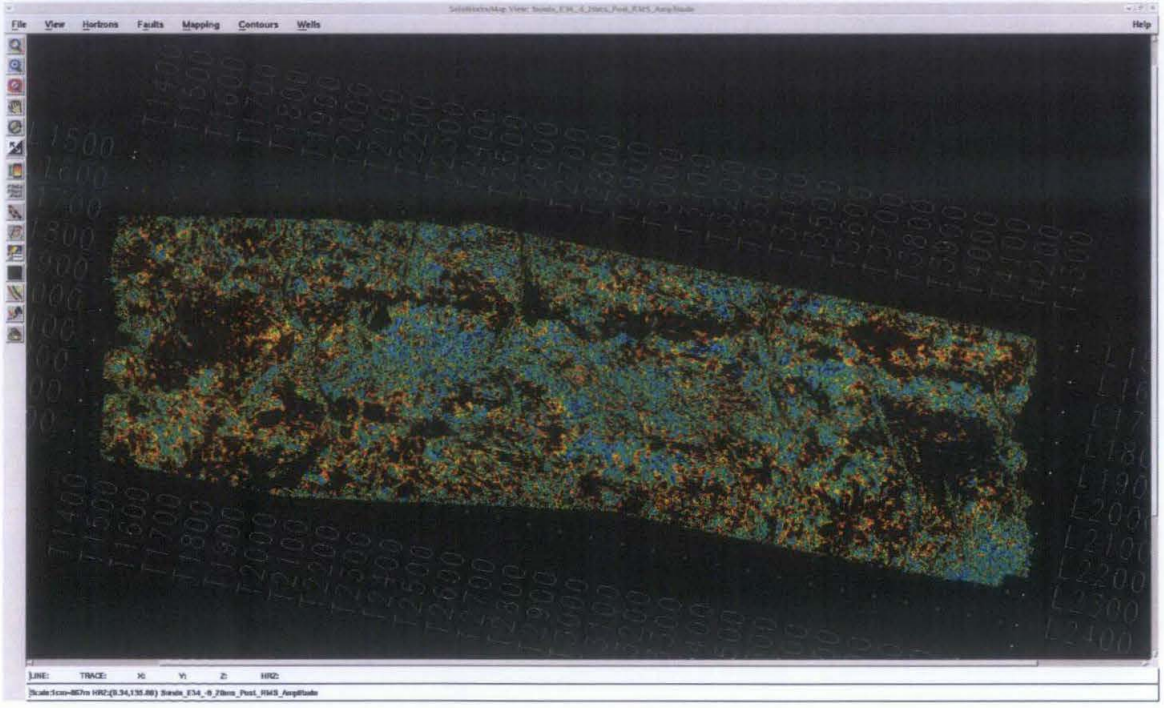

Figure 5.20: RMS Amplitude extracted on 8 to 20 ms window with color scale 10 to 50 amplitude values showing the hydrocarbon sand extent.

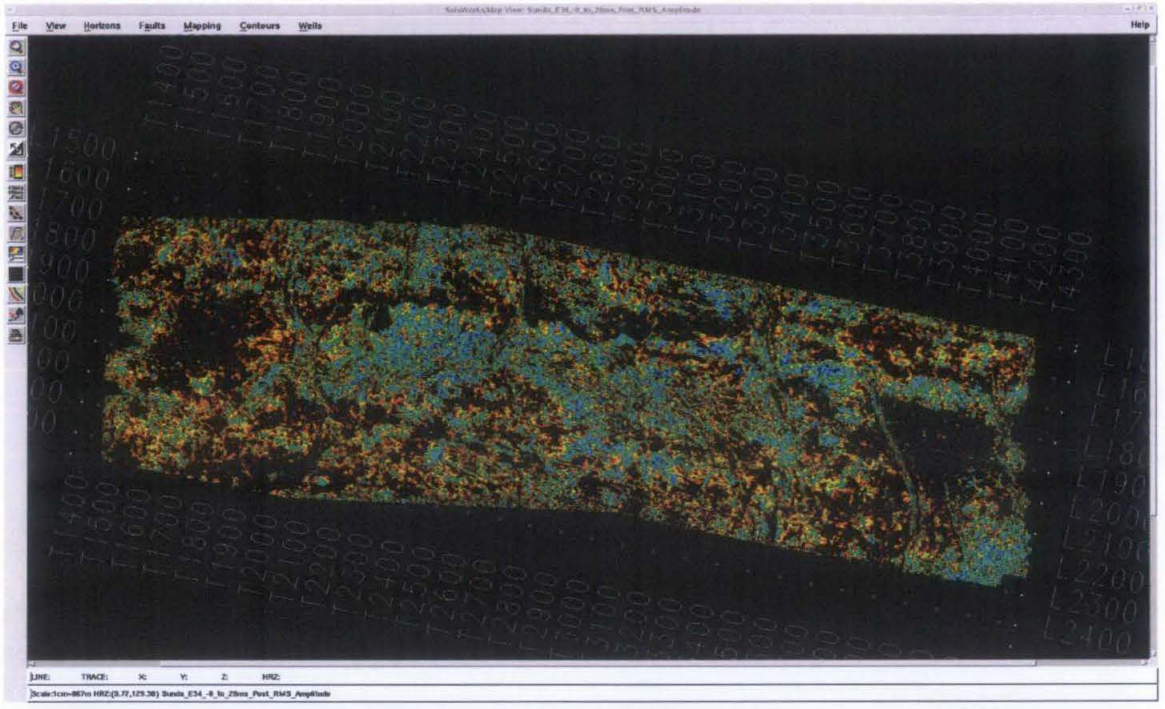

Figure 5.21: RMS Amplitude extracted on 8 to 28 ms window with color scale 10 to 50 amplitude values showing the hydrocarbon sand extent.

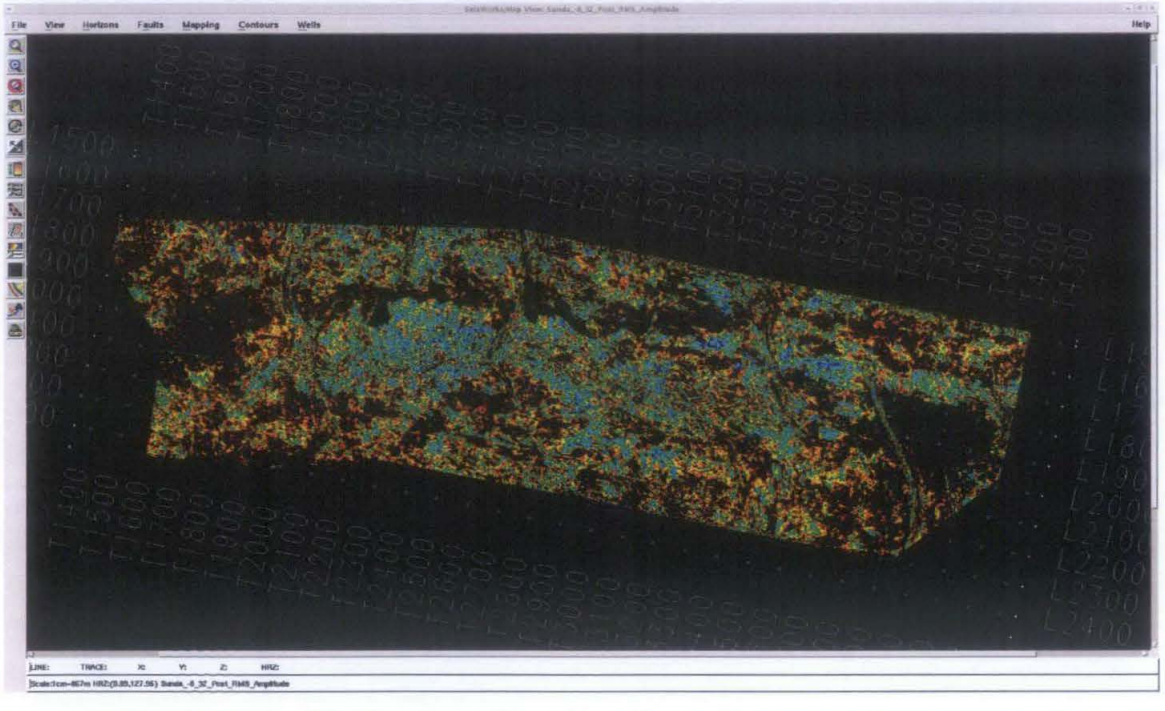

Figure 5.22: RMS Amplitude extracted on 8 to 32 ms window with color scale 10 to 50 amplitude values showing the hydrocarbon sand extent.

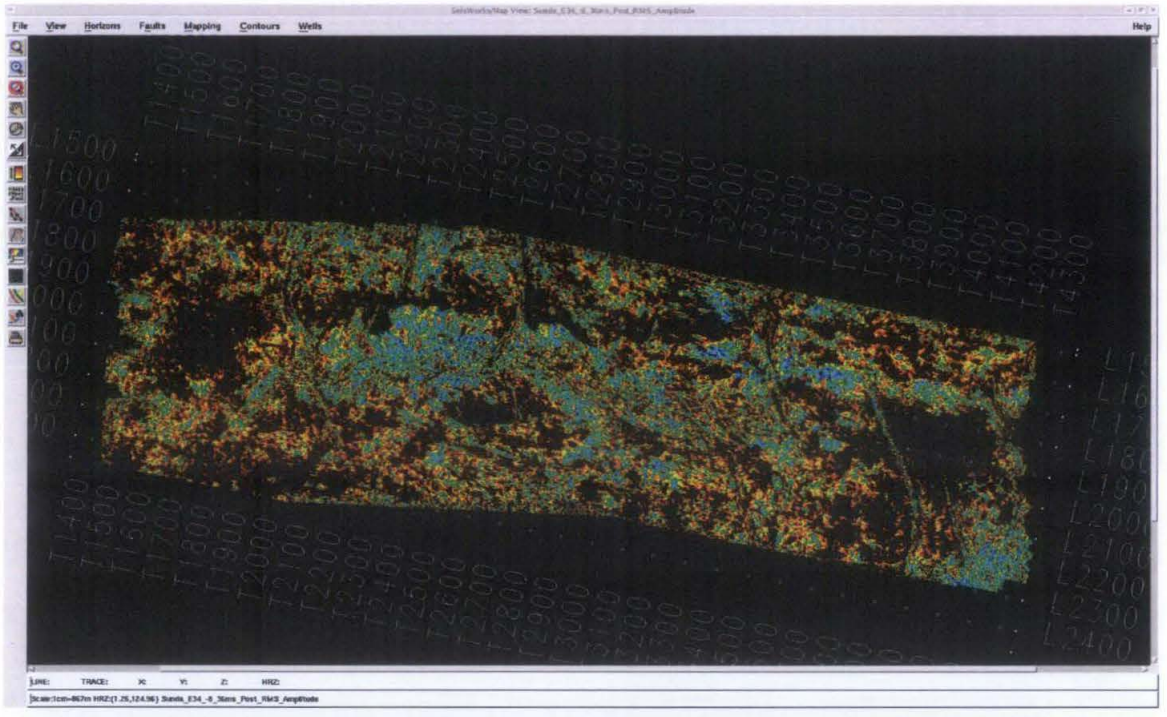

Figure 5.23: RMS Amplitude extracted on 8 to 36 ms window with color scale 10 to 50 amplitude values showing the hydrocarbon sand extent.

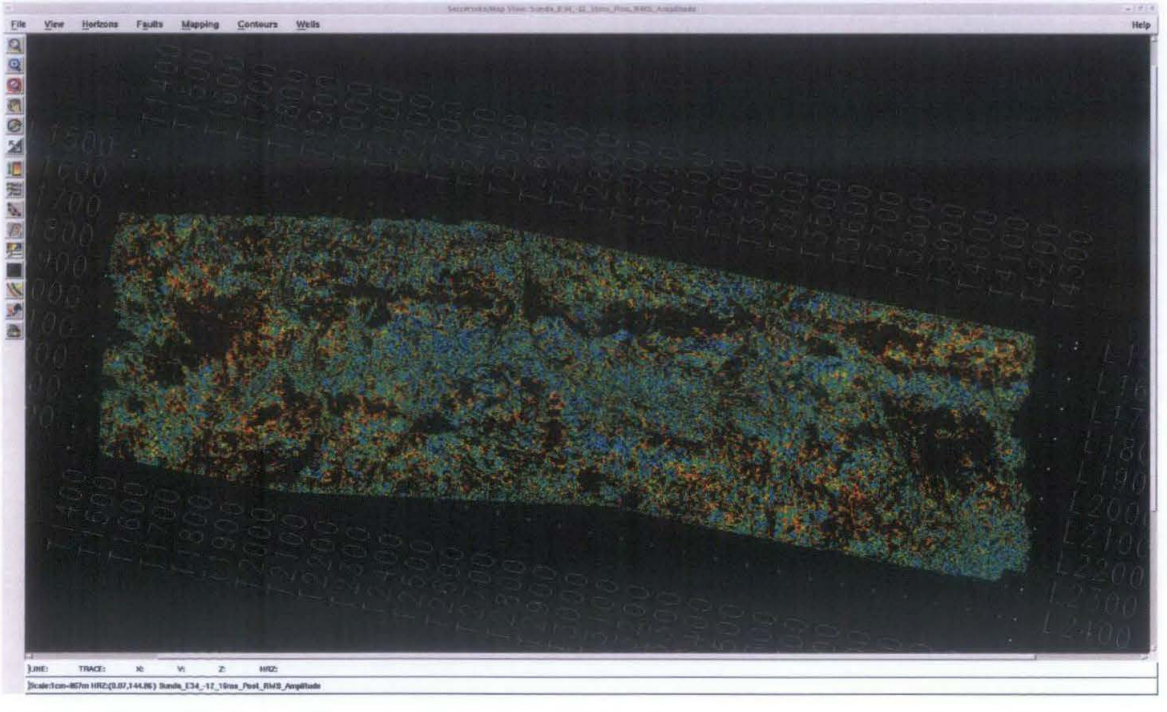

Figure 5.24: RMS Amplitude extracted on 12 to 16 ms window with color scale 10 to 50 amplitude values showing the hydrocarbon sand extent

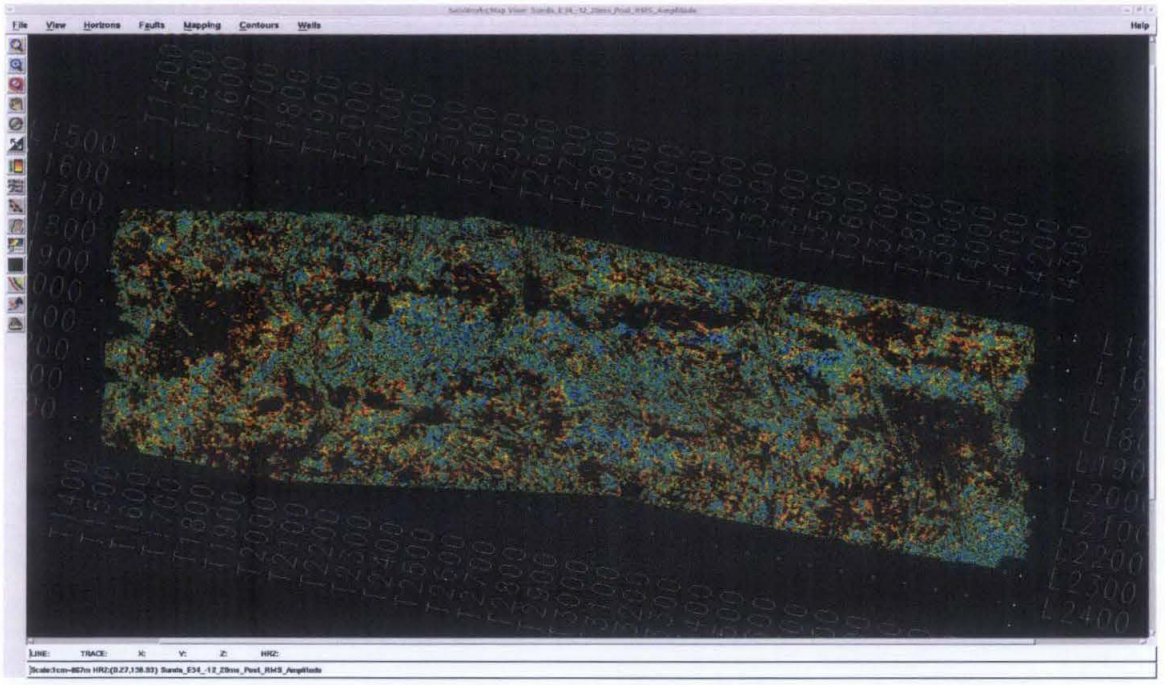

Figure 5.25: RMS Amplitude extracted on 12 to 20 ms window with color scale 10 to 50 amplitude values showing the hydrocarbon sand extent

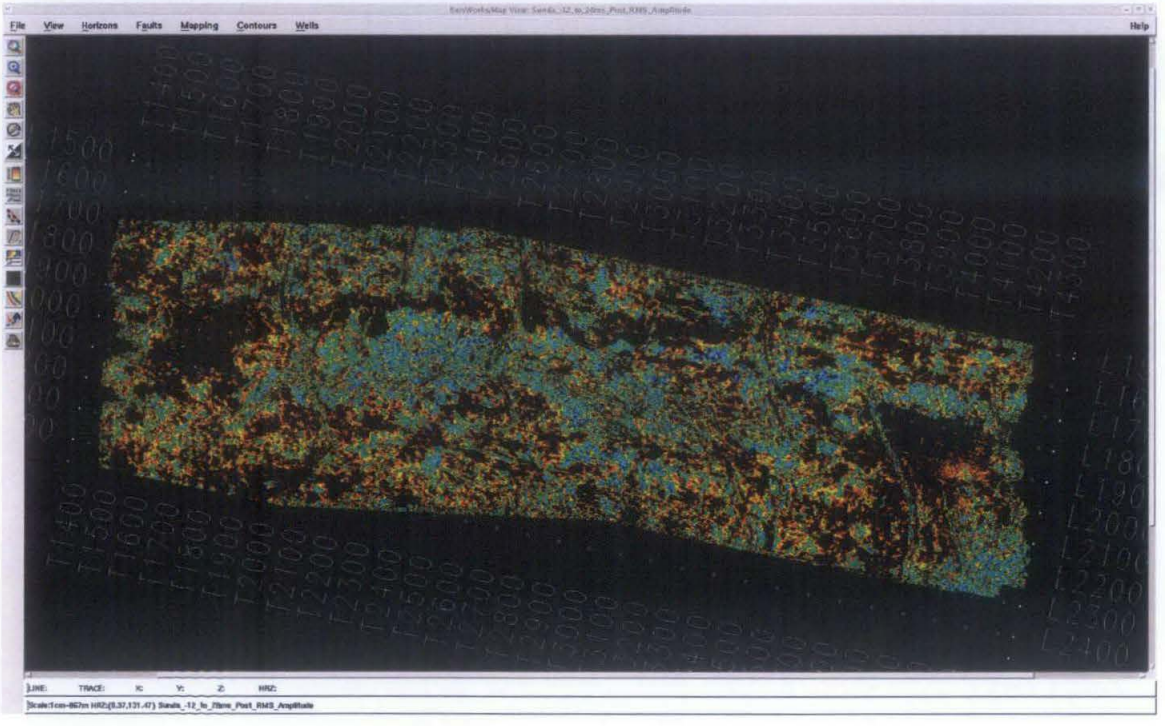

Figure 5.26: RMS Amplitude extracted on 12 to 28 ms window with color scale 10 to 50 amplitude values showing the hydrocarbon sand extent

5.5.2 Average Absolute Amplitude Results

Absolute Amplitude replaces all samples with the absolute value of the original sample. For each trace, the absolute values of the amplitudes in the analysis window are added, and then the total is divided by the number of samples in the window to yield the mean.

The same method as RMS amplitude was adopted to define the hydrocarbon sand using the average absolute amplitude. The similar windows were adopted to check on hydrocarbon sand as the depths define from well logs. The initial extraction scale is 0 to 120 ms, which later the amplitudes observed, are used to define the hydrocarbon sand.

Figure 5.27: Average Absolute Amplitude extracted on 4 to 8 ms window with color scale 0 to 120 ms showing the hydrocarbon sand extent

The amplitude observed is noted on Table 4 below. Figure 5.27 shows the average absolute amplitude extraction for a window of 4ms below E34 horizon up to 8 ms below the E34 horizon. The well location on Figure 5.28 is zoomed and shown in Figure 5.29. The attribute map on Figure 5.29 shows the well D-07, D-03, D-08, D-02, D-A03 and D-01 location where the amplitude reading were extracted. Other wells are used to crosscheck the observed amplitude values.

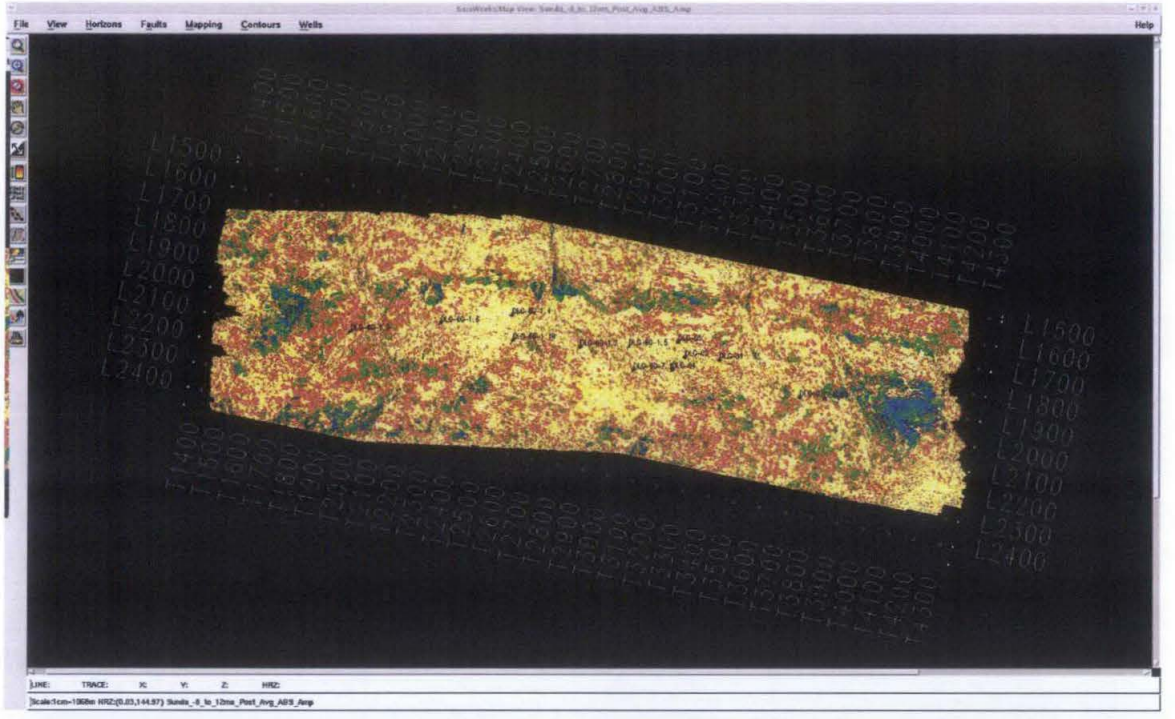

Figure 5.28: Average Absolute Amplitude extracted on 8 to 12 ms window with color scale 0 to 120 ms.

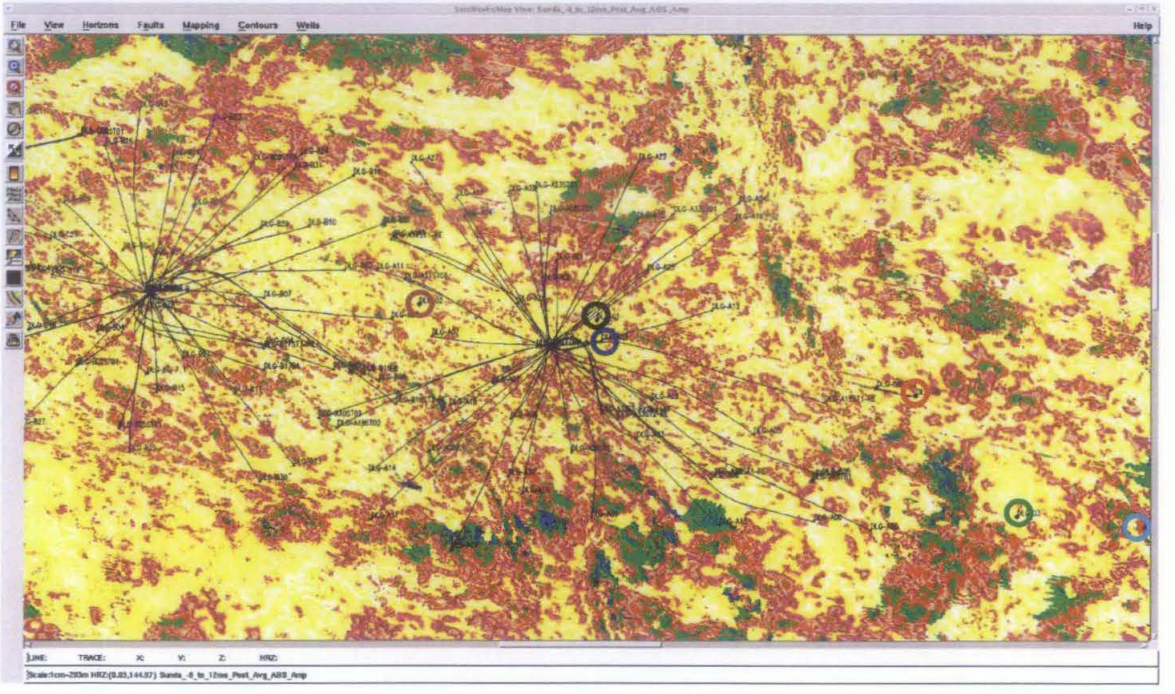

Figure 5.29: Zoom plot of Average Absolute Amplitude extracted on 8 to 12 ms window with color scale 0 to 120 ms. The attribute map shows the well D-07, D-03, D-08, D-02, D-A03 and D-01 location

On the average absolute amplitude attribute method the changes on type of hydrocarbon sand either oil or gas should be more visible because the absolute amplitude attribute, will enable zones of high acoustic impedance change be identified. As explained earlier, the seismic data used in this project uses the SEG negative polarity convention. Therefore, the reflection coefficient from shale to gas sand is negative whereas from gas to oil is positive. The acoustic impedance on gas is low whereas oil is higher. Therefore, the well logs are displayed on Syntool as on Figure 5.2 and 5.3 and the shalely coal E34 horizon shows a negative reflection coefficient whereas the impedance log show a increase sudden increase.

The amplitude reading on Table 3 shows that the amplitude range varies between gas sand and oil sand. The gas sand shows amplitude between 15 to 24 ms whereas the oil sand shows amplitude readings varies between 25 to 45 ms. Considering the results of amplitude extraction, the preferred range for hydrocarbon sand is 15 to 45 ms. Therefore, all the average absolute amplitude attribute maps are scaled to the mention range as shown in figures below.

Average Absolute Amplitude at HC location						
Extraction	D-03	D-08	D-07	D-01	D-02	D-A03
E34 to top HC	5	4	5	3	3	9
E34 to Bottom HC	15	10	8	21	17	12
4 to 8 ms window	28.65	19.86	36.12	41.46	30.23	30.28
4 to 12 ms window	19.96	23.95	39.17	37.22	30.57	44.98
8 to 12 ms window	29.37	20.06	50.8	23.01	31.67	20.06
8 to 16 ms window	15.73	11.93	73.44	80.79	31.52	39.69
8 to 20 ms window	21.76	28.6	55.27	37.17	46.32	48.29
8 to 28 ms window	53.67	40.21	45.8	45.8	37.65	44.85
12 to 16 ms window	37.65	50.51	52.5	51.7	48.68	54.81

Table 3: Average Absolute amplitude extracted at each well location. The yellow highlight the wells that show gas sand.

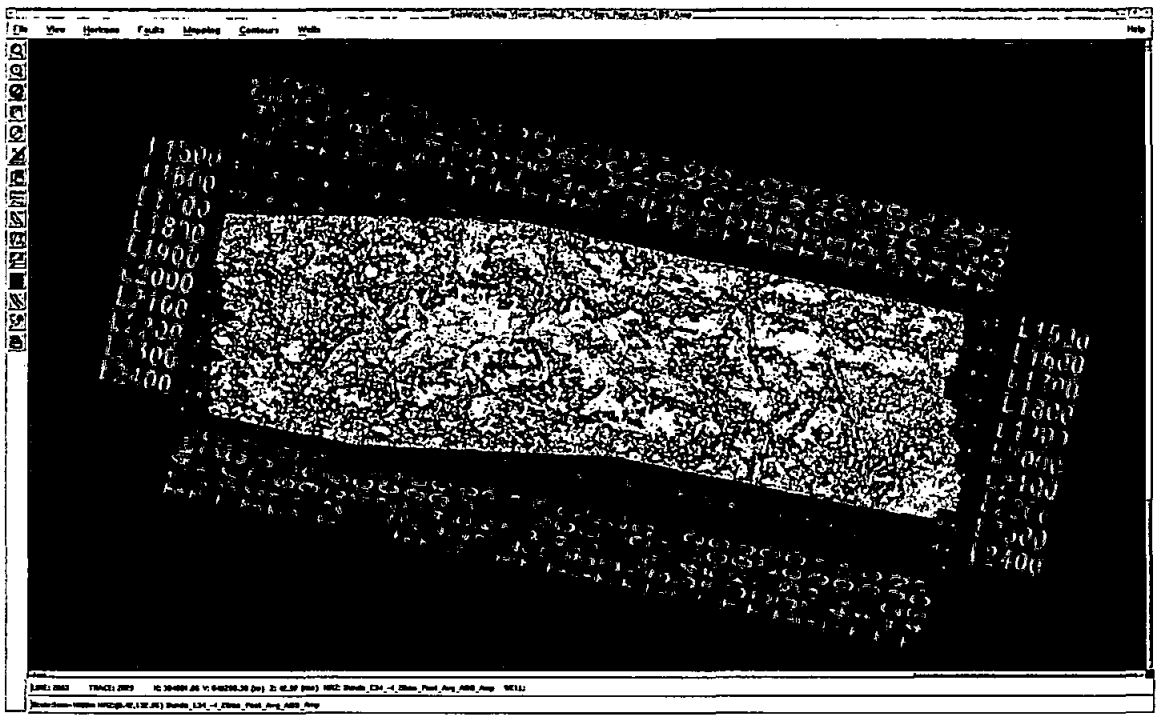

Figure 5.30: Average Absolute Amplitude extracted on 4 to 20 ms window with color scale 0 to 120 ms showing the hydrocarbon sand extent

Figure 5.31: Average Absolute Amplitude extracted on 4 to 8 ms window with color scale 15 to 45 amplitude values showing the hydrocarbon sand extent

Figure 5.30: Average Absolute Amplitude extracted on 4 to 20 ms window with color scale 0 to 120 ms showing the hydrocarbon sand extent

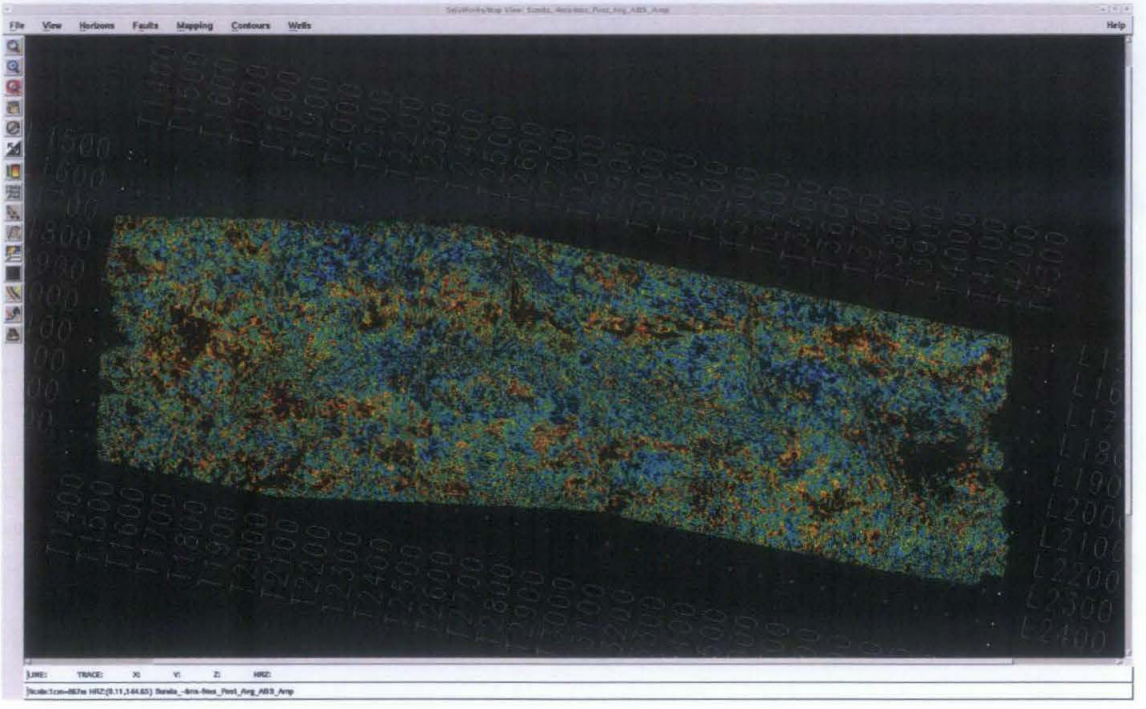

Figure 5.31: Average Absolute Amplitude extracted on 4 to 8 ms window with color scale 15 to 45 amplitude values showing the hydrocarbon sand extent

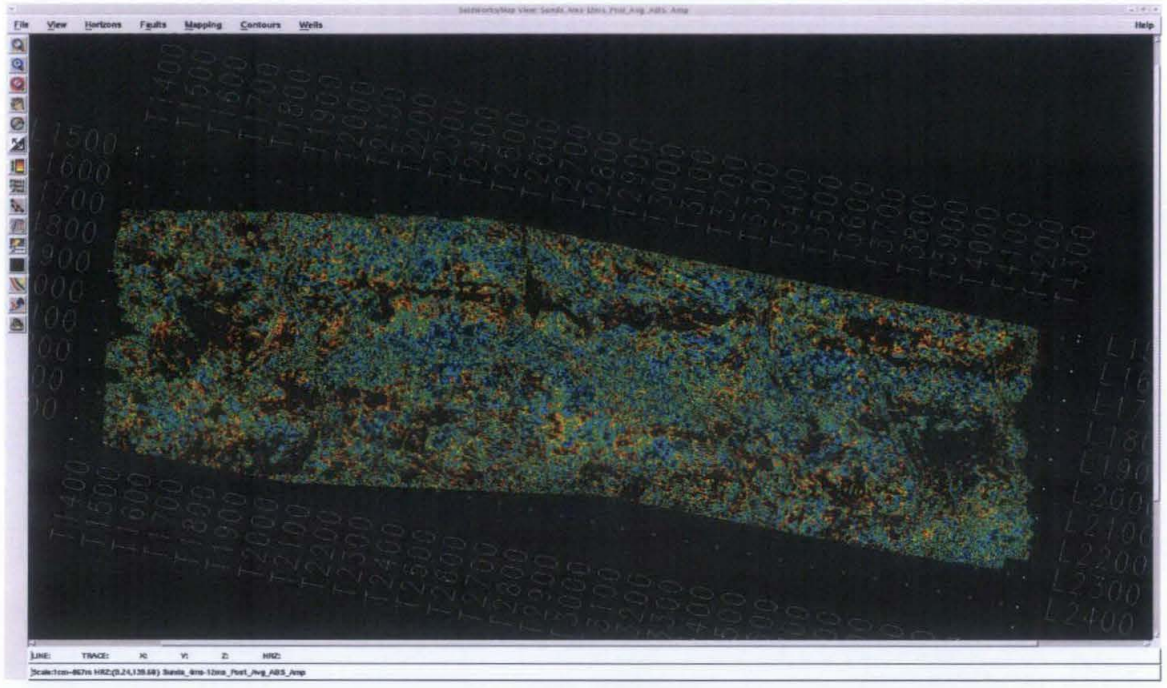

Figure 5.32: Average Absolute Amplitude extracted on 4 to 12 ms window with color scale 15 to 45 amplitude values showing the hydrocarbon sand extent

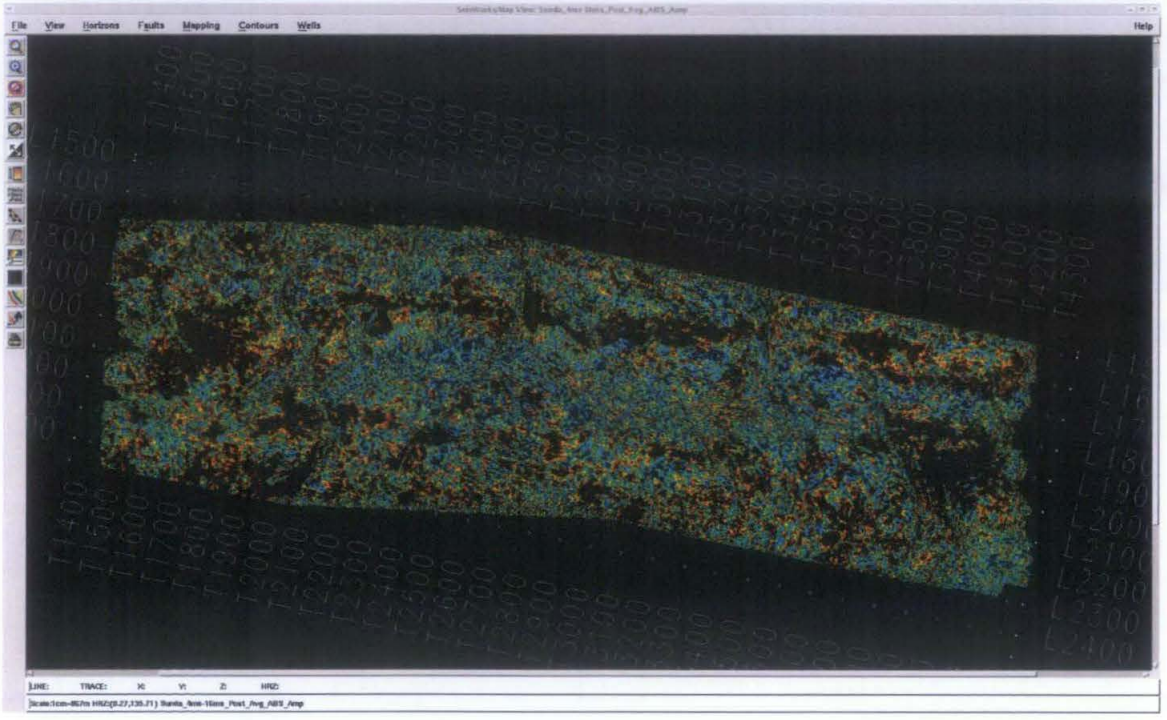

Figure 5.33: Average Absolute Amplitude extracted on 4 to 16 ms window with color scale 15 to 45 amplitude values showing the hydrocarbon sand extent

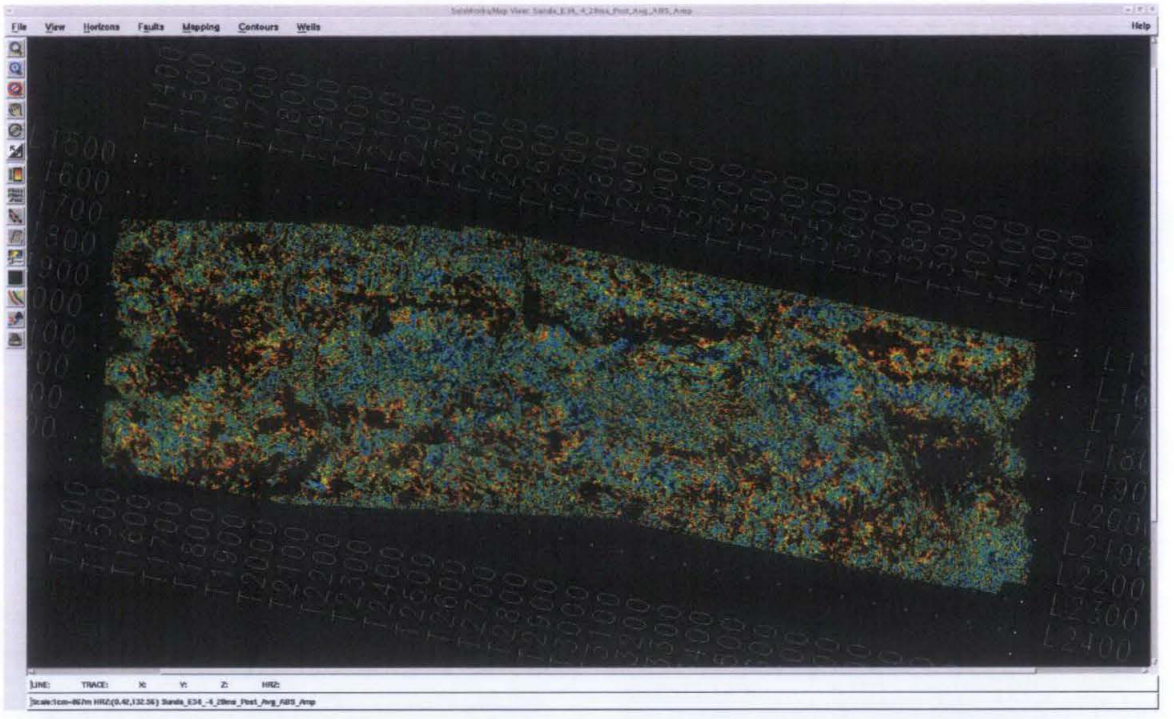

Figure 5.34: Average Absolute Amplitude extracted on 4 to 20 ms window with color scale 15 to 45 amplitude values showing the hydrocarbon sand extent

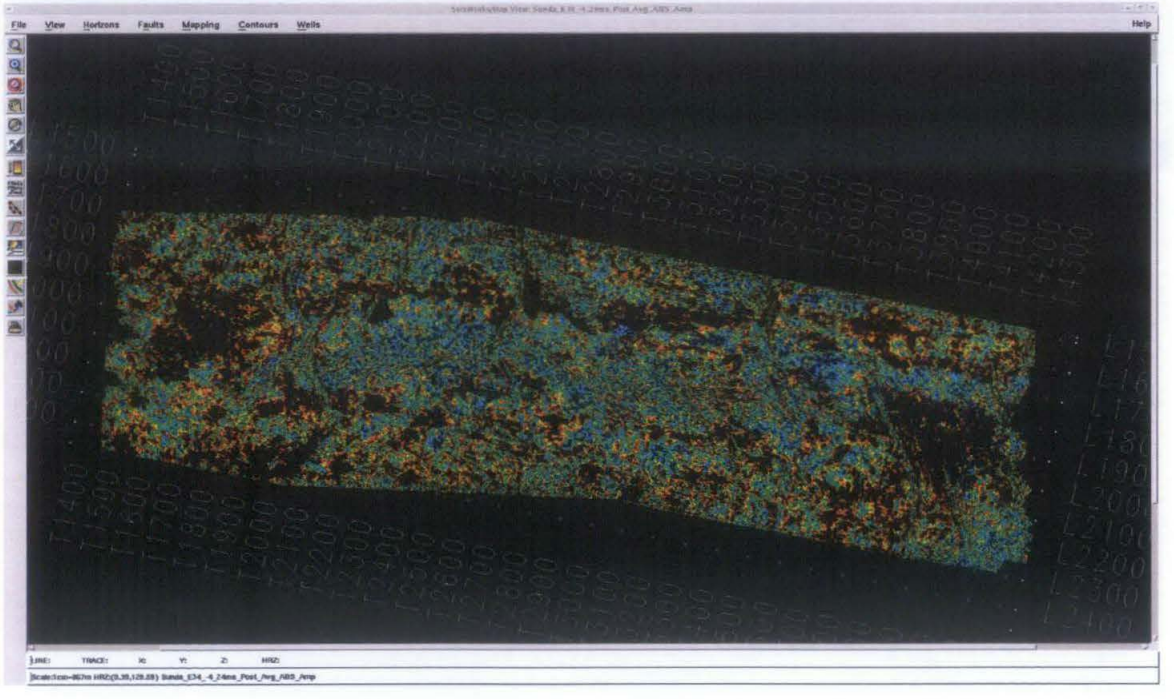

Figure 5.35: Average Absolute Amplitude extracted on 4 to 24 ms window with color scale 15 to 45 amplitude values showing the hydrocarbon sand extent

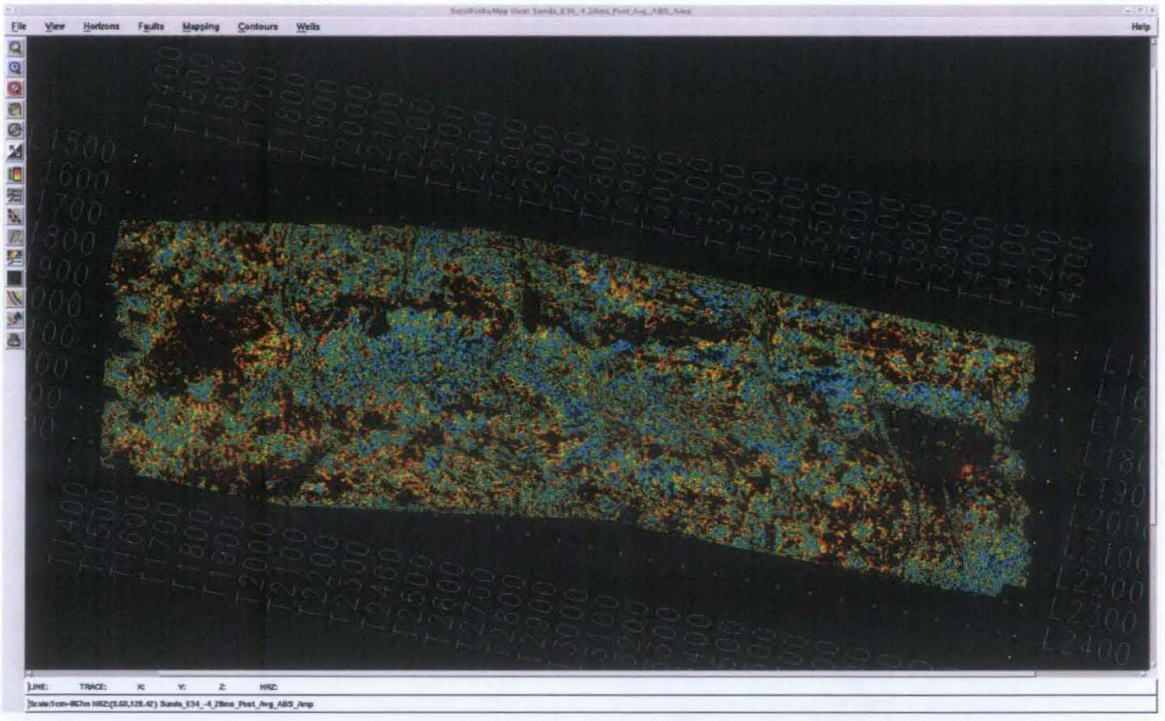

Figure 5.36: Average Absolute Amplitude extracted on 4 to 28 ms window with color scale 15 to 45 amplitude values showing the hydrocarbon sand extent

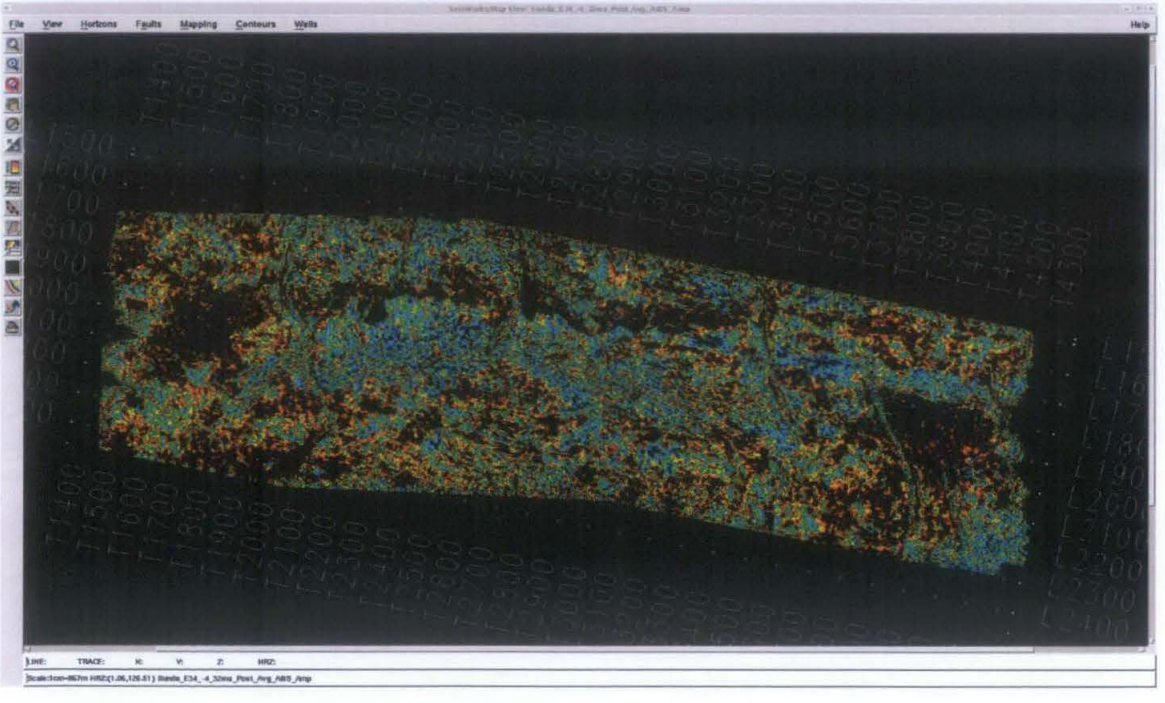

Figure 5.37: Average Absolute Amplitude extracted on 4 to 32 ms window with color scale 15 to 45 amplitude values showing the hydrocarbon sand extent

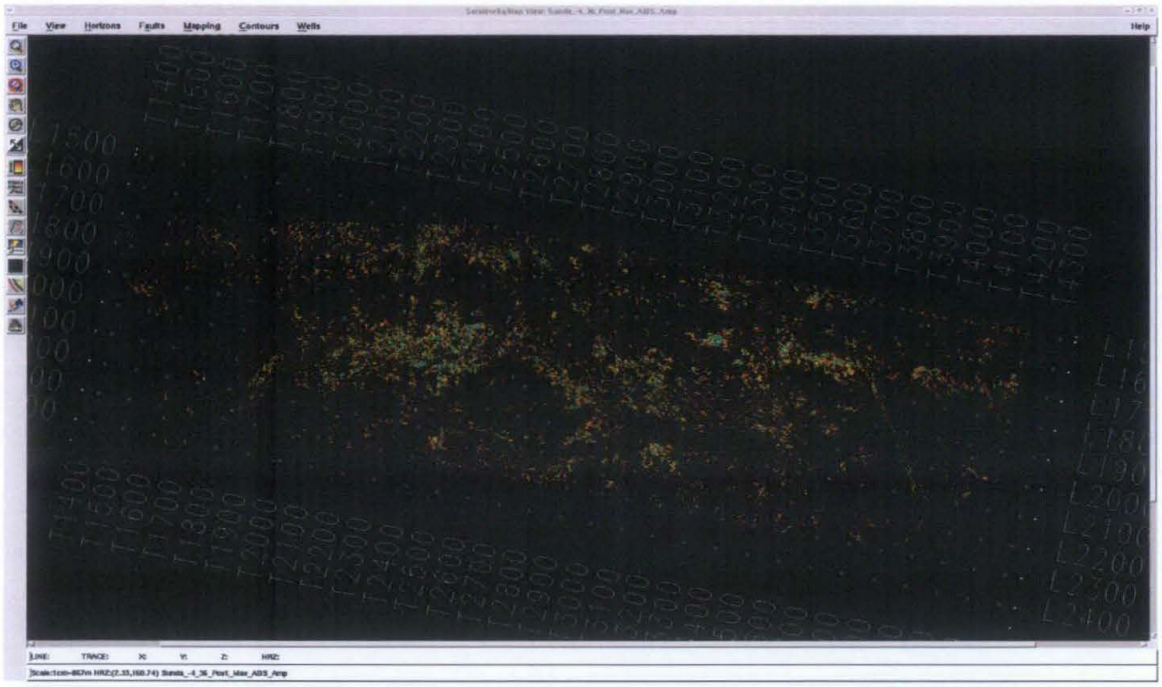

Figure 5.38: Average Absolute Amplitude extracted on 4 to 36 ms window with color scale 15 to 45 amplitude values showing the hydrocarbon sand extent

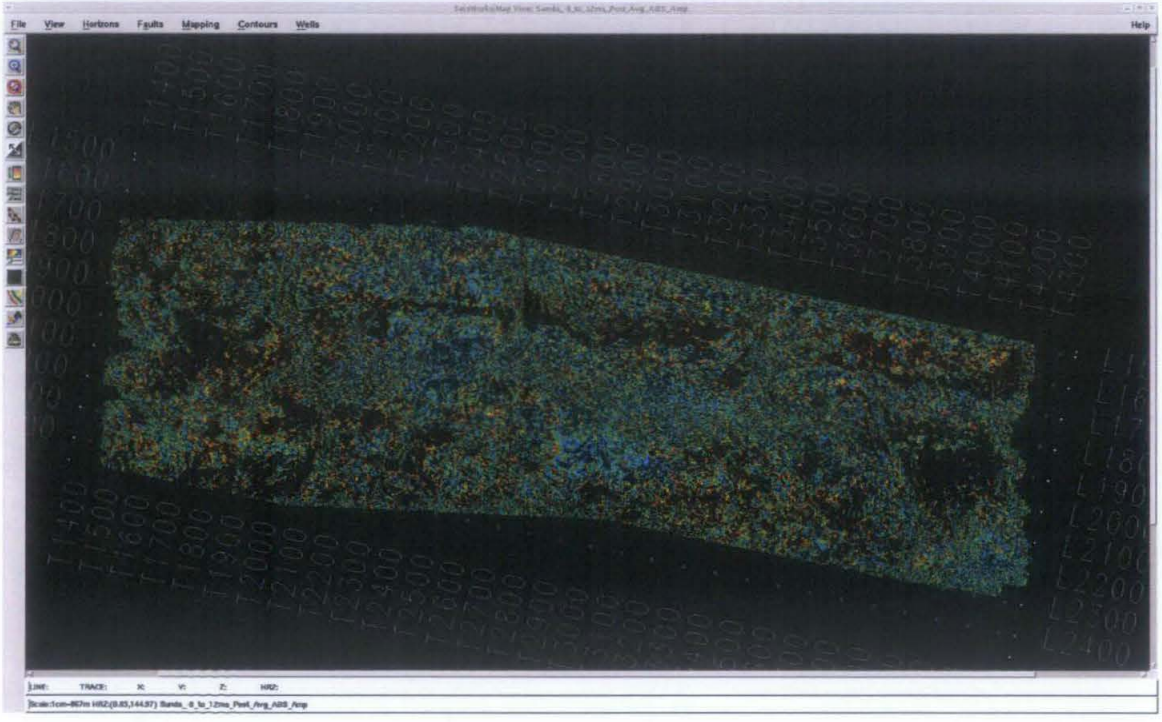

Figure 5.39: Average Absolute Amplitude extracted on 8 to 12 ms window with color scale 15 to 45 amplitude values showing the hydrocarbon sand extent

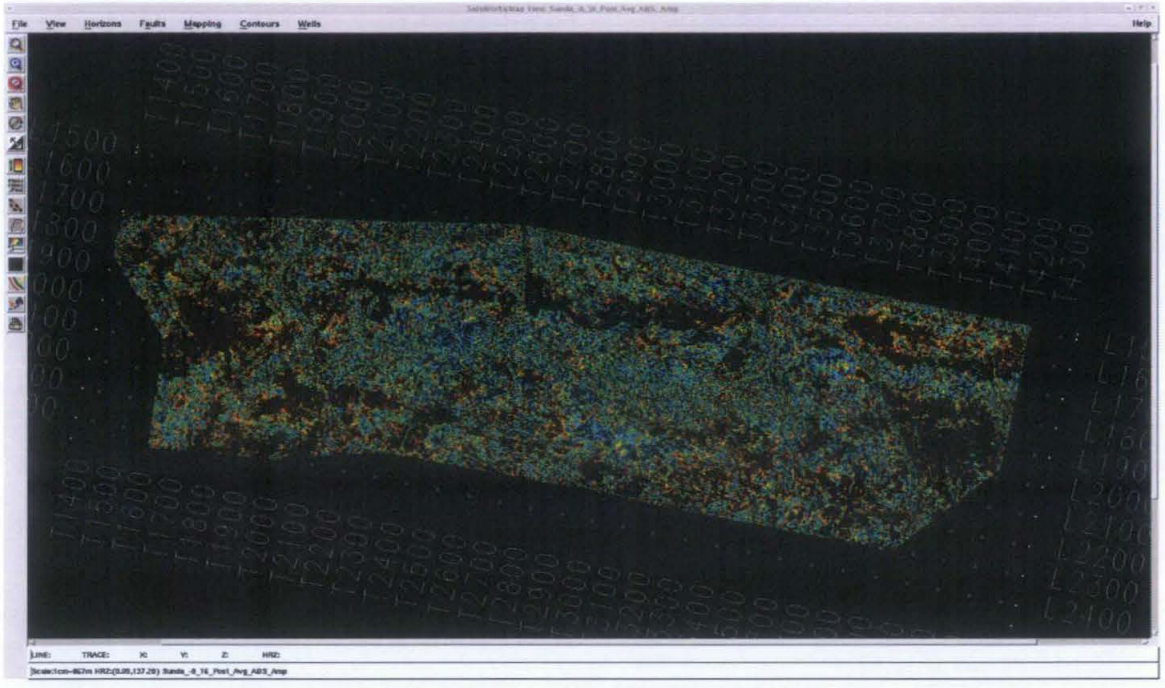

Figure 5.40: Average Absolute Amplitude extracted on 8 to 16 ms window with color scale 15 to 45 amplitude values showing the hydrocarbon sand extent

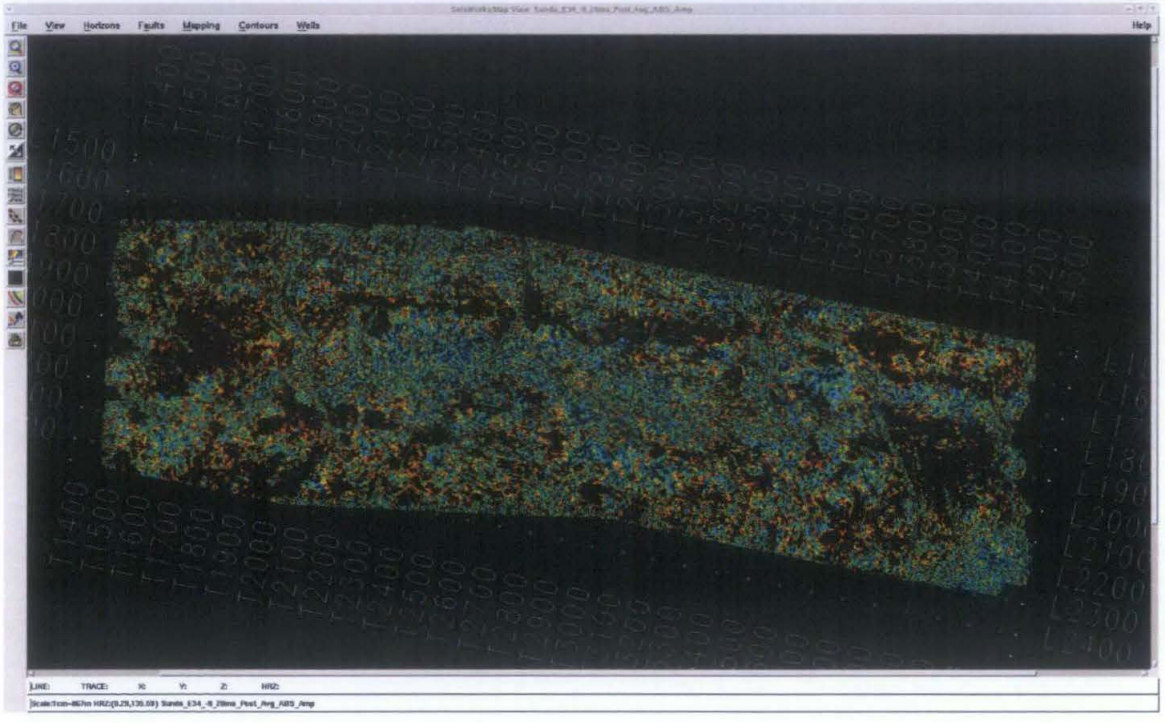

Figure 5.41: Average Absolute Amplitude extracted on 8 to 20 ms window with color scale 15 to 45 amplitude values showing the hydrocarbon sand extent

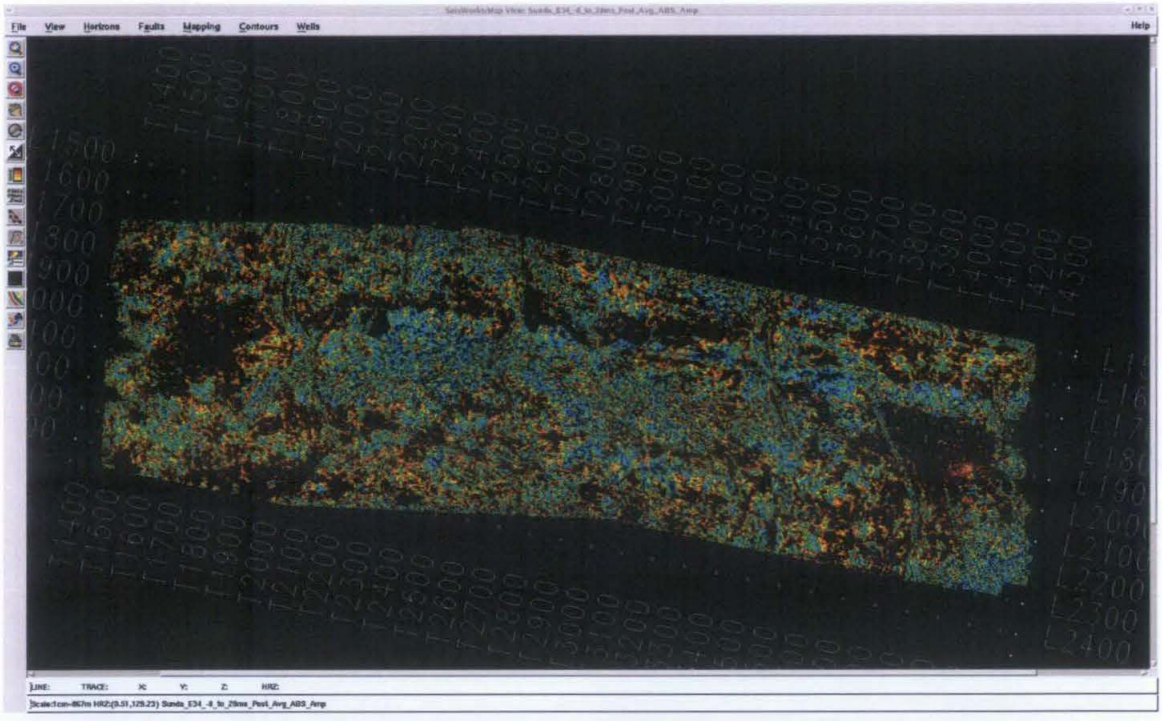

Figure 5.42: Average Absolute Amplitude extracted on 8 to 28 ms window with color scale 15 to 45 amplitude values showing the hydrocarbon sand extent

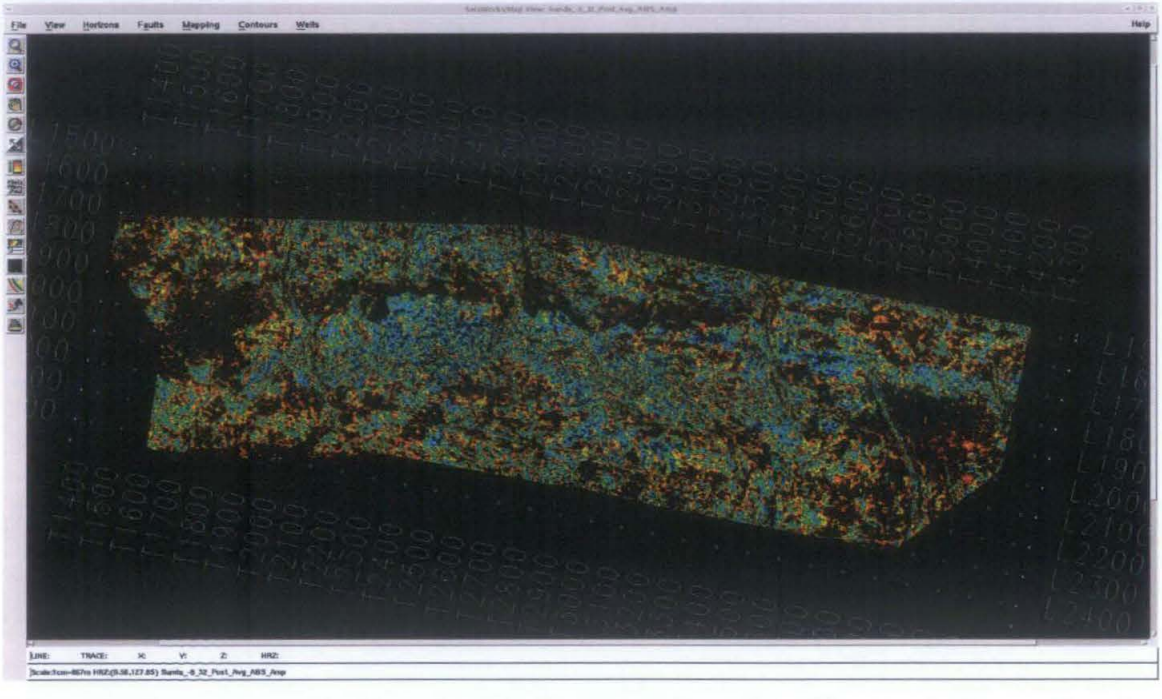

Figure 5.43: Average Absolute Amplitude extracted on 8 to 32 ms window with color scale 15 to 45 amplitude values showing the hydrocarbon sand extent

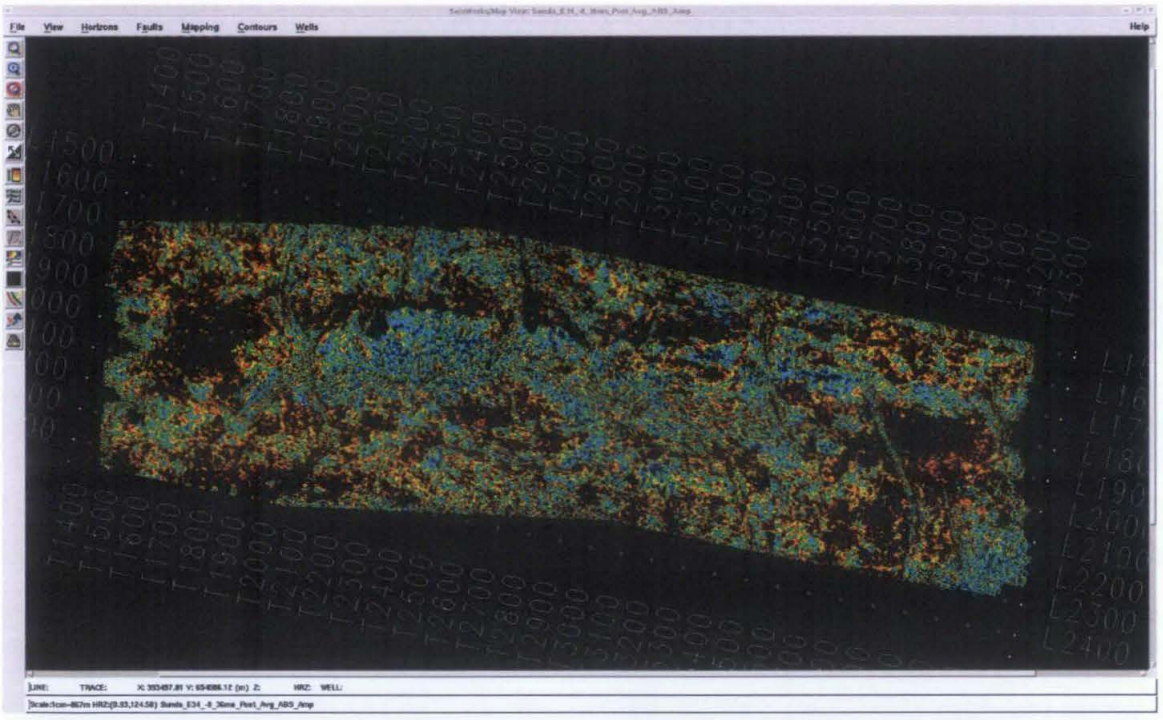

Figure 5.44: Average Absolute Amplitude extracted on 8 to 36 ms window with color scale 15 to 45 amplitude values showing the hydrocarbon sand extent

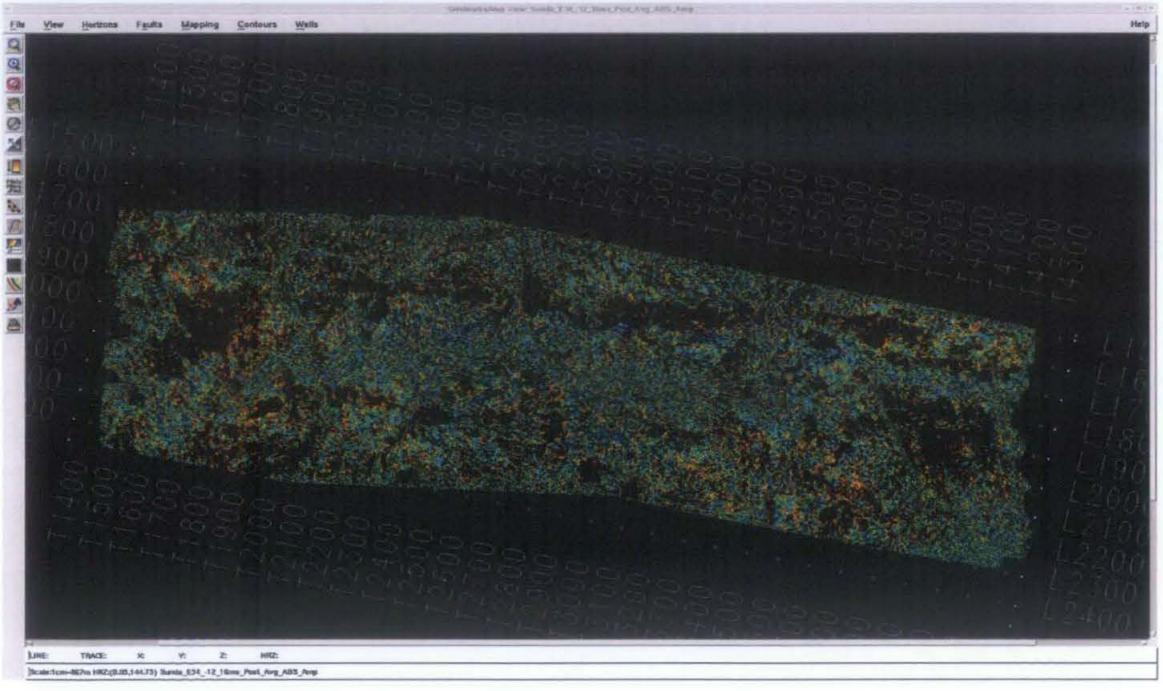

Figure 5.45: Average Absolute Amplitude extracted on 12 to 16 ms window with color scale 15 to 45 amplitude values showing the hydrocarbon sand extent

5.5.3 Maximum Peak Amplitude Results.

The Landmark Post Stack PAL does a parabolic fit trough the maximum positive amplitude in the analysis window determined earlier. The sampling rate is 4 ms and the windows used are able to identify at least an amplitude value. The same method as other attributes is adopted to determine amplitude at the hydrocarbon windows.

Maximum Peak Amplitude at HC location						
Extraction	D-03	D-08	D-07	D-01	D-02	D-A03
E34 to top HC	5	4	5	3	3	9
E34 to Bottom HC	15	10	8	21	17	12
4 to 8 ms window	8.73	9.58	8.42	14.25	9.16	8.29
4 to 12 ms window	21.37	29.04	38.71	29.53	23.39	39.55
8 to 12 ms window	20.57	15.93	46.31	31.13	13.01	15.13
8 to 16 ms window	30.84	49.37	90.73	78.98	37.04	58.05

Table 4: Maximum Peak Amplitude extracted at each well location. The yellow highlight the wells that show gas sand.

The amplitude readings are extracted from attribute map between 0 to 120 ms scale as shown on Figure 5.46, 5.47, 5.48 and 5.49. The amplitudes extracted are shown in Table 4. Result shows that the gas sand and oil sand are not clearly showing differences. For instants, the oil sand represent between 8 to 40 ms whereas the gas sand represented between 8 to 16 ms. These observation are noticed on other deviated wells too. These differences are possibly because the maximum peak amplitude takes the highest amplitude within the extraction window. Therefore, the amplitude value for larger windows may appear to dominate the highest reading, which occurs at lower range window too. For example, the highest amplitude value at 4 to 8 ms my dominate the amplitude value taken at 4 to 36 ms window if the then dominate amplitude value is maximum or anomalous. Therefore, the amplitude variations are not evenly studied on all window ranges. The maximum peak is the measurement of the highest amplitude noted on a curve as shown and explained on section 5.3.3 Maximum Peak Amplitude.

Observation on well logs on section 5.4 Attribute Analysis Methodology briefly explains that the hydrocarbon extent does not actually falls up to the peak of the curve which is approximately 124 ms. The hydrocarbon sand suppose to be within a lower peak amplitudes range between 0 ms to value lower than 124 ms. Therefore, the maximum amplitude if recorded for a bigger window range will only gives the higher range amplitudes than happens at the peak of the curve. These cases are shown clearly on Figure 5.53 for window 4 to 32 ms, Figure 5.56 for window 8 to 36 ms and Figure 5.60 for window 12 to 36 ms. Other windows showing the similar effect are window 4 to 36 ms and 8 to 36 ms. Therefore, the maximum peak amplitude is suitable for a shorter-range window in this project. The hydrocarbon extents on shorter range windows are more reliable than higher range windows.

Considering the limitation, the anomalous readings are ignored and the results for amplitude extraction shows that the preferred range for hydrocarbon sand is 5 to 40 ms. All the average maximum peak amplitude attribute maps are scaled to the mention range as shown in Figures 5.50 to 5.60.

Figure 5.46: Maximum Peak Amplitude extracted on 4 to 8 ms window with color scale 0 to 120 ms.

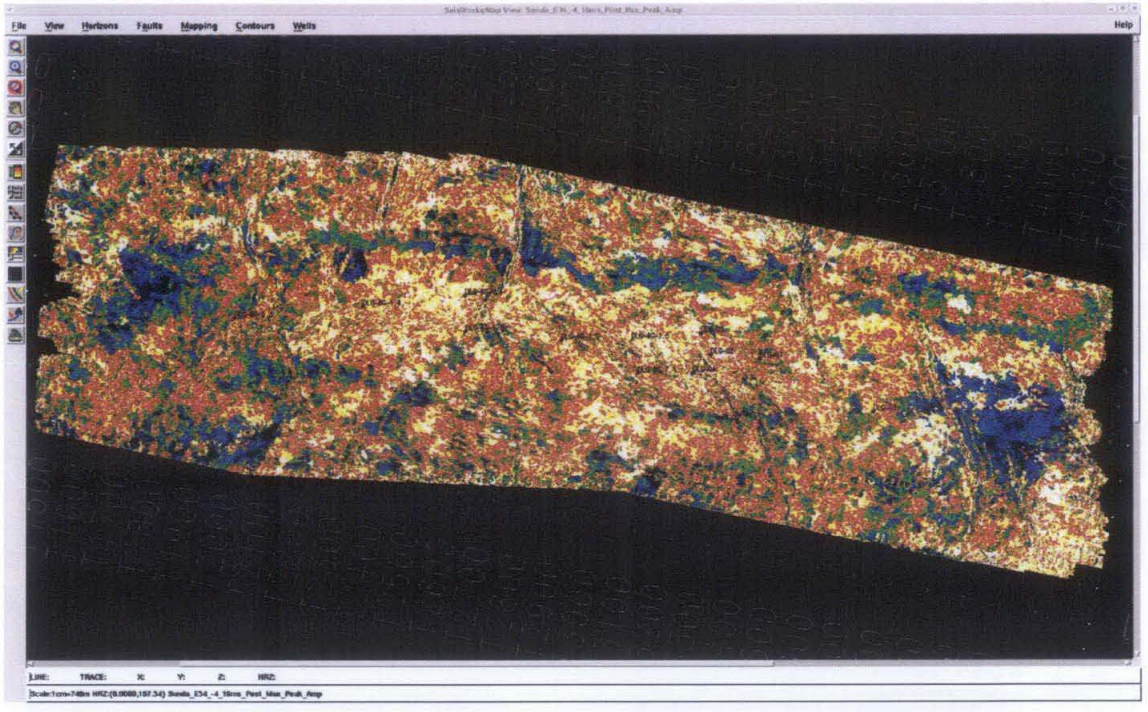

Figure 5.47: Maximum Peak Amplitude extracted on 4 to 16 ms window with color scale 0 to 120 ms.

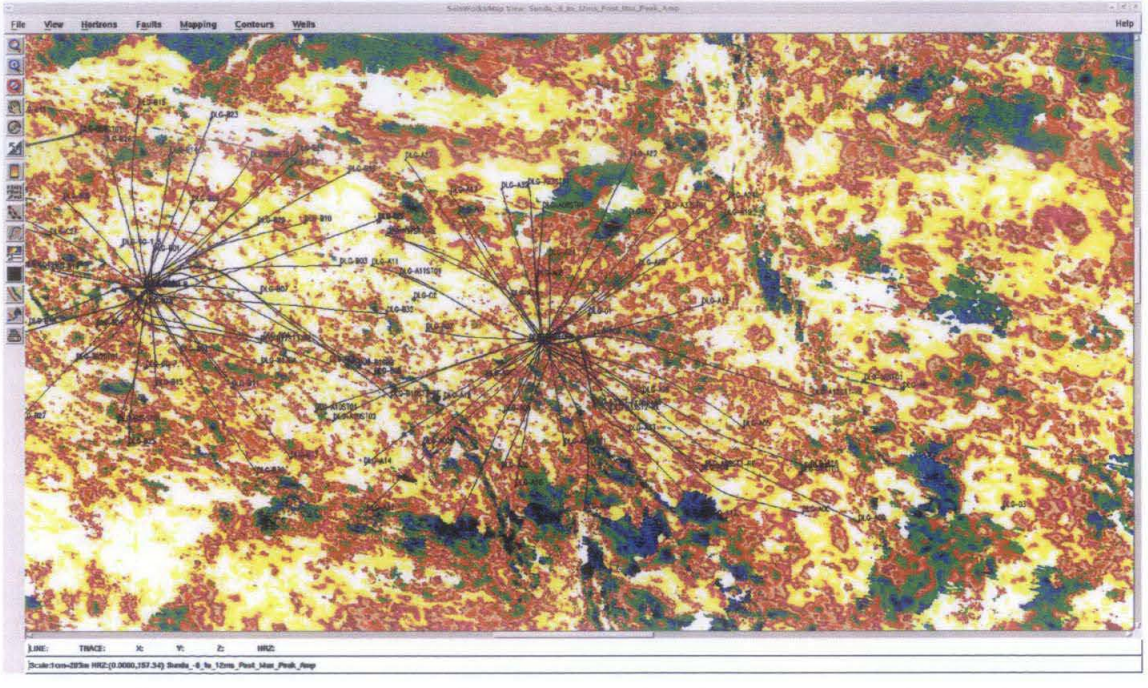

Figure 5.48: Maximum Peak Amplitude extracted on 8 to 12 ms window with color scale 0 to 120 ms. Zoom for closer look on wells.

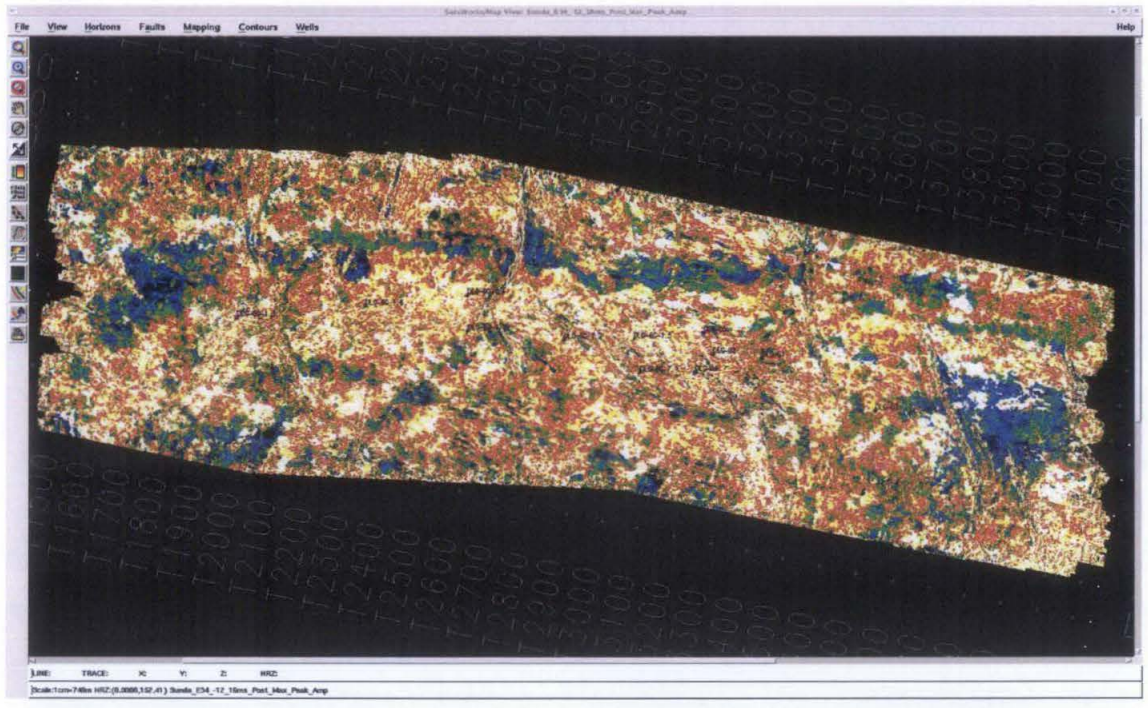

Figure 5.49: Maximum Peak Amplitude extracted on 12 to 16 ms window with color scale 0 to 120 ms.

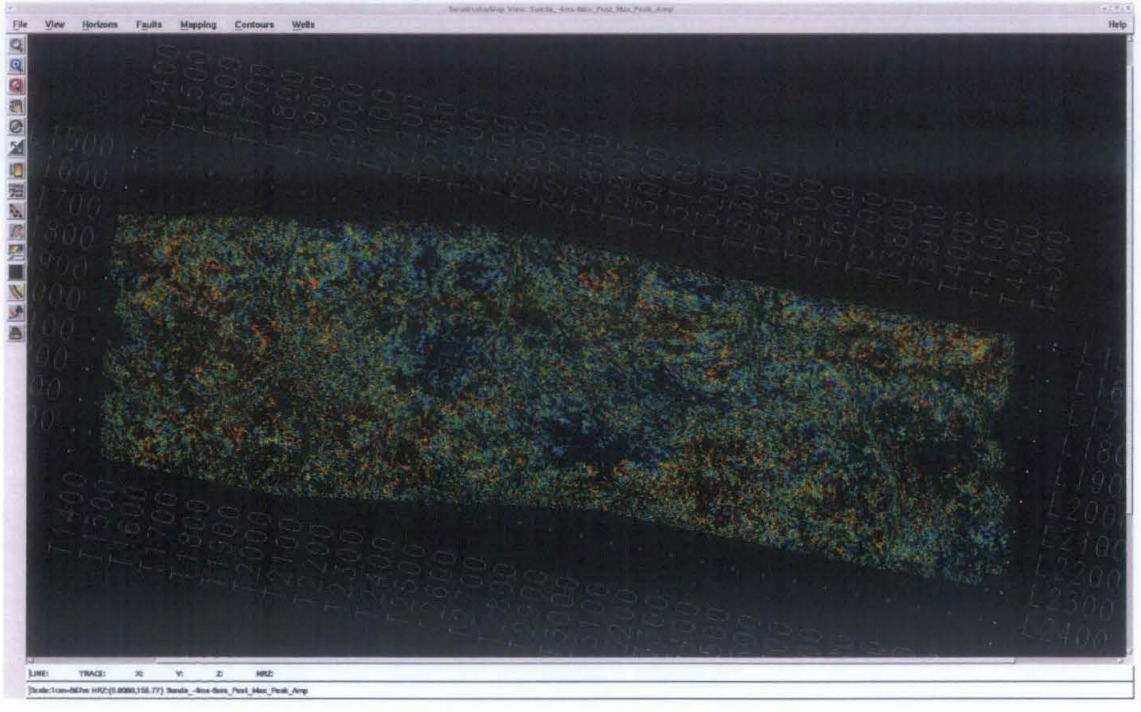

Figure 5.50: Maximum Peak Amplitude extracted on 4 to 8 ms window with color scale 5 to 45 amplitude values showing the hydrocarbon sand extent

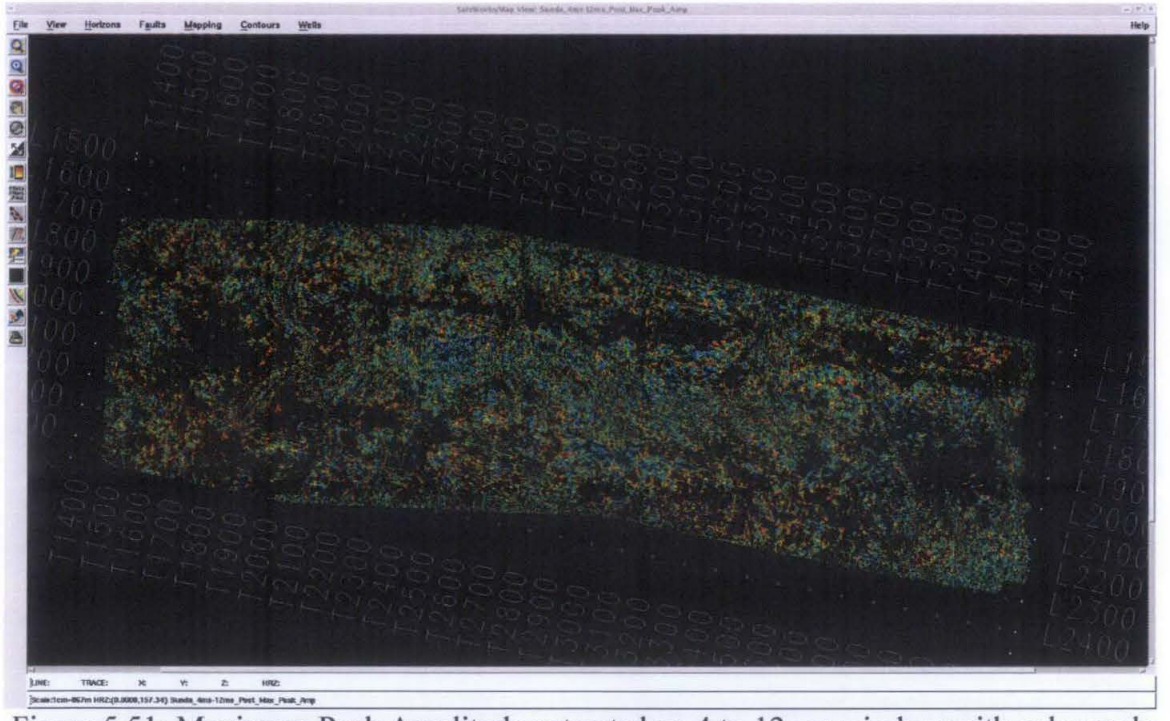

Figure 5.51: Maximum Peak Amplitude extracted on 4 to 12 ms window with color scale 5 to 45 amplitude values showing the hydrocarbon sand extent

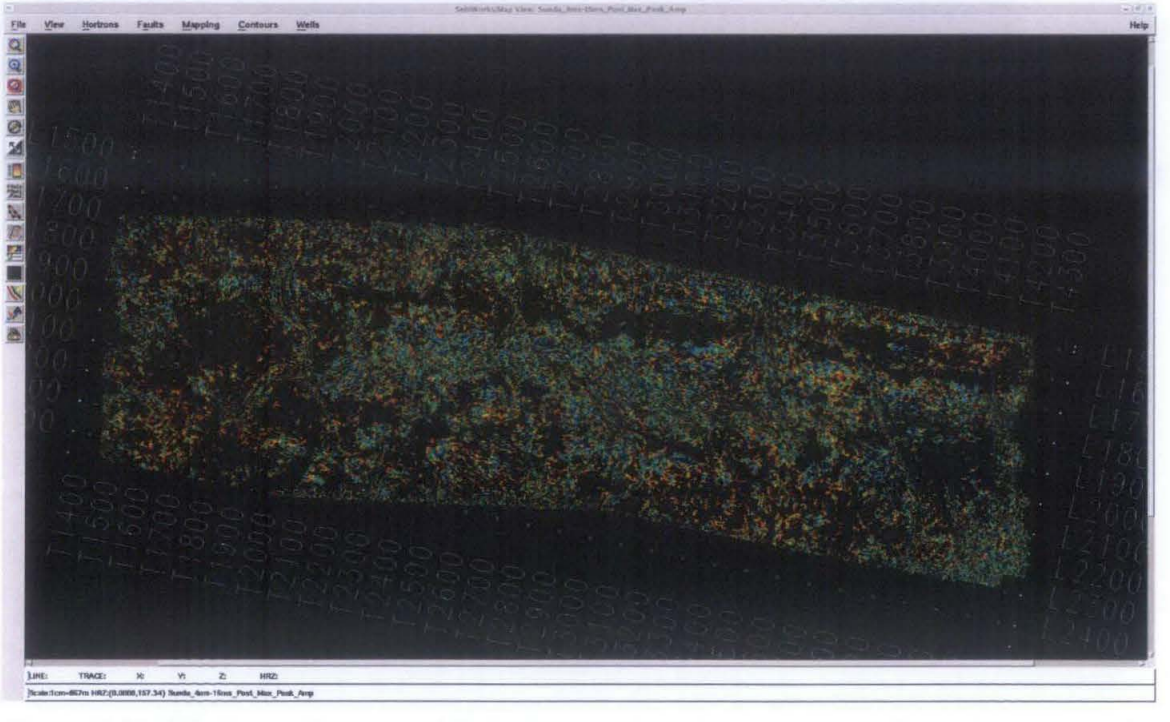

Figure 5.52: Maximum Peak Amplitude extracted on 4 to 16 ms window with color scale 5 to 45 amplitude values showing the hydrocarbon sand extent

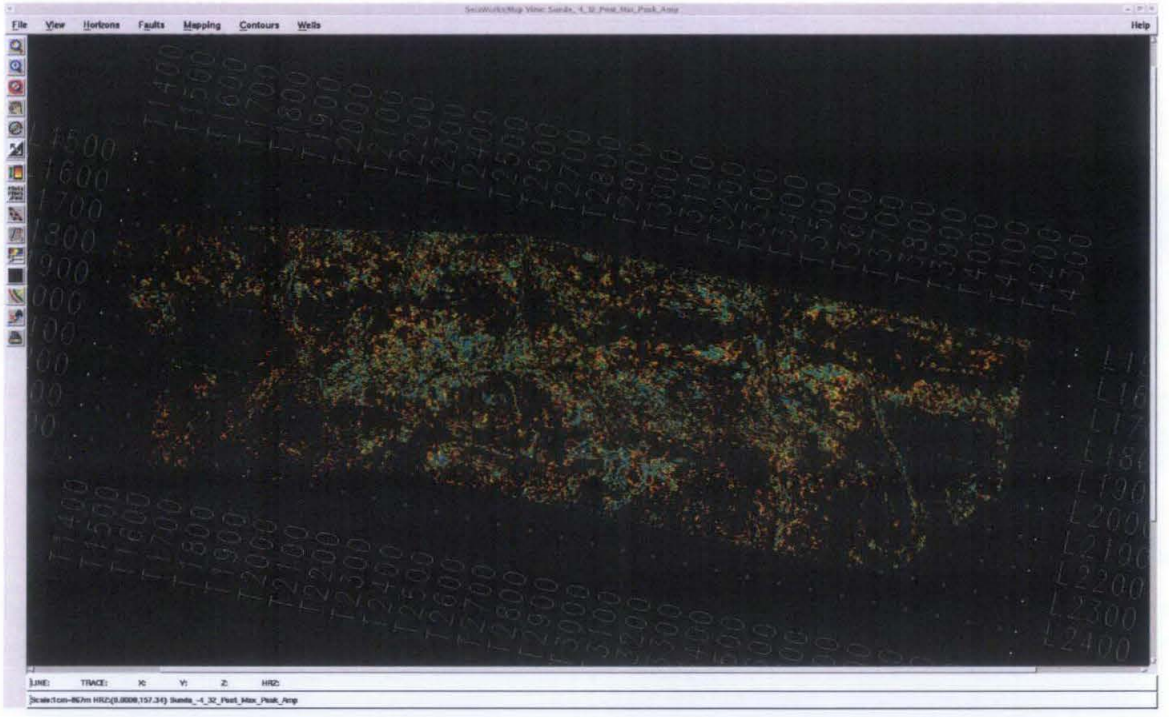

Figure 5.53: Maximum Peak Amplitude extracted on 4 to 32 ms window with color scale 5 to 45 amplitude values showing the hydrocarbon sand extent

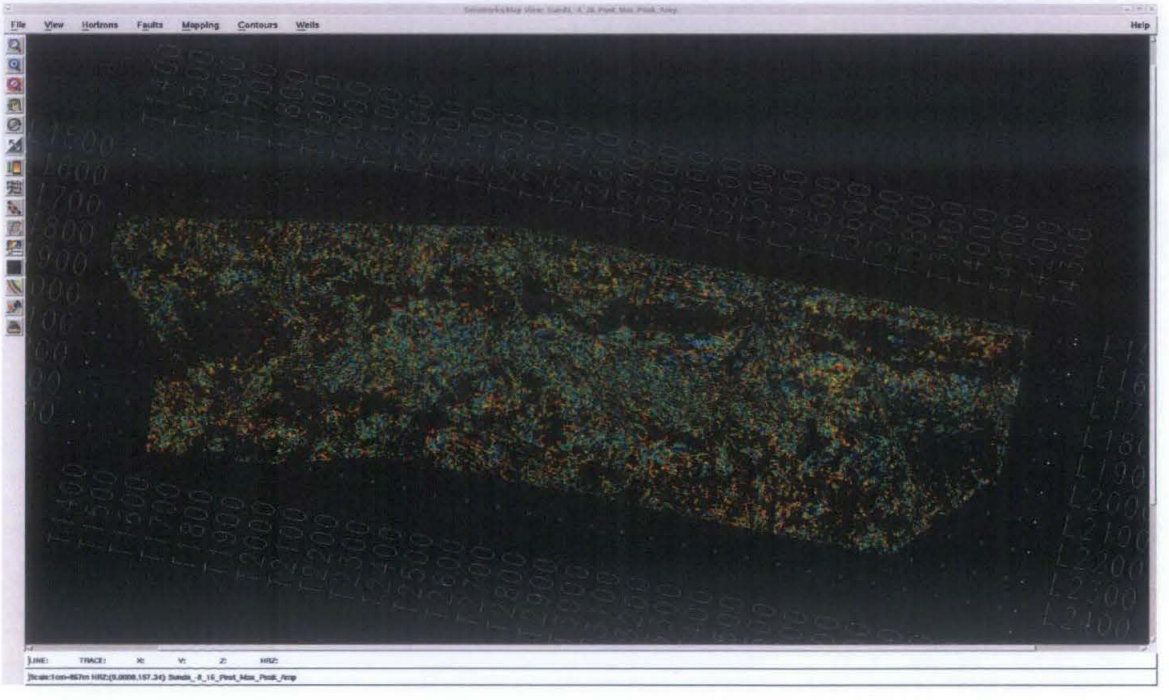

Figure 5.54: Maximum Peak Amplitude extracted on 8 to 16 ms window with color scale 5 to 45 amplitude values showing the hydrocarbon sand extent

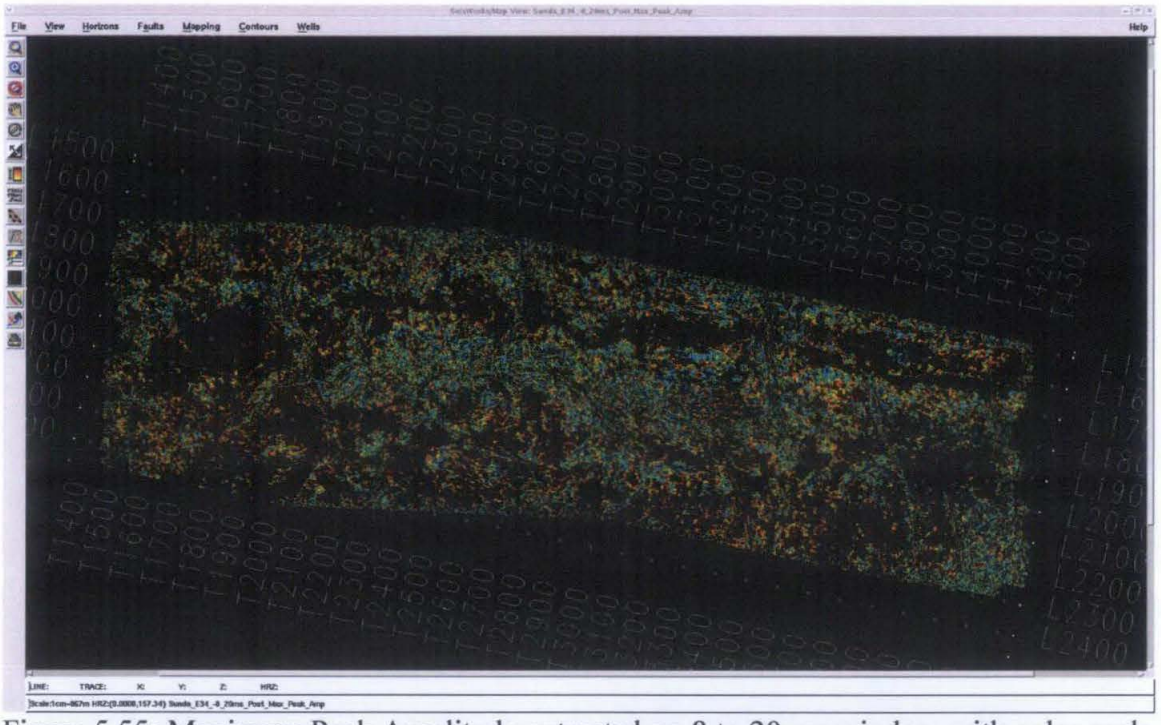

Figure 5.55: Maximum Peak Amplitude extracted on 8 to 20 ms window with color scale 5 to 45 amplitude values showing the hydrocarbon sand extent

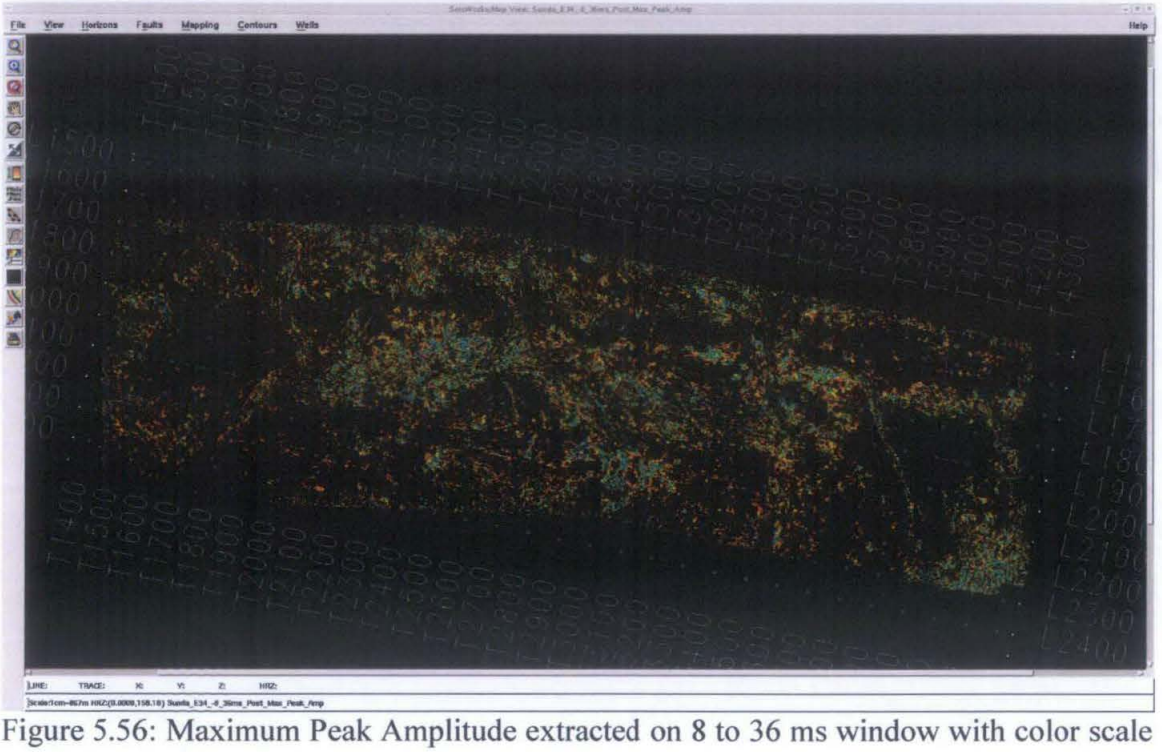

Figure 5.56: Maximum Peak Amplitude extracted on 8 to 36 ms window with color scale 5 to 45 amplitude values showing the hydrocarbon sand extent

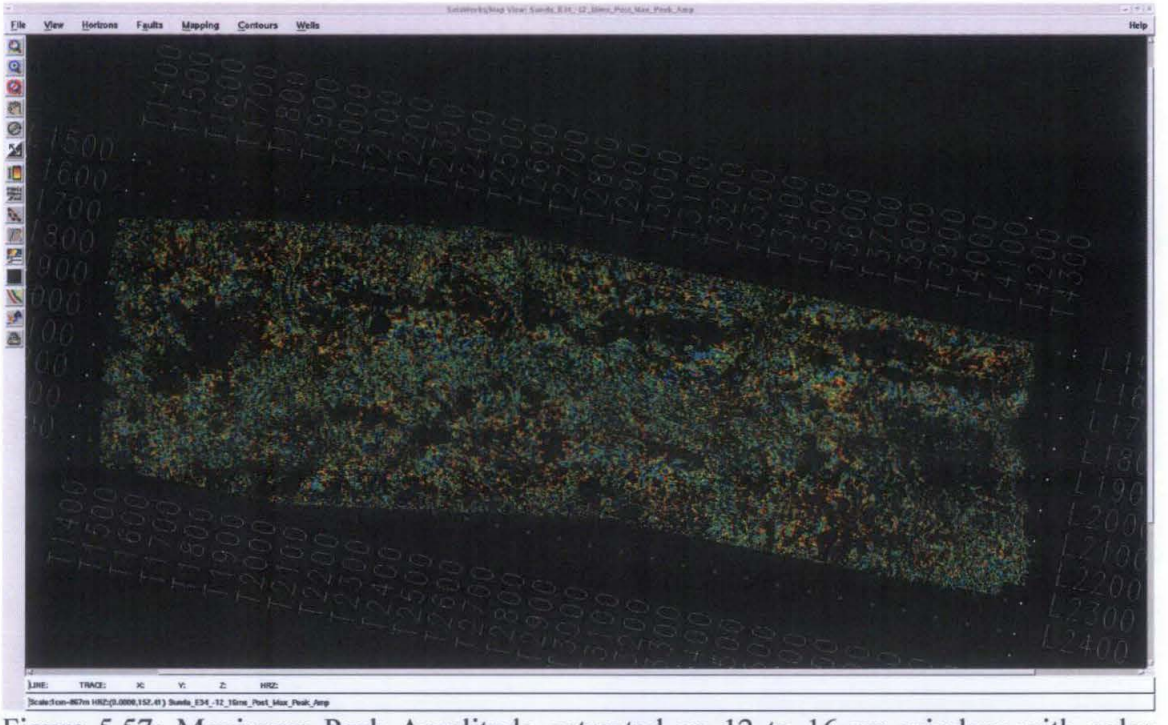

Figure 5.57: Maximum Peak Amplitude extracted on 12 to 16 ms window with color scale 5 to 45 amplitude values showing the hydrocarbon sand extent

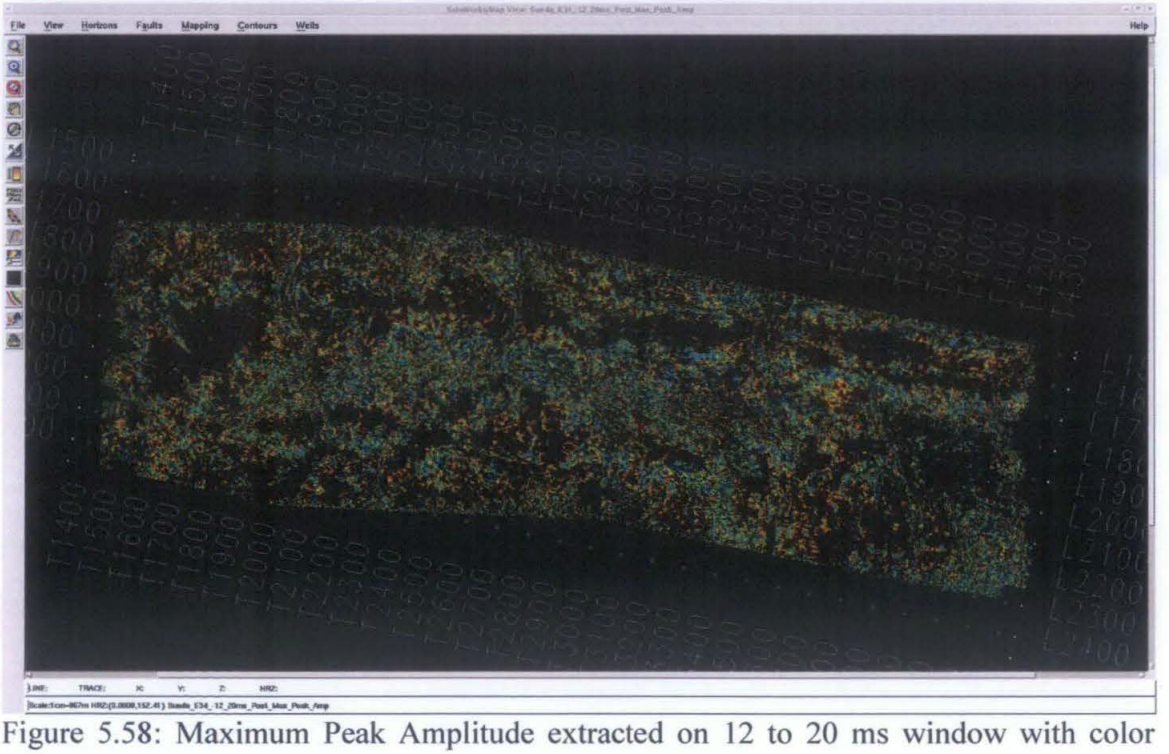

Figure 5.58: Maximum Peak Amplitude extracted on 12 to 20 ms window with color scale 5 to 45 amplitude values showing the hydrocarbon sand extent

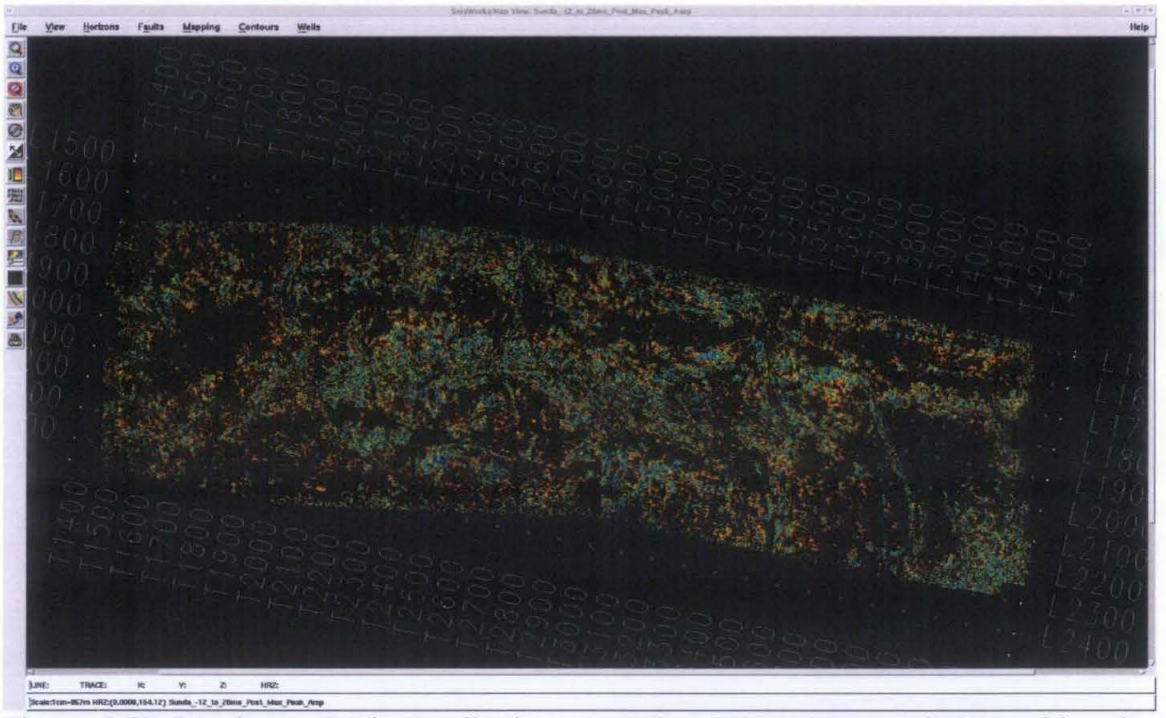

Figure 5.59: Maximum Peak Amplitude extracted on 12 to 28 ms window with color scale 5 to 45 amplitude values showing the hydrocarbon sand extent

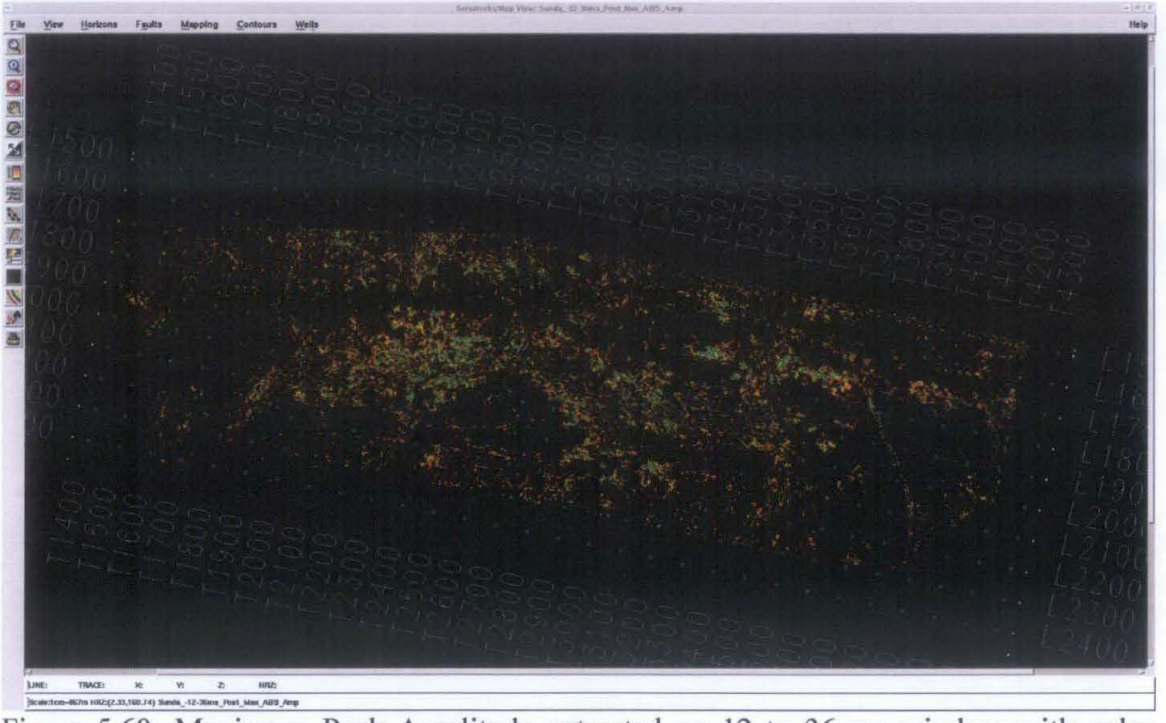

Figure 5.60: Maximum Peak Amplitude extracted on 12 to 36 ms window with color scale 5 to 45 amplitude values showing the hydrocarbon sand extent

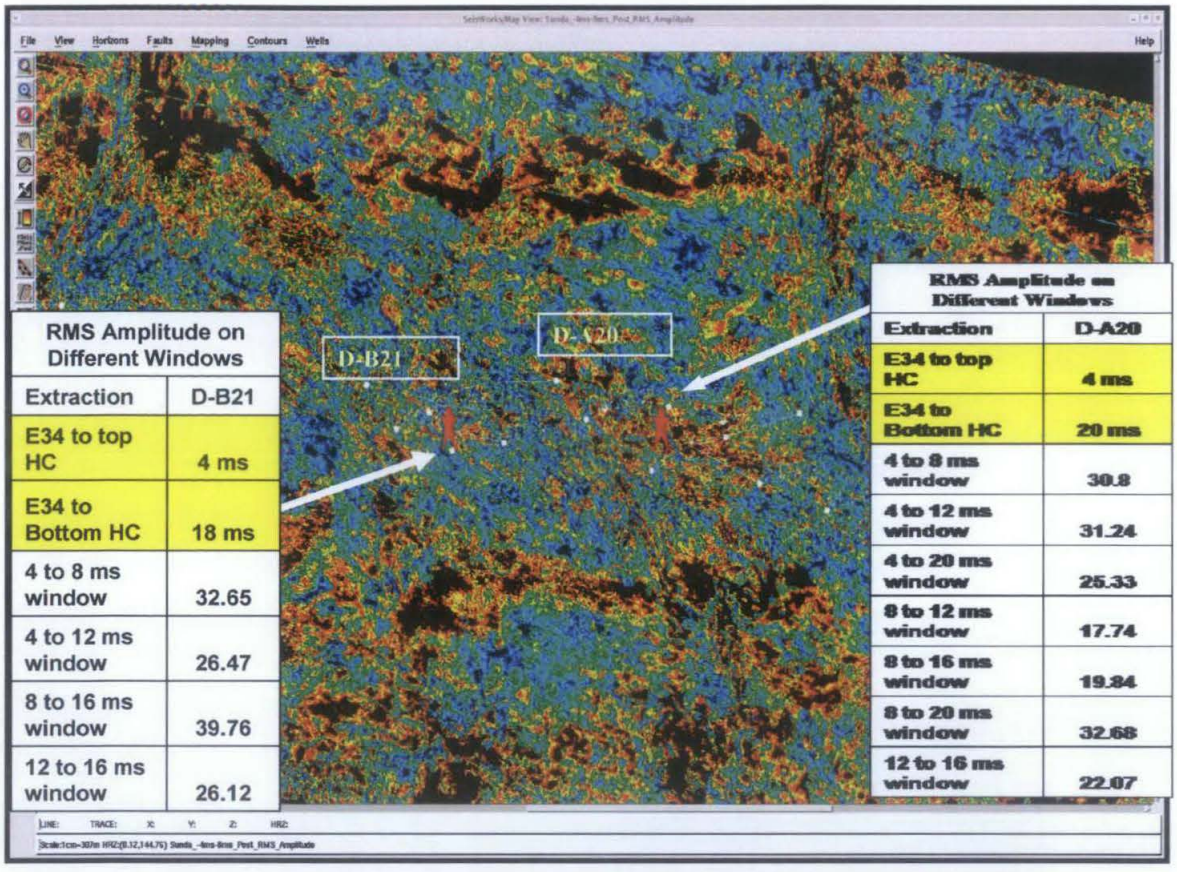

Figure 5.61: RMS Amplitude extracted at Blind wells D- A20 and D-B21 at each respective window. The amplitudes are extracted between 10 to 50 amplitude values showing the hydrocarbon sand extent

The figure 5.61 shows the results of extraction on several windows on well D-B21 and D-A20. The amplitude values were noted between 10 to 50 RMS amplitude values. Similar observations were done on other blind wells and the values are listed down on table 5.

The hydrocarbon thicknesses were defined as shown on red font on table 5. The number shows the top and bottom hydrocarbons, which were defined between the window that shows the amplitude, values within the range of 10 to 50 RMS amplitude value.

RMS Amplitude on Different Windows						
Extraction	D-D15	D-B04	D-A20	D-B32	D-B28	D-B21
E34 to top HC	4	4	4	4	4	4
E34 to Bottom HC	16	20	20	12	12	16
4 to 8 ms window	19.16	10.05	38.8	28.39	23.52	32.65
4 to 12 ms window	41.96	12.32	31.24	23.86	26.34	26.47
4 to 20 ms window	31.13	18.36	25.33	59.12	84.49	34.91
8 to 12 ms window	34.65	20.82	17.74	20.83	39.74	47.5
8 to 16 ms window	91.68	37.19	19.84	66.78	75.56	39.76
8 to 20 ms window	13.82	23.63	32.68	56.74	99.64	46.25
8 to 28 ms window	20.93	44.97	45.99	53.48	82.55	61.94
12 to 16 ms window	20.77	24.54	22.07	52.76	54.87	26.12

Table 5: RMS amplitude extracted at the well location. The green highlight shows the amplitude values at hydrocarbon sand.

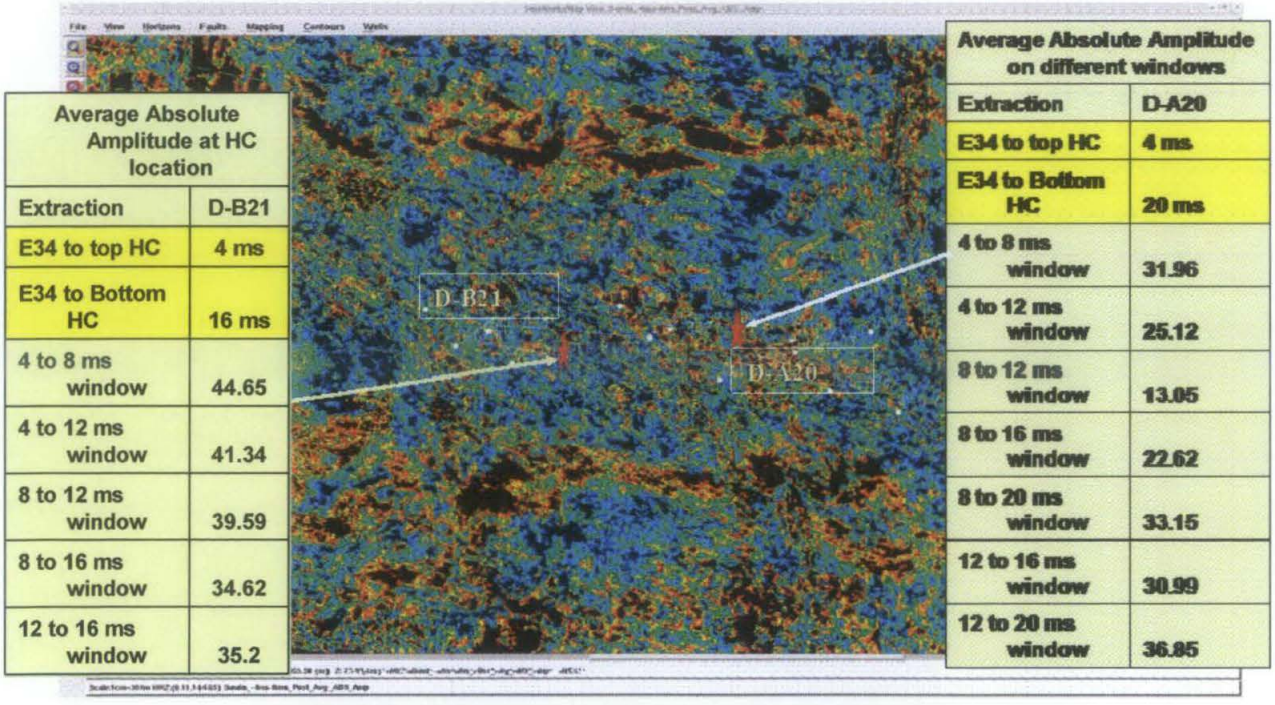

Figure 5.62: Average absolute Amplitude extracted at Blind wells D- A20 and D-B21 at each respective window. The amplitudes are extracted between 15 to 45 amplitude values showing the hydrocarbon sand extent

The similar observation for average absolute amplitude on deviated wells also agrees with hydrocarbon expected range between 15 to 45 amplitude values. The results for the six blind wells are listed on table 6.

Average Absolute Amplitude at HC location						
Extraction	D-D15	D-B04	D-A20	D-B32	D-B28	D-B21
E34 to top HC	4	4	4	4	4	4
E34 to BottomHC	16	20	20	12	16	16
4 to 8 ms window	18.05	36.24	31.96	37.96	31.32	45.66
4 to 12 ms window	19.1	17.39	25.12	26.77	20.78	41.34
4 to 20 ms window	15.39	45.21	56.57	36.5	67.02	21.75
8 to 12 ms window	20.85	42.24	13.05	18.74	12.82	39.59
8 to 16 ms window	59.32	32.51	22.62	52.49	85.81	34.62
8 to 20 ms window	13.17	34.03	33.15	51.41	80.85	22.87
8 to 28 ms window	19.47	48.52	42.06	47.51	84.94	16.44
12 to 16 ms window	7.83	17.39	30.99	44.29	28.7	35.2

Table 6: Average Absolute Amplitude extracted at the well location. The green highlight shows the amplitude values at hydrocarbon sand.

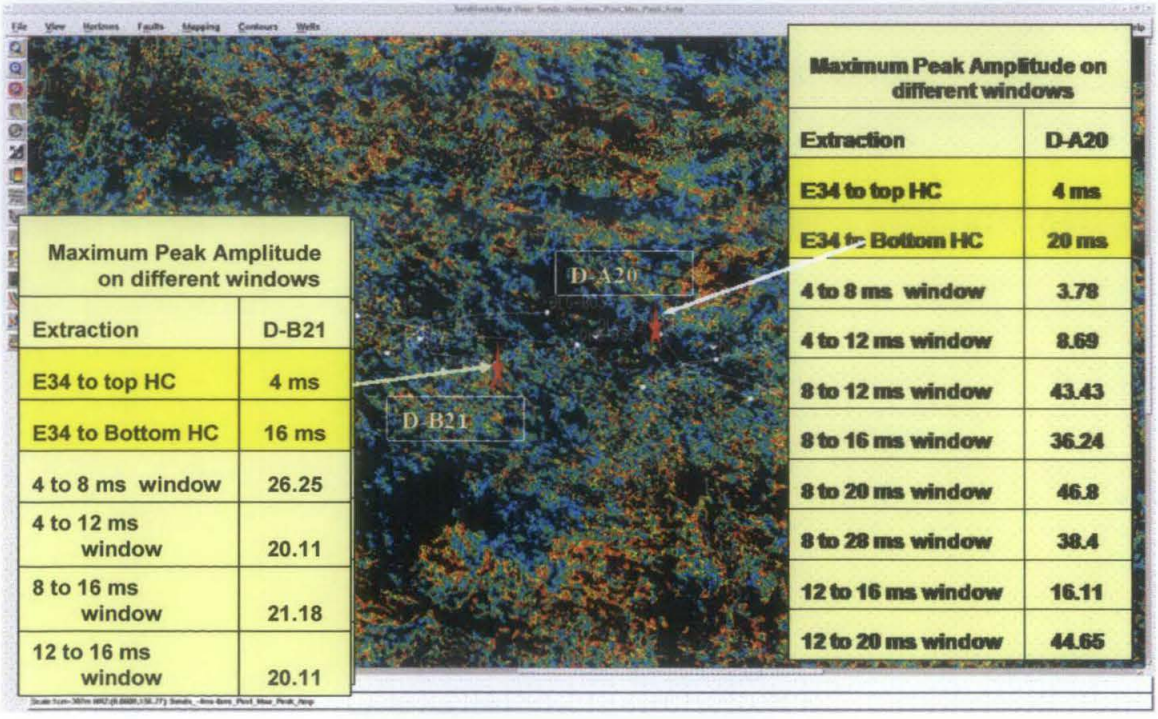

Figure 5.63: Maximum Peak Amplitude extracted at Blind wells D- A20 and D-B21 at each respective window. The amplitudes are extracted between 5 to 45 amplitude values showing the hydrocarbon sand extent

Maximum Peak Amplitude at HC location/ ms						
Extraction	D-D15	D-B04	D-A20	D-B32	D-B28	D-B21
E34 to top HC	4	4	4	4	4	4
E34 to BottomHC	16	20	20	12	12	16
4 to 8 ms window	1.42	3.17	3.78	8.7	3.1	26.25
4 to 12 ms window	108.69	12.66	8.69	18.74	31.07	20.11
4 to 20 ms window	12.52	43.61	44.07	56.35	110.63	62.76
8 to 12 ms window	1.89	17.8	43.43	41.85	17.2	58.44
8 to 16 ms window	6.71	21.68	36.24	55.56	113.08	21.18
8 to 20 ms window	78.75	21.69	38.4	76.57	92.98	21.18
8 to 28 ms window	98.72	46.63	46.8	79.21	77.15	64.19
12 to 16 ms window	16.61	46.63	16.11	74.14	76.36	64.19

Table 7: Maximum Peak Amplitude extracted at the well location. The green highlight shows the amplitude values at hydrocarbon sand.

Similar observations as for other amplitude attributes are conducted on Maximum Peak amplitude attribute. The results from the Maximum Peak amplitude extraction on vertical wells agrees with the blind well results. The hydrocarbon sand varies between 5 to 45 amplitude values. Results observed on deviated wells are shown on Table 7 (Maximum Peak Amplitude).

These values were checked on well markers at respective vicinities to confirm the consistency of the method. Results of observation from two wells were shown on Figure 5.62 and Figure 5.63 respectively. The D-A20 wells shows a depth of 16 ms whereas the D- B21 shows a depth of 14 ms. These results agree with the observation on amplitude maps where the D-A20 shows a depth of 16 ms and the D-B21 shows a depth of 12 ms. The depth measurement here can give an error of ± 2 ms because the windows are measured on 4 ms interval considering the seismic sample rate of 4 ms.

Similar observations were done on all other wells and the hydrocarbon thickness is noted to be within the range with error of ± 2 ms. Anyhow, ambiguous values does present on the records, which cannot be avoided. This is probably because of the final migrated data used on this project is only 8 bit that may cause amplitude clipping. Furthermore, the studied windows are small with minimum of two samples on 4 to 8 ms and maximum is

up to 6 samples on 8 to 28 ms window extraction. Considering the 8-bit data limitation, the amplitude results that showing reasonable amplitude value are noted to define amplitude ranges that classify the hydrocarbon sand.

Shortly, the amplitude extraction method introduced on this project agrees on the blind wells. Therefore, this method confirms to represent the hydrocarbon thickness at each location within the X field.

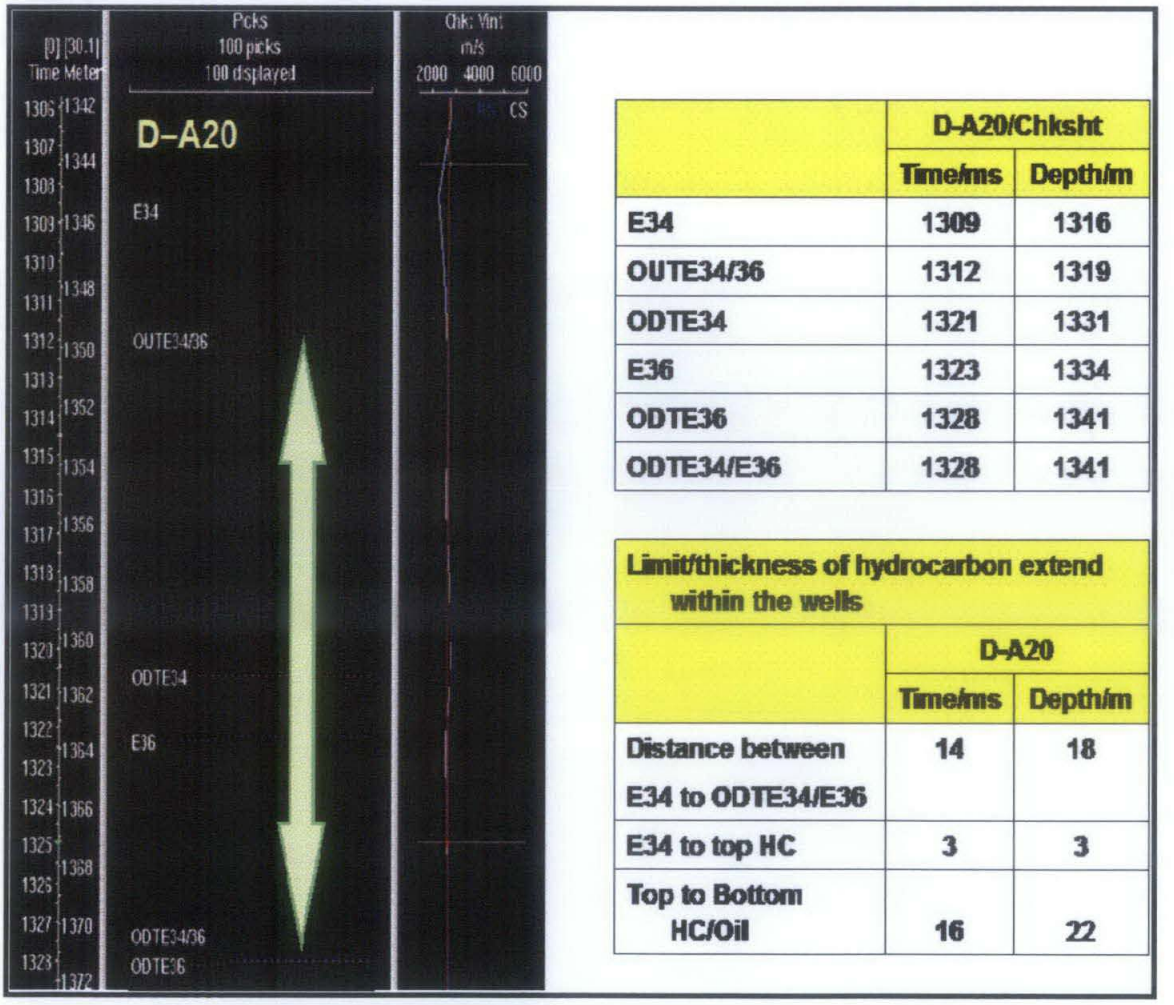

	D-A20/Chksht	
	Time/ms	Depth/m
E34	1309	1316
OUTE34/36	1312	1319
ODTE34	1321	1331
E36	1323	1334
ODTE36	1328	1341
ODTE34/E36	1328	1341

Limit/thickness of hydrocarbon extend within the wells		
	D-A20	
	Time/ms	Depth/m
Distance between E34 to ODTE34/E36	14	18
E34 to top HC	3	3
Top to Bottom HC/Oil	16	22

Figure 5.64: Limit/thickness of hydrocarbon extend observed at well D-A20. Left diagram shows the limit observed on well D-A20 check shot corrected markers. Right shows the thickness of hydrocarbon on Time/ms and Depth/m.

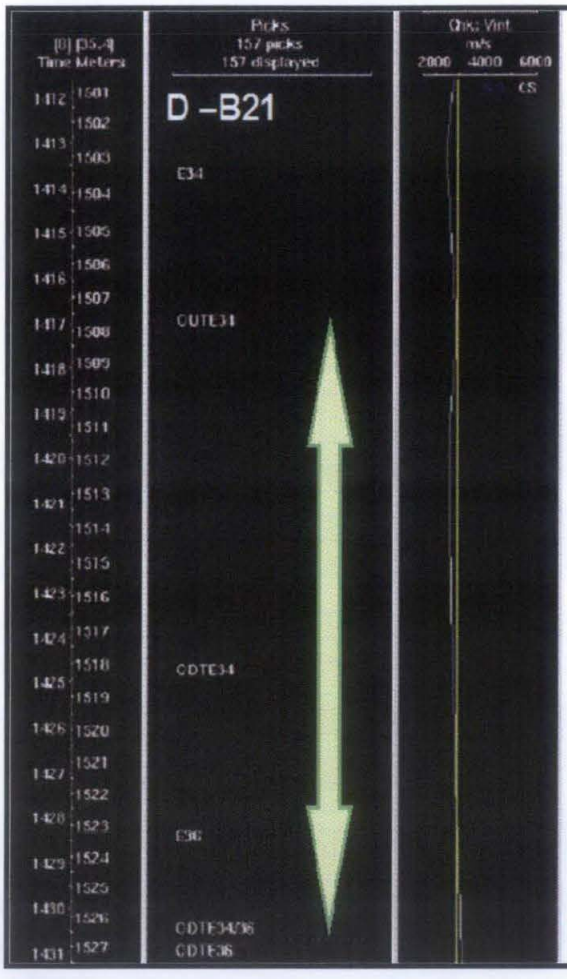

	Dig-B21/Chksht	
	Time/ms	Depth/m
E34	1414	1304
OUTE34/36	1417	1307
ODTE34	1424	1316
E36	1428	1321
ODTE36	1431	1324
ODTE34/E36	1431	1324

Limit/thickness of hydrocarbon extend within the wells		
	Dig-B21	
	Time/ms	Depth/m
Distance between E34 to ODTE34/E36	17	21
E34 to top HC	3	4
Top to Bottom HC/Oil	14	17

Figure 5.65 Limit/thickness of hydrocarbon extend observed at well D-B21. Left diagram shows the limit observed on well D-B21 check shot corrected markers. Right shows the thickness of hydrocarbon on Time/ms and Depth/m.

5.7 Summary: Results of hydrocarbon sand detection.

The amplitude variation has been adopted to define the hydrocarbon sand extent. The E34E36 reservoirs are considered as homogenous and the amplitude values throughout the reservoir are considered to be on a specified range for each type of attributes. These values are taken at the well markers at various vertical wells. The markers are check shot corrected and correspond to the actual depth where the hydrocarbon sand occurs.

All the three type of attributes used in this project for hydrocarbon sand distribution shows variation for different range of windows. The amplitude ranges defined for each window differ due to the mathematical computation adopted by each attributes. Generally, the RMS amplitude as the result of root mean square of the amplitudes shows slightly lower value compare to Average Absolute and Maximum peak amplitudes.

The maximum peak amplitudes does not give detail image for a larger window observation such as 4 to 36ms or 8 to 36 ms. This is probably because the hydrocarbon indication on the well markers on seismic does not actually shows the peak amplitude as hydrocarbon sand. On another word, the hydrocarbon sand is shown between the zero crossing and peak location of a single wavelet. Therefore, once peak amplitude is achieved then the corresponding windows tend to show the same peak amplitude value. Considering this constrain, the maximum peak amplitude must be derived on small scale windows.

Both RMS and Average Absolute amplitude attributes show the hydrocarbon sand distribution for various windows for specified ranges. The Hydrocarbon sand distribution within the Unit area of X field is seen to be averagely continuous within the E34E36 reservoirs on both the attributes. The Average Absolute amplitude is able to show the oil and gas distribution on hydrocarbon sand. The impedances log and reflection coefficient characteristic are used to define these hydrocarbon distribution on Average Amplitude attribute.

The hydrocarbon sand extent does tie with the E34 structure map. The closure within the anticline structure was mapped clearly on all attribute maps. These amplitude maps will be useful to define the hydrocarbon sand distribution within the studied area.

The studied was conducted on Unit area because the availability of well logs. The amplitude attribute maps are more accurate for Unit area compare to Eastern and Western area. More studies and well analysis can be used to confirm the attribute studies on Eastern and Western area. Anyway, there are high possibilities that the amplitude ranges may change. This is due to the sealing capacity shown by the major faults, which has compartmentalized the units. Anyway, the general steps to be followed with remain the same as the Unit area. The crucial part of this survey is to have a calibrated and check shot corrected well data and seismic data with good resolution. Post-stack amplitude attributes extraction method is a manageable approach for observing large amounts of data in initial reconnaissance investigations. Therefore, in future, ADD Oil Company should consider this available information to further study the Western and Eastern field.

On this project, the final migration seismic data has been utilized. Stacking is an averaging process that eliminates offset and azimuth related information. Input data could be CDP stacked or migrated. The time migrated data will maintain their time relationships, hence temporal variables, such as frequency, will also retain their physical dimensions. The major lack on this project is the 8-bit data used as an input for attribute extraction. These data was processed on year 2002 and data made available for loading into workstation is only of 8-bit. Furthermore, the workstation capacity at the research centre currently cannot allocate space for 32-bit data loading. Landmark Seiswork recommend using 16-bit or 32-bit files, if available, for attribute extractions since these formats give greater data precision.

CHAPTER SIX: CONCLUSION

6.1 Method Conclusion

The final migrated seismic data made available on this project was sufficient for the interpretation work. The 8-bit data utilized in the attribute analysis work are considered not adequate for attribute extraction. However, due to unavailability, the 8-bit data was used as input to PAL attribute analysis software and taking into account that valuable information can be lost due to clipping, and that the resolution is not as good as with 16-bit or 32-bit data. Therefore, the initial assumption was made prior to conduct the attribute extraction was that any anomalous amplitude reading shown from amplitude extraction are not taken into consideration.

The amplitude extraction method using various attribute analysis are proven works for the X field seismic data. The blind wells indicate the precision of this study on how well the well information ties with the amplitude extraction analysis. These extracted amplitude maps at different window ranges can be used to define the hydrocarbon occurrence at each interval and together provide information to ADD Oil Company on expected amount of hydrocarbon that can be recovered at the period of drilling at the mentioned window intervals.

The seismic and well information are integrated to illustrate the relationship between geologic and geophysical events. The E34 horizon interpretation is considered the most crucial to achieve the objective of this project. The E34 horizon interpretation used the Landmark Seiswork software to tie time interpretation with wells via a 1D synthetic seismogram, thus matching the time data with depth data. Therefore, the interpretation made is considered as precise as possible.

The fault interpretation was done using Poststack ESP and consistently checked with Poststack Curvature attribute analysis. The Planner Dip Constrained method is sufficient to detach event termination such as faults and other discontinuity features. The Semblance and Manhattan method adopted in the ESP Planner has enabled the software

to calculate the similarity and unsimilarity between traces on a scanning window process. The advantage of dissimilarity data is that it reveals and heightens lateral seismic changes that often relate to geologic changes. These dissimilarity measurements yield the visual identification of such features as faults, facies changes, and other geologic patterns. Faults and stratigraphic changes often stand out as prominent anomalies feature. The precision of the interpretation was enhanced by cross checking the ESP interpreted results on Curvature attribute analysis. The fault information has been crucial to obtain the best-interpreted E34 horizon prior to extract the hydrocarbon sand extent on attributes. The results obtained are satisfactory and meet the requirement to enhance E34 horizon interpretation accuracy.

RMS amplitude, Average Absolute amplitude and Maximum Peak amplitude attributes can give precise attribute maps to detach the hydrocarbon sand extent. The results are satisfactory and drive with the well markers information within the Unit area. Both RMS and Average Absolute amplitude attributes show the hydrocarbon sand distribution for various windows for specified ranges. The maximum peak amplitudes do not give detail image for a larger window observation. Therefore, all the three attribute methods should be studied together and observe the variation on them to obtain the best hydrocarbon sand extent.

6.2 Recommendation

Amplitude is one of the key geophysical parameters that determine the changes either geological or non-geological changes on seismic data. This project only checked on amplitude variation to define the litological changes, which was classified as hydrocarbon sand as the information adopted from various geological reports. More parameters need to be studied to enhance the accuracy of this prediction on actual. Other parameters such as porosity, permeability and water saturation are among the key elements that need to be studied. Considering the numbers of fault within this block, the faults sealing capacity associate with the hydrocarbon migration pathway must be incorporated on this project.

The amplitude extraction classification on this project at X field may only be used at this area only. The amplitude range may change for different area, which may be represented by different range of amplitudes. Anyway, the similar method may be adapted for different area considering the amplitude as the major direct hydrocarbon indicator (DHI) used to determine hydrocarbon.

The overall performances to identify the hydrocarbon sand in this project were based on well information and the final migrated seismic data interpretation. The well here refers to vertical exploration wells that shows hydrocarbon and shown as well markers on well logs. Wells within the X field Western, Eastern and Unit areas are covered with wells mainly deviated wells with few exploration vertical wells. Assumption made in this project was that the E34E36 reservoir has no drastic amplitude variations. Considering this statement, more work should be carried out to study the deviated wells. The wells with deviation survey information should be used to conduct this study. The new hydrocarbon windows could be established once we have studied all the available deviated wells.

The 2002 seismic data over the X field does not provide seismic data with good resolution below and within the E34E36 reservoirs. The focus and objective were for imaging the shallower reservoirs at that time of exploration. The seismic acquisition acquired on 4800 metres cable is not actually adequate to image the Top E34E36

reservoirs, which extent up to 2500 ms depth. Therefore, it is recommended to conduct another 3D seismic acquisition with finer acquisition parameters and longer cable offset.

The X field reservoirs are classified as stacked reservoirs. Therefore, an accurate horizon interpretation should be carried out prior to attribute extraction. E34 interpreted horizon was utilized as an input for various amplitude attribute extractions for E34E36 reservoir studies. In order to crosscheck the reliability of attribute extraction method, the shallower layer that proven reservoirs should be interpreted. The similar amplitude extraction approach should be utilized to determine the hydrocarbon sand distribution on those reservoirs. The results should be compared with the well results to confirm that the method proposed works for all these reservoirs.

A detail horizon interpretation should be conducted on seismic lines and traces on 5 ms interval. The accurate interpretation will enhance the accuracy of the attribute extraction results. The auto tracking should only be used after horizon interpretation is done at the mentioned intervals. The horizon interpretation is conducted on final migrated seismic data which also been used as input data for attribute extraction.

The synthetic tie well with horizons on the shallow part of the seismic and does not fit very well with the deeper reflectors especially below the SMECoal layers. The well synthetic seismic tie were done for all the vertical wells and crosschecked with other nearest deviated wells where the synthetics are available in the database. The current available processed seismic data should be reprocessed with other processing technique to preserve the amplitude within the E34 reservoir mainly and below the SMECoal layer generally. The ADD Oil Company should bear on mind that the attribute extraction for the reservoirs below the SMECoal layer needs amplitude preservation for more detail study.

The X field seismic data was acquired on 4 ms sample rate which leads to attribute window selection on 4 ms multiple. It is recommended that the current available seismic data to be processed on 2ms sample rate. ADD Oil Company should invest on high-resolution seismic method or the Q-Marine acquisition technique to enhance the data

resolution and amplitude-sampling interval for attribute extraction and horizon interpretation.

Another step should be taken into consideration is the sealing capacity of the faults. Fault seal can arise from reservoir/nonreservoir juxtaposition or by development of fault rock having high entry pressure. The methodology for evaluating these possibilities uses detailed seismic mapping and well analysis. The X field has 227 faults where 220 exist on the database and 7 newly found possible faults. These faults are interpreted on both seismic and attribute maps, which can be used for further study on fault sealing capacity. Two types of lithology dependent attributes can be used here namely gouge ratio and smear factor. Gouge ratio is an estimate of the proportion of fine-grained material entrained into the fault gouge from the wall rocks. Smear factor methods (including clay smear potential and shale smear factor) estimate the profile thickness of shale drawn along the fault zone during faulting.

These parameters vary over the fault surface, implying that faults are sealing or nonsealing. These parameters are calibrated in areas where across-fault pressure differences are known from wells on both sides of a fault. This information should give a threshold value (on percentage) between minimal across-fault pressure difference and significant seal. The mentioned threshold value will be able to define the sealing capacity of all the faults in X field.

Understanding the fault sealing capacity will enable us to define the composition of the fluid or similarity between the hydrocarbon sand within the E34E36 reservoir. Please bear in mind that this project is done by considering the E34E36 reservoir as homogenous with constant amplitude variation. Therefore, understanding the faults sealing capacity will enable us to define the hydrocarbon delineation along this reservoir which probably will vary on the amplitude readings.

Bibliographical References

1. Satinder Chopra, Kurt Marfut and Vladimir Alexeev; 2006. Practical aspects of curvature computations from seismic horizons.

2. Fernando A. Nevis, Mohammad S. Zahrani and Stehen W. Bremkamp, Saudi Aramco, Dahran, Saudi Arabia, The Leading Edge, 2004; Detection of potential fractures and small faults using seismic.

3. Fred Aminzadeh, Paul de Groot, Tim Berge, Herald Ligtenberg, AAPG Hedberg conference, September 16-19, 2001; Determining Migration Path from Seismically derived Gas Chimney.

4. M. Turhan Taner, Rock Solid Image, Houstan U.S.A, CSEG September 2001; Seismic Attributes

5. Mario E. Sigismondi, Petrobras Energia SA, Neuquen, Argentina, Juan C. Soldo, Heriot Watt University, Scotland; Curvature attributes and seismic interpretation: Case studies from Argentina basin.

6. Y. Berthoumieu, M. Doias, C. David, 2004: Geometrical model based method for fault detection

7. Ligtenberg, Herald, dGB Earth Science, Enshede, the Netherlands. AAPG international conference, October 2004; Fault seal analysis by enhancing fluid flow paths and fault irregularities in seismic data.

8. Satinder Chopra, Arcis Coporation, Kurt J. Marfut, 2007, CSPG CSEG Convention ; Seismic attributes for fault/fracture identification.

9. Satinder Chopra, Arcis Coporation, Kurt J. Marfut, 2006, Distinguished instructor short course, SEG : Seismic attributes mapping of structure and stratigraphy.

10. Alister R. Brown, AAPG Publication, 3rd edition, 1991; Interpretation of 3D seismic data

11. Institute France Petroleum (IFP), 2007; MSc Petroleum Geoscience, 2D and 3D seismic data interpretation course manual

12. Landmark Cooperation, 2004; PostStack Family Reference Manual.

13. Landmark Cooperation, ver 3, 2003; SynTool Reference Manual

14. Landmark Cooperation, 2003; SeisWork Reference Manual

15. Project No.: CH2/C3/2001/XES/295(T) CGGAP Sdn. Bhd, May 2002; 3D Processing Report.

16. Petrophysics Report No.: CTR-402/403/404b/405/407/408a/409/4 11, July 2006; X Field Full Field Review Report.

17. C.R Johnson, EPMI. August 1984. A General Description of the Geological Interpretation Parameters and Interpolation Technique of X Field.

18. Dr. Venkataraman, PRSS, April 1994; X Field Sand Study for ADD Oil Company.

1. Appendix I: ESP Unconstrained and ESP Planner Dip Color Bar (Figures 4.1, 4.2, 4.3, 4.4, 4.5, 4.6, 4.7, 4.9, 4.10, 4.11, 4.12, 4.13, 4.14, 4.15, 4.16, 4.17, 4.18, 4.19, 4.20, 4.21, 4.22, 4.23, 4.24)

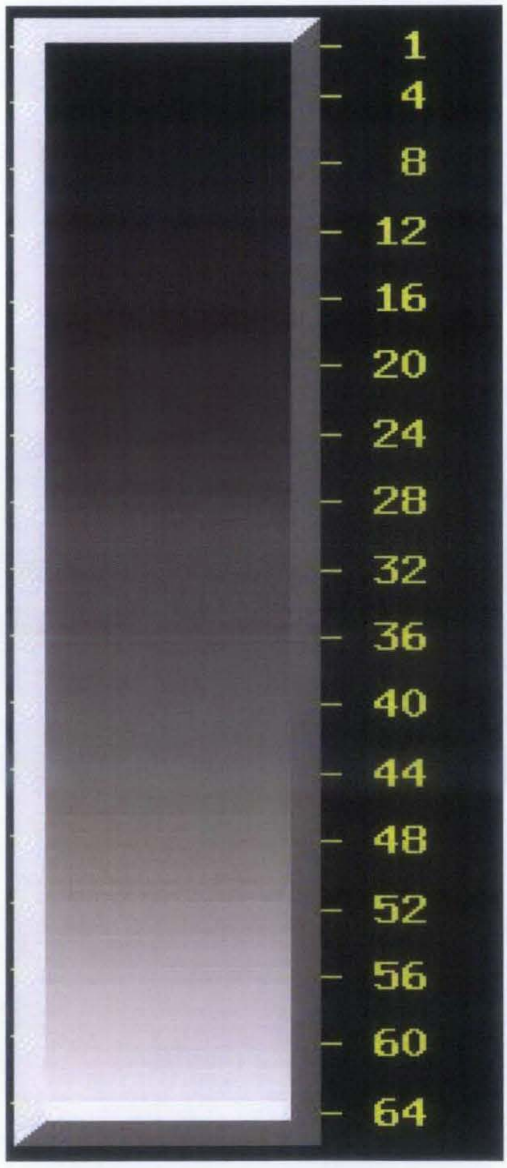

2. Appendix II: Positive Curvature Color Bar (Figures 4.27, 4.28, 4.29, 4.30, 4.31)

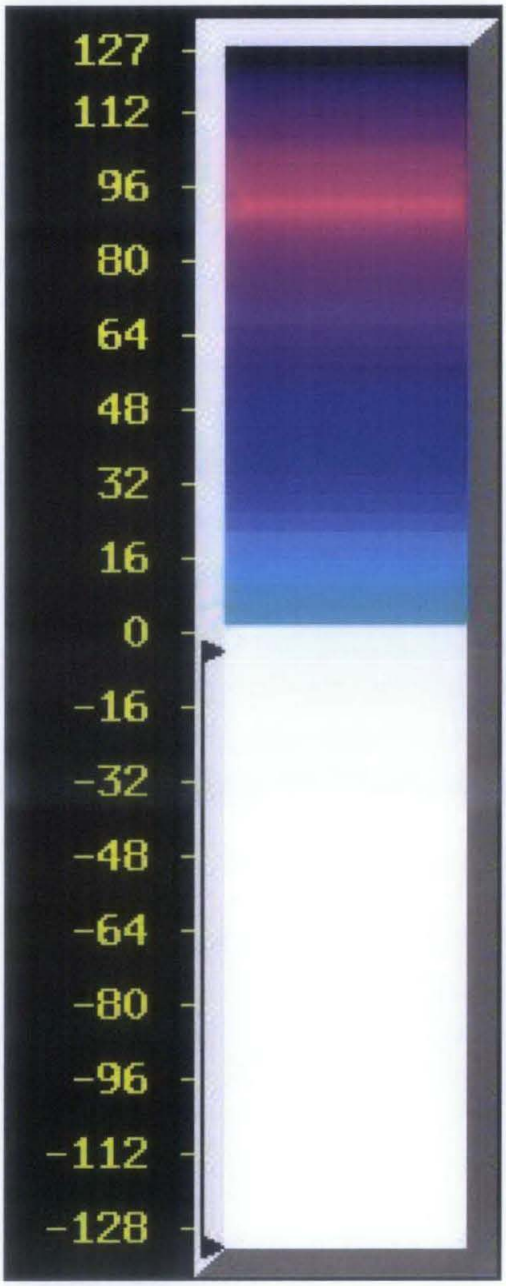

3. Appendix III: Negative Curvature Color Bar (Figures 4.32, 4.33, 4.34, 4.35)

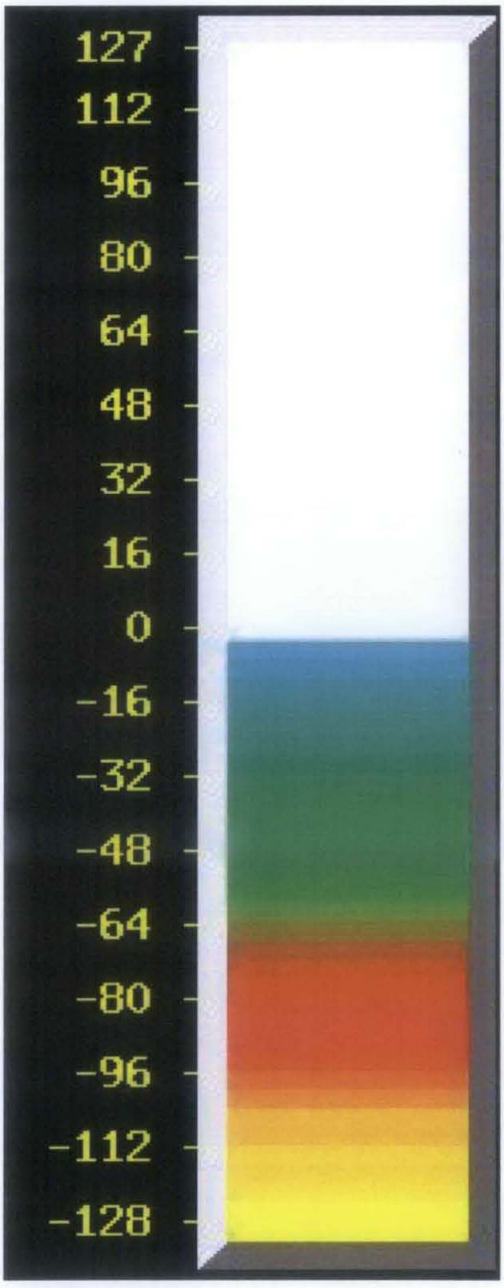

4. Appendix IV: Combination of both Positive and Negative Curvature (Figures 4.36, 4.37, 4.38, 4.39)

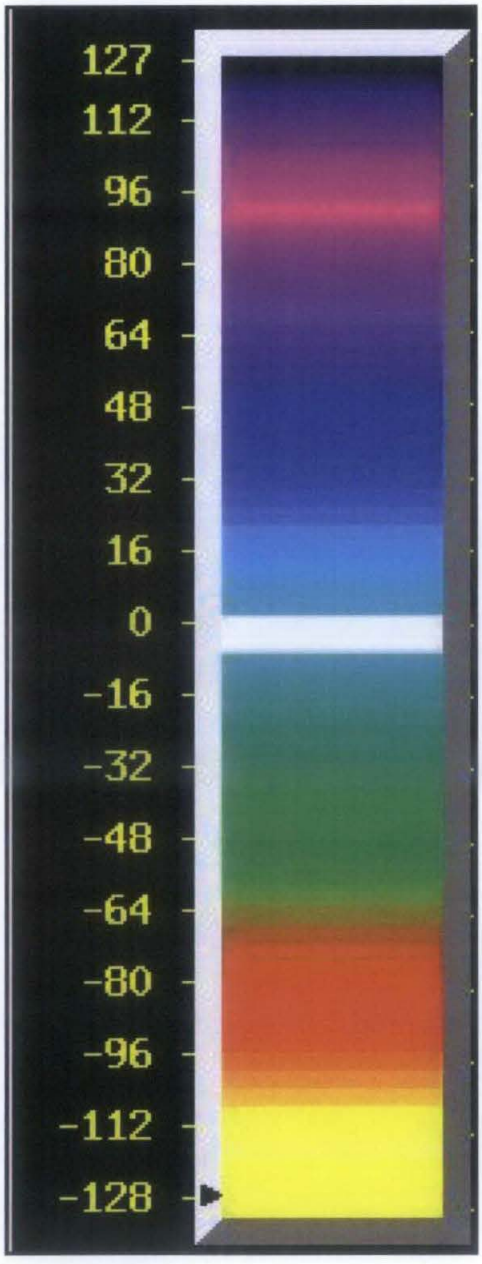

5. Appendix V: RMS amplitude, Average Absolute amplitude and Maximum Peak amplitude extraction within 0 to 120 amplitude values scale Color Bar (Figures 5.8, 5.9, 5.10, 5.27, 5.28, 5.29, 5.30, 5.46, 5.47, 5.48, 5.49)

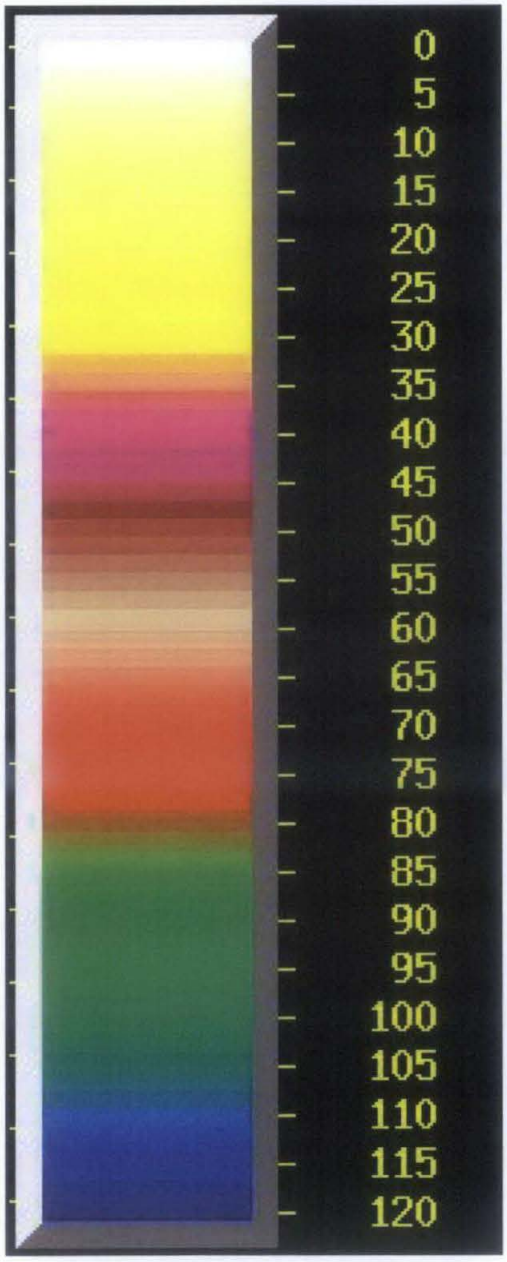

6. Appendix VI: RMS amplitude within 0 to 50 amplitude values scale Color Bar (Figures 5.12, 5.13, 5.14, 5.15, 5.16, 5.17, 5.18, 5.19, 5.20, 5.21, 5.22, 5.23, 5.24, 5.25, 5.26)

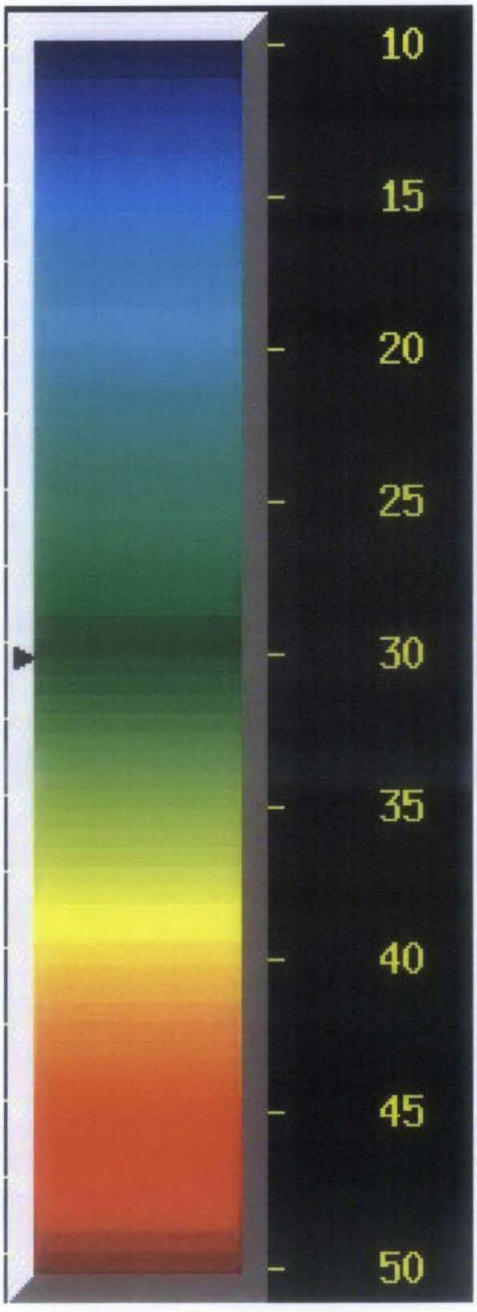

7. Appendix V: Average Absolute amplitude extraction within 15 to 45 amplitude values scale Color Bar (Figures 5.31, 5.32, 5.33, 5.34, 5.35, 5.36, 5.37, 5.38, 5.39, 5.40, 5.41, 5.42, 5.43, 5.44, 5.45)

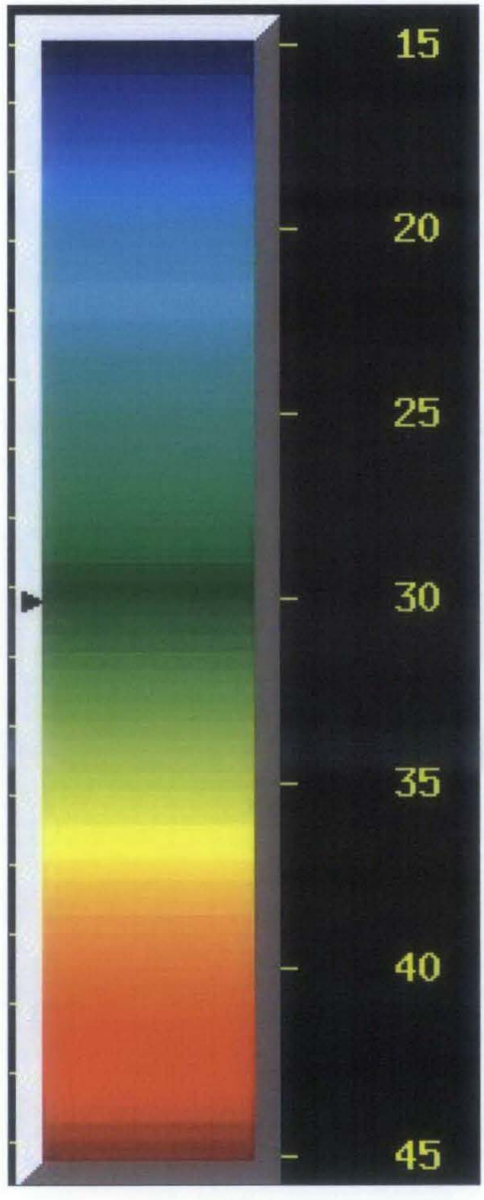

8. Appendix VII: Maximum Peak amplitude extraction within 0 to 40 amplitude values scale Color Bar (Figures 5.50, 5.51, 5.52, 5.53, 5.54, 5.55, 5.56, 5.57, 5.58, 5.59, 5.60)